Design of Riverbed Infiltration Gallery for sustainable water supply in Jhargram Municipality, West Bengal: An approach to mitigate groundwater exploitation

A thesis submitted towards partial fulfilment of the requirements for the degree of

Master of Engineering in
Water Resources and Hydraulic Engineering

Submitted by:

KABEER AHMED TAIYABJI

Examination Roll No. M4WRE22012
Registration No. 127307 of 2014-2015
Class Roll No. 002030301012
Session: 2020-22

Under the guidance of

PROF. (DR.) ASIS MAZUMDAR
Professor
School of Water Resources Engineering, Jadavpur University

and

DR. GOURAB BANERJEE
Assistant Professor
School of Water Resources Engineering, Jadavpur University

School of Water Resources Engineering
M.E. (Water Resources & Hydraulic Engineering)
Course affiliated to Faculty of Engineering and Technology
Jadavpur University
Kolkata-700032, India

2022

School of Water Resources & Hydraulic Engineering

Faculty of Interdisciplinary Studies, Law & Management

Jadavpur University

Kolkata, India

Certificate of Recommendation

This is to certify that the thesis entitled "**Design of Riverbed Infiltration Gallery for sustainable water supply in Jhargram Municipality, West Bengal: An approach to mitigate groundwater exploitation"** is a bonafide work carried out by **Mr. Kabeer Ahmed Taiyabji** under our supervision and guidance for partial fulfilment of the requirement for the Post Graduate Degree of Master of Engineering in Water Resources & Hydraulic Engineering during the academic session 2020-2022.

THESIS ADVISOR

Prof. (Dr.) Asis Mazumdar
Professor
School of Water Resources Engineering
Jadavpur University

THESIS ADVISOR

Dr. Gourab Banerjee
Assistant Professor
School of Water Resources Engineering
Jadavpur University

DIRECTOR

Prof. (Dr.) Pankaj Kumar Roy

School of Water Resources Engineering
Jadavpur University

DEAN

Prof. (Dr.) Subenoy Chakraborty

Faculty of Interdisciplinary Studies, Law & Management
Jadavpur University

M.E. Water Resources & Hydraulic Engineering
Jadavpur University
Kolkata, India

CERTIFICATE OF APPROVAL

This foregoing thesis is hereby approved as a credible study of Water Resources Engineering and presented in a manner satisfactorily to warranty its acceptance as a prerequisite to the degree for which it has been submitted. It is understood that by this approval the undersigned do not endorse or approve any statement made or opinion expressed or conclusion drawn therein but approve the thesis only for purpose for which it has been submitted.

Signature of Examiner

_____

Signature of Supervisor

1. _____

2. _____

Declaration of Originality and Compliance of Academic Ethics

I hereby declare that this thesis contains a literature survey and original research work by the undersigned candidate, as part of my **Master of Engineering** in **Water Resources & Hydraulic Engineering** in the Faculty of Interdisciplinary Studies, Law & Management, Jadavpur University during the academic session 2020-22.

All information in this document has been obtained and presented in accordance with academic rules and ethical conduct.

I also declare that, as required by these rules and conduct, I have fully cited and referenced all material and results that are not original to this work.

Name	: Kabeer Ahmed Taiyabji
Exam Roll Number	: M4WRE22012
Thesis Title	: Design of Riverbed Infiltration Gallery for sustainable water supply in Jhargram Municipality, West Bengal: An approach to mitigate groundwater exploitation.

Signature with Date

ACKNOWLEDGEMENT

I would like to extend my sincerest gratitude to my master's Thesis Advisors Prof. (Dr.) Asis Mazumdar, Professor, School of Water Resources Engineering, Jadavpur University and Dr. Gourab Banerjee, Assistant Professor, School of water Resources Engineering, Jadavpur University, under whose valuable guidance this research has been carried out. Without their assistance and dedicated involvement in every step throughout the process, it would have been impossible to carry out this research work with confidence without their whole-hearted involvement, advice, support, and constant encouragement throughout. My advisors have not only helped me to complete my thesis work but also has given valuable advice to proceed further in my life.

I would also like to show gratitude to, Prof. (Dr.) Arunabha Majumder, Emeritus Professor, School of Water Resources Engineering, Jadavpur University, Prof. (Dr.) Pankaj Kumar Roy, Director & Professor of School of Water Resources Engineering, Jadavpur University, Dr. Subhasish Das, Associate Professor, School of Water Resources Engineering, Jadavpur University, and Dr. Rajib Das, Assistant Professor, School of Water Resources Engineering, Jadavpur University, for their valuable guidance and suggestions.

I would also like to express my gratitude to all Senior and Junior Research Fellows of School of Water Resources Engineering, Jadavpur University, the entire staff at School of Water Resources Engineering, Jadavpur University & my friends for their constant help and encouragement during my thesis.

Getting through my dissertation required more than academic support, and I have many, many people to thank for their help and support. I cannot begin to express my gratitude and appreciation for their friendship. Most importantly, I am very grateful to my family for their constant support and encouragement over the last two years.

Date: _____

Kabeer Ahmed Taiyabji

Place: Jadavpur University, Kolkata Roll no: M4WRE22012

ABSTRACT

With the rising population in the subcontinent, water demand is also increasing over time. To meet the demand people are using the most available source of water and especially the groundwater. But the world water resources are limited and especially the groundwater resources. People are extracting groundwater without knowing the limitations of it. Which in upcoming decades may turn into a huge problem of water scarcity. The Government has been taking several measures by supplying the demand using available surface water and their further treatment and imposing restrictions on irregular extraction of groundwater. But the problems arise when there is less availability of surface water especially during summer seasons. Thereby groundwater extraction could be a sole solution in these cases. To mitigate the groundwater exploitation, this study concerns about a sustainable water supply by extracting the groundwater using a River Bed Infiltration Gallery at Kangsabati River, Jhargram. In spite of being a perennial river, the Kangsabati usually dries up in the extreme summer which affects the entire region. To proceed the study, a long duration pumping test has been performed to get the aquifer details to further estimate the safe yield of the aquifer so that the groundwater resources can be well maintained. Various methods have been followed in places, to estimate the required parameters necessary for the design of the gallery. To make the design sustainable and economical a gravel pack can also be provided to reduce the treatment cost. Few software have also been used e.g. QGIS, Strater etc. wherever needed. The purpose of the study is to supply the adequate demand to the Jhargram Municipality region to reduce the groundwater exploitation.

Keywords: Groundwater exploitation, Infiltration Gallery, Aquifer Parameters, Gravel Pack.

CONTENTS

List of Figures

List of Tables

Infiltration galleries should be seen as one of a number of techniques available for diverting/abstracting river water. Natural filtration is one of the main benefits of an infiltration intake and is used to reduce water quality variance. However in geological environments beneath the river bed where the aquifer is in semi-confined aquifer or where the water table is very deep in an unconfined aquifer infiltration gallery is not feasible. In such an environment collector well with radials are constructed (Sikdar, et al., 2020). In most cases, the groundwater beneath the river bed system is the unconfined aquifer, where shallow depth infiltration galleries are feasible. Apart from abstraction of groundwater, infiltration galleries are also suitable for groundwater recharge as well depending upon the purpose and location. Inclusion of additional gravel pack around the gallery also minimises the chances of groundwater contamination. This is highly recommended in the areas where groundwater contamination level is high.

1.1 Background of the study

Water is, beyond any doubt, the most abundant liquid to be found on the earth crust. About 71% of the Earth's surface is water-covered, and the oceans hold about 96.5% of all Earth's water. And only 2.5% of Earth's water is freshwater - the amount needed for life to survive. Figure 1.1 shows the distribution of water on earth crust out of which groundwater is the only source to supply a better degree of potable water up to a certain extent. And this is the reason it is getting exploited because of its irregular and unplanned use throughout the world. Though several measures have been taken and policies and restrictions have been introduced, it is the utmost need to supply the sufficient demand to the population.

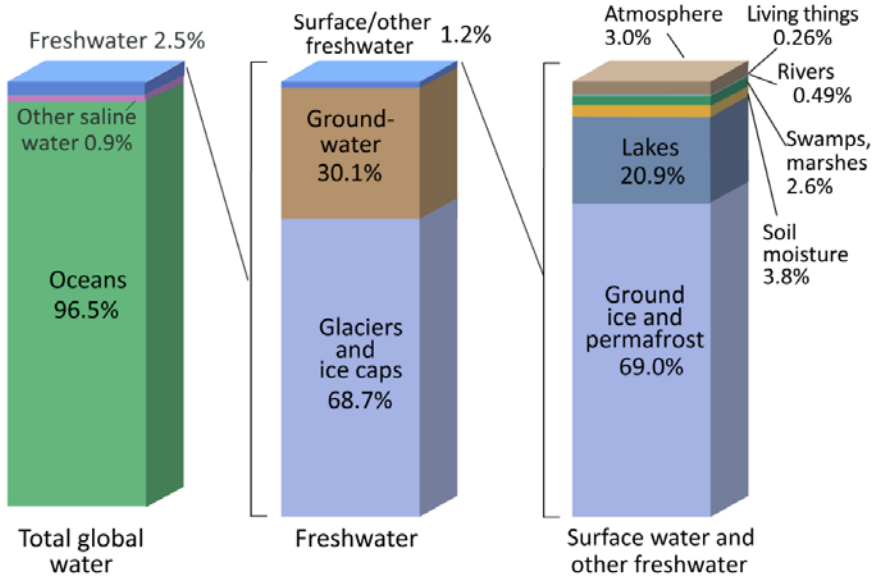

Figure 1.1: Distribution of Water on Earth (source: US Geological Survey, Water Science School)

Availability of groundwater varies depending upon the location. It also depends upon the possibilities of recharging from time to time. The quality of the groundwater in this case usually depends upon the quality of the water being infiltrated. The constituency of soil is such that it itself acts as a filter media which somehow provides a little better quality of the water. This technique is widely used nowadays to use a natural filter media to reduce the cost of the supply water. Infiltration galleries, vertical and horizontal intake wells etc. are the underground structural engineering techniques to use soil as a filter media and are widely used nowadays to make it economical. Studies are being carried out both nationally and globally to optimize the use of underground intake structures which is further discussed in this study.

Despite several threats from polluting activities, groundwater is often surprisingly resilient because of its filtration capacity. This natural filtration ability of the aquifer media can reduce the significant cost for water treatment. The contamination level of groundwater varies depending upon the location, and many areas have still remained unnoticed due to various socio-political reasons. Though people are using groundwater directly using hand pumps or domestic pumps for drinking purposes as well as daily demand. India is a fast growing country with its population growth is around 15% in the last decade. Meeting the water demand of the entire population with limited freshwater resources is thereby very challenging and thorough research works are vital.

1.1.1 Global Scenario

Groundwater has been a global concern since decades, as its availability is not even around the globe. Moreover recharging of the groundwater table is largely dependent on the precipitation and the climatic conditions vary largely around the globe. Therefore to meet the community water demand and to avoid groundwater exploitation, well and proper designing of underground intake structures are very crucial. In the Middle Eastern region especially Saudi Arabia, underground qanat systems were being used since the ancient times because of the water scarcity (Amin, et al., 1983). The places of tropical region where groundwater availability is abundant but the quality remains a discussion, uses gravel packed infiltration gallery to extract ground water and thereby reduce the pre supply treatment cost. Infiltration galleries are among the oldest known means used for small public water fountains. Owing to its ancestral origin they are usually associated with high quality water. Thirty-one compounds, including pesticides and oestrogens from different chemical families, were analysed in waters from infiltration galleries collected in Alto Douro Demarcated Wine region (North of Portugal). A total of twelve compounds were detected in the water samples collected from the gallery (Mansilha et. al 2011).

1.1.2 National Scenario

Rainfall is the primary source of groundwater recharge in India, supplemented by other sources such as recharge from canals, irrigated fields, and surface water bodies. As

the civilization developed around of water bodies that could support agriculture and transportation as well as provide drinking water but the quality has remained a larger issue. Due to pollution the quality of water in these rivers has gone down and in few areas it is so much polluted due to which water is not even fit for irrigation. The surface flow of these rivers is negligible in summer on account of which required amount of water is not available from the month of January to June every year. Hence there is problem of quality as well as of quantity of available drinking water. An adequate supply of pure water is absolutely essential to human existence. The consequence of contaminated water supply results in outbreak of water Borne diseases like Cholera and Typhoid (Jurel et. al 2013). One of the most suitable solution for getting potable water at low cost and throughout the year is the provision of Infiltration Galleries in the river bed which will provide clean filtered water continuously even in summer. Though in most cases it may need fewer pre supply treatments, it reduces the cost with respect to full scale treatment of water from open sources. Moreover it significantly reduces groundwater exploitation by imposing restrictions on unauthorised groundwater extraction using hand pumps and domestic centrifugal pumps.

1.1.3 Regional Scenario (West Bengal)

The western part of West Bengal has an acute scarcity of water because of its high altitude and hilly regions especially in the summer seasons. The scope of groundwater recharge via infiltration is hence minimum. Moreover the available ground water resources is highly contaminated with fluorides and arsenic etc. At present, factors like limited water reservoirs, water supply, global water demand, regional disparities, and climate change make water resource management a significant challenge in regions like Jhargram. Brackish water-bearing aquifers have been deciphered in the different depth zones in the Kolkata Municipal Corporation area, South 24 Parganas parts of North 24 Parganas, Haora, and East Medinipur districts. In the last decade a few intake structures in various parts of the state have been proposed and few of them have been executed under “West Bengal Drinking Water Sector Improvement Project” to get rid of the contaminations as well as the scarcity during the summer seasons.

1.2 Study area

Jhargram is a district in the western part of West Bengal. The study area is located on the Kangsabati River near the Baita Gram panchayat office at Jhargram District to supply the daily demand in Jhargram Municipal Region. The Jhargram Municipal region accommodates a population of 61682 (Census India, 2011) with a land coverage of 21.4 sq. km. The Baita Gram panchayat region which is 8 kms to the east of Jhargram Municipal region, is located in a humid tropical region with a maximum temperature of 42 ^{o}C during the months of summer and receives an annual average rainfall of 1300 mm. The stream is perennial in nature, however in summer seasons, it almost dries up.

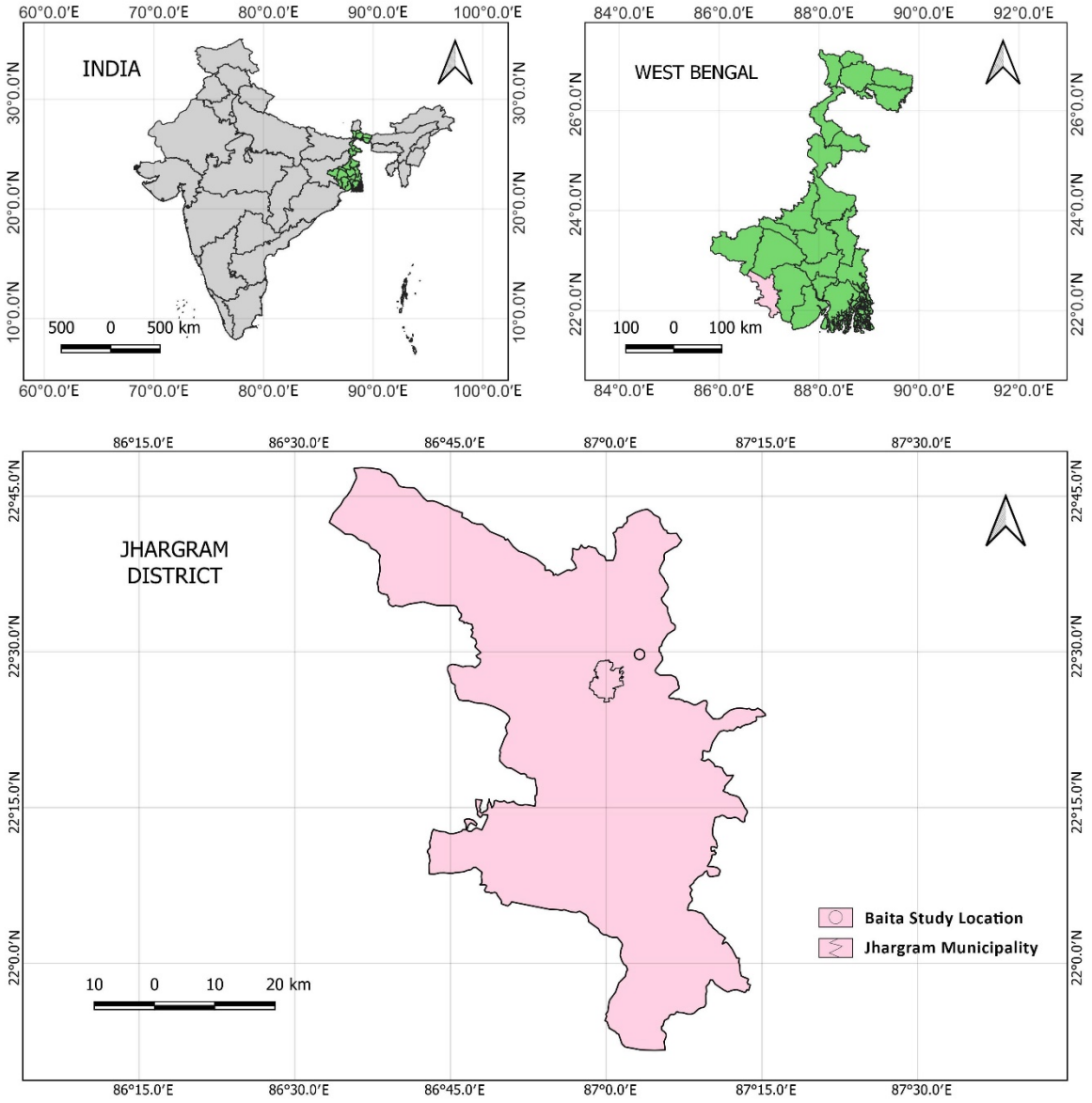

Figure 1.2: Location Map of the study area

1.3 Research Objectives

The main objective of the present research study is to reduce groundwater exploitation through estimation of in-situ aquifer parameters by performing a 72 hour long pumping test at Baita Village, Jhargram, West Bengal and design an infiltration gallery for sustainable water supply in the target area.

1.4 Methodology Adopted for the Research

The overall research study methodology is mainly divided into five components: Literature Review for Identification of goal and objective, collection of the information of the present situation by performing primary survey and detailed field and lab

experiments, data presentation and organisation of data analysis. Discussion about the details of the study area for proper evaluation of the work, and also the target area for the present study. Proper analysis of the field data using suitable scientific methods to pop out the hydro geological parameters and thereby safely design the targeted infiltration gallery to achieve the research goal. Along with the hydraulic design of the gallery suitable gravel pack design is also favourable for better yield.

1.5 Proposed Outcomes of the Research Study

The following outcome would possibly have emerged through this research study:

1. River morphology including preparation of lithological strata from the slim boring operation.
2. Details of the Aquifer properties of the study area to design the target infiltration gallery
3. Detailed hydraulic design of the infiltration gallery to meet the requirements of the target area.

1.6 Outline of the Thesis

The thesis consists of mainly six chapters. After briefly discussing about the thesis introduction, Literature Review is described in the second chapter. The third chapter describes the study area: location, topography, demographics, lithology etc. Fourth chapter describes the conceptualization of the theory behind the study. The fifth chapter describes the methodologies adopted to get to the research objectives. The sixth chapter discusses the results of the detailed experiments and the analysis and designs. And the final chapter is the conclusion of the thesis. And References are given at the end of the dissertation.

Chapter 2 Literature Review

There are various studies that have been made to analyse the aquifer characteristics and using them to design infiltration galleries for various purposes depending upon the location, topography and uses. Infiltration galleries are used to recharge the ground water and on the other hand to extract them for various purposes which includes drinking in many places where quality has also come out to be an important parameter to count on. Water quality in the aquifer varies with the location therefore quality check is also a criteria for the researchers and designers.

2.1 Research Review on International and National Scale

- **Asare** et. al. (2004) studied on infiltration gallery which was successfully installed at a small rural community of Goviefe-Agodome in Ghana, South Africa. The facility consists of three shallow wells located in series which are 54 to 74 m away from the pond. Two of the wells were constructed and filled with locally available filter media e.g. (Sand of effective size 0.52 mm and uniformity co-efficient of 2.308). Sand D30 of 0.52 mm and CU of 2.308. Results obtained from laboratory analysis carried out on water samples taken from the infiltration gallery showed that most of the physio-chemical characteristics of the filtered water were within the WHO (1993) guidelines and were higher than the raw water parameters. Leaching of lime and other constituents of cement used in the construction work accounted for the increase in ionic content. The bacteriological quality of the filtered water was acceptable. The iron levels in the filtered water are, however, high and may require further treatment.

- **Jones** (2008) studied to develop an intake system that would not be depended on local geological characteristics; a site-independent indirect intake system that would deliver sufficient quantity of feed water while pre-filtering the feed water to remove as much biological material as possible. The quantity and quality of feed water for desalting is critical for efficient operation of a desalination plant. The considerations include a synthetic permeable system designed to take advantages of the advances in directional drilling as well as incorporate the use of geotextile fabrics to transfer the preferred infiltration characteristics to any coastal site. The filtered seawater collection system removes undesirable elements from feed water. Elimination of all stages of plankton greatly reduces impingement and eliminates entrainment from fouling the system. The synthetic infiltration gallery overcomes existing limitations due to constraints imposed by the geological conditions at the construction site. This system comprises a subterranean reservoir installed at a sheltered location; a borehole created by directional drilling, a pipe or series of pipes extending from the reservoir into the open ocean. The terminal end of the intake is overlain with marine mattresses with filtration media sachets. The intake receives water infiltrated through these sachets. As with well designs, the compelling objective is to obtain the greatest yield, taking into account life cycle costs

over a 25-year period of operation. Gallery placement under water bodies is known to produce twice the typical yields of galleries placed adjacent to water bodies on the bank or shoreline. In terms of maintenance, the system can be backwashed by isolating sections and flushing with up to twice the infiltration rate, around 200–600 $m^3/d/m^2$ of filter surface area of sachets.

- **Bhattacharya** et. al. (2009) developed practical design for groundwater withdrawal consisting of qanats coupled with vertical risers to obtain groundwater of satisfactory quality and quantity. And presented the phenomena of saline water intrusion and up-coning below wells. Saline water intrusion takes place in all coastal aquifers and pumping of fresh water increases the saline water intrusion. In coastal aquifers, where the fresh water lies above saline water, and is pumped by a well, the interface rises below the well due to drawdown of the groundwater table around the well. The pressure on the interface is reduced and saline water rises as a conical mound beneath the well. Ghyben-Herzberg relation has been used to find the depth of interface. As the deep tube wells are not preferable to avoid coning horizontal infiltration galleries called qanats coupled with vertical risers can be used to supply the required demand by avoiding the coning. Design parameters can be obtained as per the demand of supply.

- **Banerjee** (2011) prepared a report on the rationality of design methods of sub-surface RC well, based on image theory and model study, which was adequately supported with geophysical investigations. An RC well-system was designed following the aforesaid two methods and was constructed at the proposed sites, which was found to be the most favourable one based on remote sensing survey, geophysical studies, and hydrological investigations. Remote sensing-based information and geophysical investigations along with the fence diagrams resulting from the borehole data (logs) establish the existence of a confined aquifer at Site I and an unconfined aquifer at Site II. The sand layer at Site I thin out to the north as well as to the west. Whereas, at Site III, there is a thin confined layer, very much irregular in nature and having no scope for pushing radials, all within the sand strata. Analyses of pump test data show that there is fairly good (for Site III) to excellent (for Site II) transmissivity (T) of the aquifers at all the sites under study having an overall range of 810–2573 m^3/day-m. However, the average coefficients of storage (S) are poor at Site I (0.0037) and Site III (0.0016), while the same at Site II is much higher (0.068). Hence, this site (II) has been selected for design of radial collector well, while the other two sites (Sites I and III) were not found suitable for such types of well systems. The model-based design approach seems to be much less conservative suggesting more yield as against that the same based on image well concept, in which case the expected safe yield was much conservative.

- **Mansilha** et. al. (2011) discussed against the conventional assumption that the quality of water collected from infiltration gallery requires a very minimal treatment. As per the discussion the potability of water collected from infiltration gallery varies from place to place. Thirty-one compounds, including pesticides and estrogens from different

chemical families, were analysed in waters from infiltration galleries collected in Alto Douro Demarcated Wine region (North of Portugal). A total of twelve compounds were detected in the water samples. Nine of these compounds are described as presenting evidence or potential evidence of interfering with the hormone system of humans and wildlife. Although concentrations of the target analytes were relatively low, many of them below their limit of quantification, four compounds were above quantification limit and two of them even above the legal limit. Trace analysis of thirty-one compounds was performed by GC/MS (Gas Chromatograph Mass Spectrometer) in nine samples of water from small public fountains of infiltration galleries. The methodology was previously validated by us according mainly the International Conference on Harmonisation recommendations using a weighted least squares linear regression procedure as heteroscedasticity has been verified for the target analytes. The general idea that water from infiltration galleries present always high quality was not confirmed. The sampling region chosen for this study was located in a small area (around 100 km^2). However, the qualitative and quantitative pesticide profile of water samples analysed and, therefore, its quality was clearly different. Target EDCs (Endocrine Disruptor Compounds) and other pesticides were found in seven of the nine samples and the most frequent was terbuthylazine and its metabolite terbuthylazine-desethyl that exceeded, in two samples, the 0.1 μg/L EU limit for individual pesticides. The intensive character of the local agriculture contributed to the diversity of pesticides that were detected and quantified.

- **Gregory** et. al. (2012) assessed a stormwater management servicing plan to lessen the impact on adjacent properties and on the receiving watercourse. Continuous hydrologic simulation was used to evaluate the long-term water balance and to verify the system's hydraulic performance under a full range of storm events, using a wider array of risk-based indicators including the depth and velocity of infiltration gallery overflows during extreme rainfall events. With the increasing popularity in Low Impact Development and green infrastructure initiatives, contemporary stormwater management is now concerned with water balance as an additional design objective that would maximize surface runoff volume reductions onsite. Continuous simulation offers a greater diagnostic tool for assessing hydraulic performance compared to event based modelling, since it can describe the full range of runoff response characteristics, versus a snapshot of selected individual return period events. With event-based simulation, the assessment of duration is only useful as a relative measure for comparing alternatives. Ultimately however, the key consideration in stormwater design is minimizing the risks to public safety and property damage. It is common practice to assess the hydraulic performance of stormwater facilities based on controlling peak flow rates, and in some cases runoff volume, to pre-development conditions. Neither one of these variables can accurately quantify the associated flood risk or property damage potential: the depth and velocity of flow are more appropriate indicators. A true assessment of risk can only be achieved by integrating these risk-based indicators with the full range of flow frequencies computed using continuous simulation.

- **Bekele** et. al. (2013) prepared a report on a 39-month pilot scale MAR (Managed Aquifer Recharge) scheme that infiltrated secondary treated wastewater through unsaturated sand into a limestone and sand aquifer. Two types of infiltration gallery were constructed to compare their hydraulic performance, one using crushed, graded gravel, the other using an engineered leach drain system (Atlantis Leach System). Both galleries received 25 kL of nutrient-rich, secondary treated wastewater per day. The performance of the Atlantis system suggests it is superior to the gravel gallery, requiring less maintenance within at least the time frame of this study. The results from a bromide tracer test revealed a minimum transport time of 3.7 days for the recharged water to reach the water table below 9 m of sand and limestone. This set a limit on the time available for attenuation by natural treatment within the unsaturated zone before it recharged groundwater. The perforated PVC pipe used to promote lateral distribution of treated wastewater in the gravel gallery was longer than the Atlantis system gallery and became blocked more often, leading to less infiltration and poor hydraulic performance. If the new scheme utilizes the Atlantis system under hydrogeological and hydraulic loading conditions that are similar to the study of pilot site, then either (a) natural processes in the unsaturated zone that effectively treat the water to an appropriate standard in less than four days must be demonstrated; or (b) an engineered treatment system is needed prior to recharge to achieve the required water quality at the water table. This decision will ultimately depend on the intended purpose and the purification requirements for recycled water at the site.

- **Jurel** et. al. (2013) discussed and reported the importance of infiltration galleries in reduction of the treatment cost for drinking water supply. Due to pollution and sewerage disposed in the river, the quality of water has become poor and the treatment cost has gone up. During summer the quantity of water flowing in the river is very less on account of which concentration of impurities is also more. On the other hand, due to over exploitation of ground water for irrigation, the ground water table is also going down at fast rate, hence availability of ground water is also not certain. The quality of ground water is also becoming poor due to pollution, intrusion of brackish/saline water, and concentration of fluoride etc. If system of infiltration galleries is provided in the bed of the river at 5 to 10m below bed level, by means of perforated pipes (Strainer) the availability of water in terms of quality and quantity will improve. Hence a solution to drinking water supply for major cities has been presented in this article, along with a typical example for design of infiltration gallery for Agra City (U.P., India). Design of infiltration gallery has also been prepared and the maximum discharge has come out to be 13600m^3/day. By provision of Infiltration galleries treatment cost will be reduced and we can have adequate drinking water in quality and quantity even in summer when practically no water is flowing on the bed of river.

- **Jennings** et. al. (2015) studied a case of municipal areas where land development is a basic and fundamental way for infrastructure development. When land is developed,

its surface is often compacted, defoliated, graded, and/or covered by less permeable materials. These changes increase the amount of storm water runoff, and this runoff is more rapidly conveyed to receiving streams where it can degrade stream morphology and aquatic ecosystems. Several methods have been proposed for reducing residential storm water runoff. The most common are disconnecting downspouts or installing rain barrels, rain gardens, permeable pavements, or infiltration galleries. The analysis of the infiltration gallery storm water-management system presented here is based on an algorithm that uses an hourly precipitation record to quantify system performance. Daily data are adequate to evaluate rain barrels since there is no ongoing discharge other than overflow that must be tracked. Analysis of the performance of the storm water infiltration gallery is accomplished by an hour by hour volume balance of water flow into and out of the system. The essential design attributes are the roof surface area and runoff coefficient, the gallery's length, width, depth, and storage medium porosity, the size of the perforated pipe used to charge the system, and the infiltration potential of the underlying soil. The issue of the hydraulic performance of rain barrels and rain gardens is significant because the infiltration gallery offers an approach that avoids the operational challenges of rain barrels and the aesthetic challenges of rain gardens while offering maintenance free performance superior to either.

- **Jeong** et. al. (2017) discussed about the clogging, which is a major obstacle in aquifer storage and recovery (ASR) applications, causes declines in recharge rates and ultimately the failure of artificial recharge systems. Clogging is generally triggered by physical processes, which involve the accumulation of suspended solids from recharge water, the release of fine particles from soils and aquifers and their migration, and the formation of gas barriers from the entrapped air in recharge water and biogenic gases. Clogging is a combined result of physical, biological, and chemical processes. Clogging can be alleviated by removing suspended solids, organic carbons, and nutrients from source water prior to recharge. For this purpose, several pre-treatment processes can be used: coagulation and filtration for removal of suspended solids, advanced oxidation using ozone or peroxide for destruction of organic matter, and post-filtration with anthracite sands or Granular Activated Carbon for sorption of nutrients.

- **Maity** et. al. (2017) discussed about a field-based study on the sub-surface characteristics and groundwater quality variation in the coastal region of Purba Midnapur district, West Bengal, India. The fact that the coastal area receives inadequate surface water, the use of groundwater has become increasingly important for domestic, irrigation and industrial purposes; however threat exists associated with groundwater over-exploitation that leads to the intrusion of seawater. This paper presents a mathematical analysis for estimating the safe yield from shallow vertical well and the qanat well structures coupled with vertical risers are presented as a viable solution to the problem of upconing below deep vertical wells. As regards the formulations developed for safe yield of vertical well considering upconing in coastal regions, it may be concluded that the well discharge initially increases with fresh water head above mean sea level

following a fairly parabolic pattern. Also, at zero discharge, the variation of the depth of well with the fresh water head above mean sea level follows parabolic pattern. Horizontal infiltration galleries are presented in this paper as a viable solution to upconing below vertical wells. As the analysis presented in this paper has shown, vertical wells may not be feasible in several situations and horizontal infiltration galleries can be successfully used in such cases.

- **Kusuma** et. al. (2018) discussed about the use of infiltration gallery to reduce the cost of preliminary treatment for water potability. The soil is used to screen out the contaminants in physical, chemical and biological means. This study drew attention as the cost of clean water production in the province of East Java, Indonesia requires a lot of cost, because the consumption of coagulant is very high. The purpose of this research is to know soil characteristics in soil samples in each region and its ability to removal TSS and Total Coliform. Also, to find good soil composition for removal TSS and total Coliform. The experimental method that has been used was consisting of a reactor made up of an acrylic tube with an internal diameter of 5.08 cm, an outer diameter of 5.48 cm and a height of 10 cm and is equipped a plastic container tub with a capacity of 80 litres as a water tank. The acrylic tube was filled with soil samples. The process of this reactor was at the water from the container flowed into each acrylic tube and each acrylic tube was taken as the water sample, to be analysed for TSS and total coliform parameters. The position of the acrylic reactor was placed vertically, which replicates the water performance in the soil during the infiltration process. The use of soil in the sample area resulted in poor quality of water, therefore it needs soil engineering to improve the soil's ability to reduce TSS and Total coliform. Soil engineering was done by changing the percentage of sand and clay. The results showed that the composition of sand and clay was 85% and 15%, able to decrease TSS and Total coliform about 63.50% and 99.67%, which resulted in savings of coagulant usage.

- **Macuha** et. al. (2019) developed a collector well with parallel infiltration galleries as laterals in Calaca, Philippines where trenchless technology is not a common practice. This paper presents applicable yield estimation techniques for collector wells with parallel laterals in the riverbed. The first method uses a source-sink pair model and image well theory, obtaining an approximate analytical solution. The second makes use of MODFLOW, a numerical approach to come up with a local groundwater model. The estimates from both are found to be in good agreement with actual yields measured in a study area. The underlying geology of the study area is primarily sand of differing density and consistency, typical of a downstream portion of catchment areas in the Philippines. The uppermost layer is silty sand, then sands of increasing density as one move deeper. This study shows that yield estimations for parallel horizontal wells both by analytical and numerical methods are easier as compared to radial collector wells. In fact, approximate analytical yield equations were derived and the resulting total yield estimate is in good agreement with the observed values. The developed equations can be

used for rapid estimation of yield to other candidate sites. Meanwhile, the FDM model using MODFLOW produced more accurate results than the analytical method.

- **Chau** et. al. (2019) developed a risk assessment model and combined with hydrogeological data to determine the permissible limit of fecal coliform in water during riverbank filtration (RBF). Analytical solutions contained flow and contaminant transport model for an infiltration gallery. The analytical element method (AEM) was used to measure the travel time of water toward the gallery for a given rise in stream stage under an unsteady state of flow condition. To study the contaminant concentration variation, pathogen transport considering dispersion and decay was analysed. The model was based on an explicit finite difference scheme, which was used to estimate the change in pathogen concentration during a stream stage rise. In this analysis, it was observed that the safe distance of an infiltration gallery should be considered carefully. The most desired log cycle reduction can be achieved from the analytical analysis presented in this study. More importantly, the AEM based LIFI-PATRAM model is capable of determining the optimal location and therefore can be applied to various field problems by incorporating different properties of the aquifer and source water quality for sustainable management of RBF. He found that optimization and cost studies of RBF with other pre-treatment methods is required to show that RBF is a reliable and cost-effective treatment technique.

- **Sikdar** et. al. (2020) assessed the aquifer properties and the potentiality of the base flow of River Brahmani in Nalhati-I block of Birbhum District, West Bengal, India for small to medium water supply for drinking and domestic purposes in the villages where groundwater is contaminated with fluoride. The aquifer is confined to semi-confined in nature extending up to at least 30m below the river bed with relatively deep water table. The aquifer can be exploited for water supply through a collector well with radials. Physical well drilling and pumping tests were done to find out different aquifer properties. In River Brahmani along the test well lines the sand which occurs below 4-6 m below the river bed is in general medium sand. The water level is very deep ranging between 6.67 and 10.34 m below the river bed. The aquifer is semi-confined to confined in nature. The water level in general rests at a depth below the base of the upper confining bed and hence the aquifer although confined by an overlying confining bed behaves as an unconfined aquifer. The transmissivity of the aquifer varies between 567 and 1303 m^2/day. Therefore, a collector well with radials may be constructed along test well line. Based on the study, the small amount of reduction in the base flow of the river that will occur due to abstraction will not have any significant adverse effect on the river regime.

- **Aslam** et. al. (2021) discussed about the sustainability of groundwater at Lahore province in Pakistan as groundwater exploitation in Lahore is not sustainable as abstraction rates are higher as compared to groundwater recharge rates. The average simulated water table decline is 1.1 meter per year in the study area. It was seen that

these infiltration galleries allow recharging the groundwater at better rate. Historical data of several parameters like rainfall, land use and runoff were analysed and hydrologic modelling was done. Infiltration galleries are shallow between 1 to 3 m deep rock-filled excavations that serve as reservoirs for storm water runoff. Potential routes/locations for Infiltration Galleries were demarcated usually at low line areas such as parks, playing fields, green belts along the roads etc. using the Digital Elevation Models of Model Town on ArcGIS software. Design of Infiltration galleries comprising of bed width, depth and filter material was carried out with respect to the amount of storm water runoff generated. Forecasting the GW depletion data concluded that groundwater depletion rate has reduced due to the installation of infiltration galleries in the study area. Average reduction in groundwater depletion rate is about 0.15 m/year.

- **Kusuma** et. al. (2021) studied to find the optimal soil composition in the infiltration gallery, used as an approach to dynamic system modelling which required to input all of variable that influence soil filtration process such as weather, conductivity hydraulic, TSS influent, percentage soil removal to TSS, capacity water, evaporation and catchment area. All variables could be changed until got TSS close to zero. The purpose of the study is to optimize the use of the filter media to a larger extent and avoid clogging and maximum yield. TSS is influenced by porosity, permeability and composition between clay and sand. If porosity and permeability are big then the value of TSS is also big, but if the percentage of clay is higher than TSS will be small because there is filtration process. A soil type has a sand, silt and clay component. If the amount of sand is high then the quantity of clay is low and vice versa. The ratio of clay and sand affect the size of the particle of soil. If the particle soil has a large size then the TSS becomes high because there is no effective screening process. Water content affects the porosity of the soil easily passed by water. The filtration rate is also affected by the permeability. If the permeability value is high, then the filtration rate is fast, so the TSS removal is reduced. While using infiltration gallery as a filter media, the discussed policy could be adopted to optimise the use of infiltration gallery and also the reduction in maintenance cost.

- **Kalwa** et. al. (2021) discussed that gravity-driven infiltration into the shallow subsurface via small-diameter wells (SDWs), i.e., wells with an inner diameter smaller than 7.5 cm (3 inches) and no gravel pack) has proven to be a cost-efficient and flexible tool for managed aquifer recharge (MAR), as it provides relatively high recharge rates with minimal construction effort. SDWs have a significantly smaller open filter area than larger diameter wells with gravel pack, making the infiltration of low-quality waters through these wells more at risk clogging. The experiments showed that smaller diameters and the lack of a gravel pack increase the well's susceptibility to both kinds of clogging. However, this effect was observed to be much more pronounced for physical than for biological clogging. SDWs show severe disadvantages with respect to the infiltration of highly turbid waters in comparison to large diameter wells with a gravel pack. Nevertheless, this disadvantage is much less severe when it comes to the infiltration of clear but nutrient-rich waters (e.g., treated wastewater). Depending on the economic

and geological circumstances of a MAR-project, this disadvantage could be outweighed by the significantly lower construction costs of SDWs.

- **Marazuela** et. al. (2022) studied and discussed about the infiltration process and the wetting front propagation from dry infiltration galleries based on a 3D unsaturated flow model to facilitate extreme precipitation and storm water. Commonly infiltration facilities are also used for managed artificial recharge (MAR) of aquifers in areas with scarcity of water. However, there is no scientific reference whatsoever to galleries excavated in consolidated volcanic rocks operating in the vadose zone as infiltration facilities, here referred to as dry galleries. Dry galleries are storm water infiltration facilities composed of a vertical well (1–2 m of diameter) that connects with a horizontal gallery (often 5–50 m long and 2–5 m wide) dug by hand into layers of consolidated permeable rocks within the vadose zone from where storm water infiltration is produced. The gallery can be located at any depth within the unsaturated zone, although it is generally between 5 and 50 m deep. The design of the dry galleries is justified by the characteristic geological configuration of volcanic rocks where layers of impermeable rocks (e.g., basaltic rocks) alternate with others much more permeable (e.g., loosely packaged pyroclasts). Storm water management is a global problem and, due to climate change, frequency and intensity will increase. Dry galleries could help to better manage storm water events, prevent or mitigate floods, and increase groundwater storage by artificial recharge, which is benign in preventing seawater intrusion. This is of utmost importance, especially for islands in dry regions and with increasing water scarcity.

- **Foucher** et. al. (2022) discussed about A gravel pack equipped with sand screen completion is commonly used in deepwater Gulf of Mexico. Over time, fines migration and asphaltenes clog the screens of the completion, which negatively affects the well production. In order to remediate the damage, openings are created in the concentric base pipe inside the screen. This process creates a flow path that allows for cleaning of debris from the screens through jetting and bull heading of stimulation fluids. The combination of these operations restores the productivity of the well. In the conventional method, the cuts are machined one at a time with a blade spinning in the horizontal plane. To achieve sufficient flow area, this step is repeated approximately hundred times to distribute the cuts along the target screen interval. Such an operation can require up to 14 days including the downhole cutting time as well as trips in and out of the well to replace the blades. The blades protrude only slightly from the base pipe to avoid damaging the screen. The screens are separated from the base pipe with standoff to maintain a constant clearance. Thus, the blades cannot damage the screen.

Chapter 3 Description of the Study Area

3.1 Location

Jhargram is district in the western region of West Bengal as shown in the map below. The study area is located at Kangsabati River near Baita Gram Panchayat Office, Jhargram. The location is 8 kms to the east of Jhargram Municipal region. The position of the Main well of pumping test is shown as per the coordinate 22°29'44.6" N, 87°03'11.6" E, in the Figure 3.1.

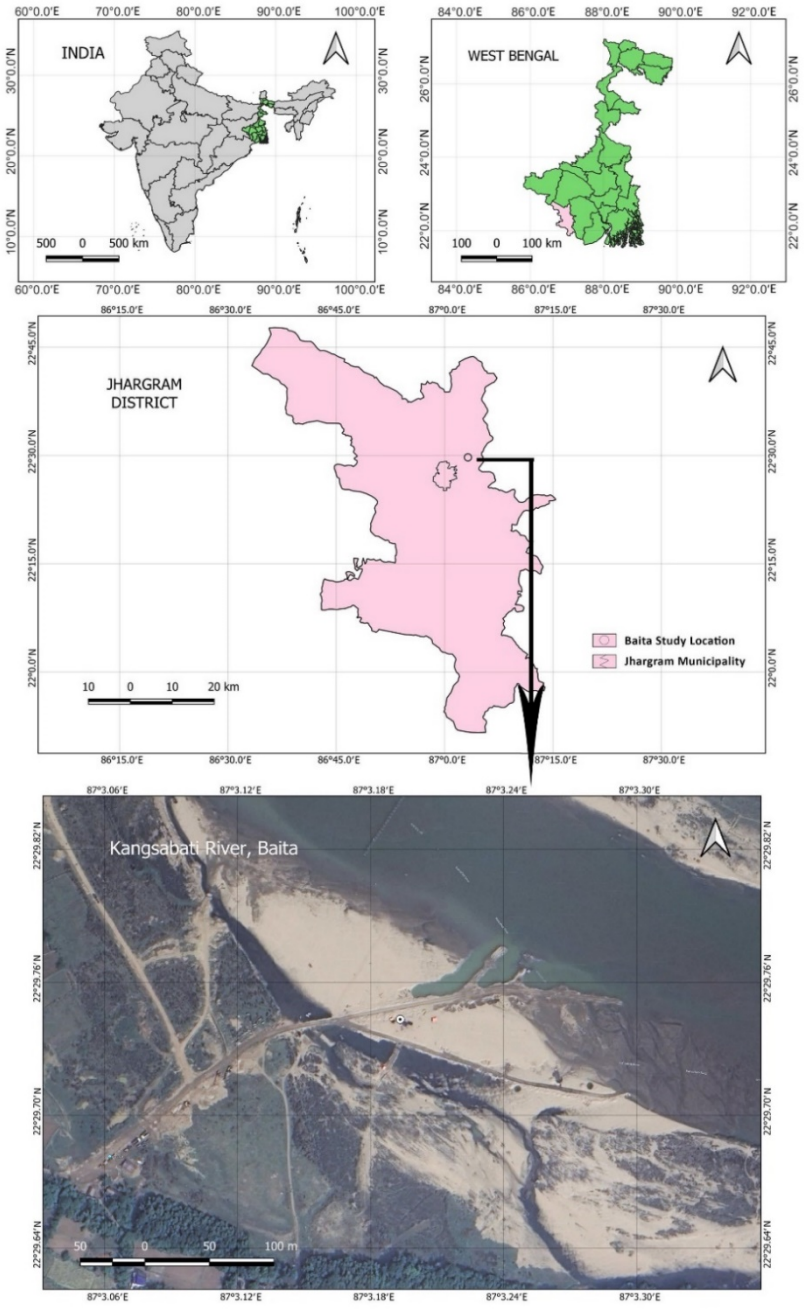

Figure 3.1: Location Map of the Study Area

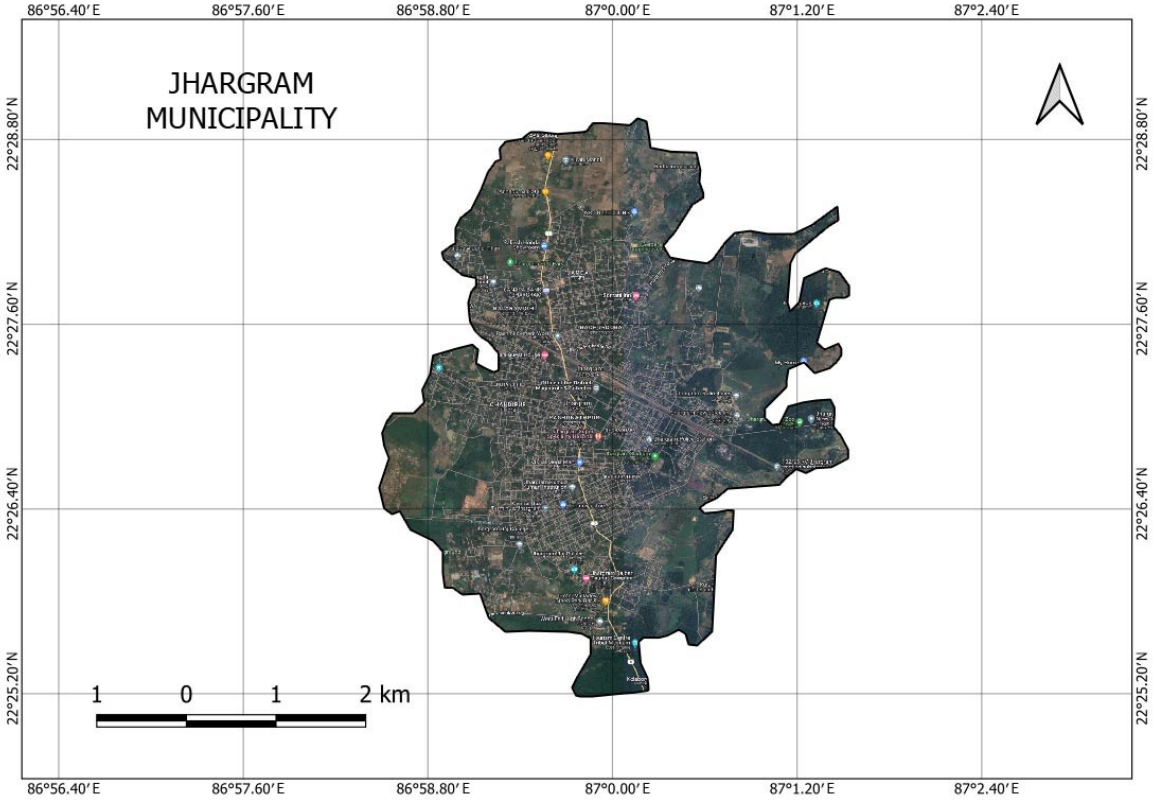

Figure 3.2: Location Map of the Target Area

Figure 3.3: Real Time Image of the Study Area

3.2 Contour Map and Drainage Basin of Study Area

The contour map and drainage basin have been prepared using the DEM (digital elevation model) in the Q-GIS (ver 3.22.7). The SRTM DEM has been downloaded from the USGS web portal. The maximum elevation is 88 meters whereas minimum is 40 meters found near the riverine tract as shown in Figure 3.4.

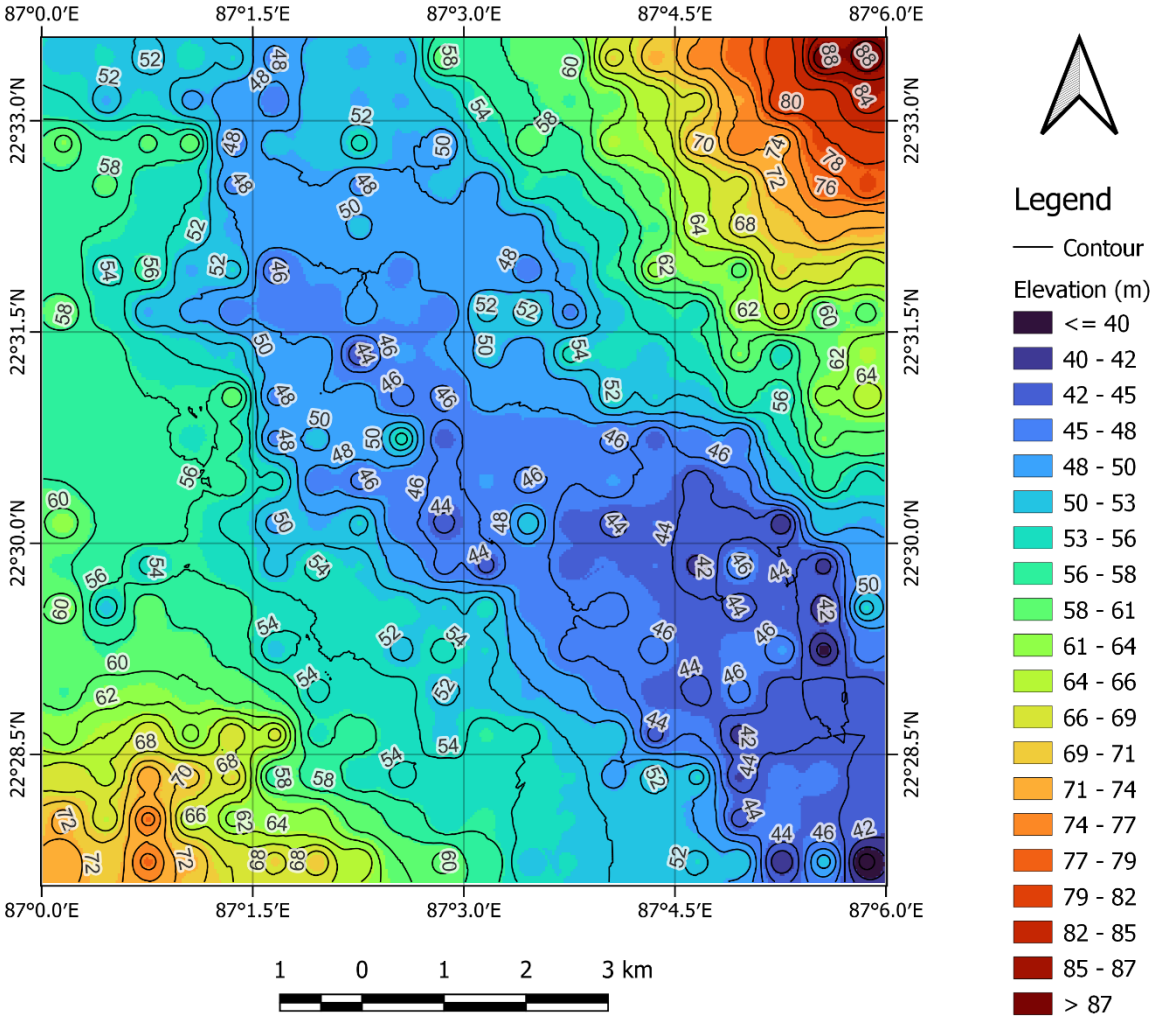

Figure 3.4: Contour Map of the Study Area

A drainage basin map of Kangsabati River has also been generated with help of Q-GIS software using the Hydrobasin and USGS data. The study area is shown in the basin map shown in Figure 3.5.

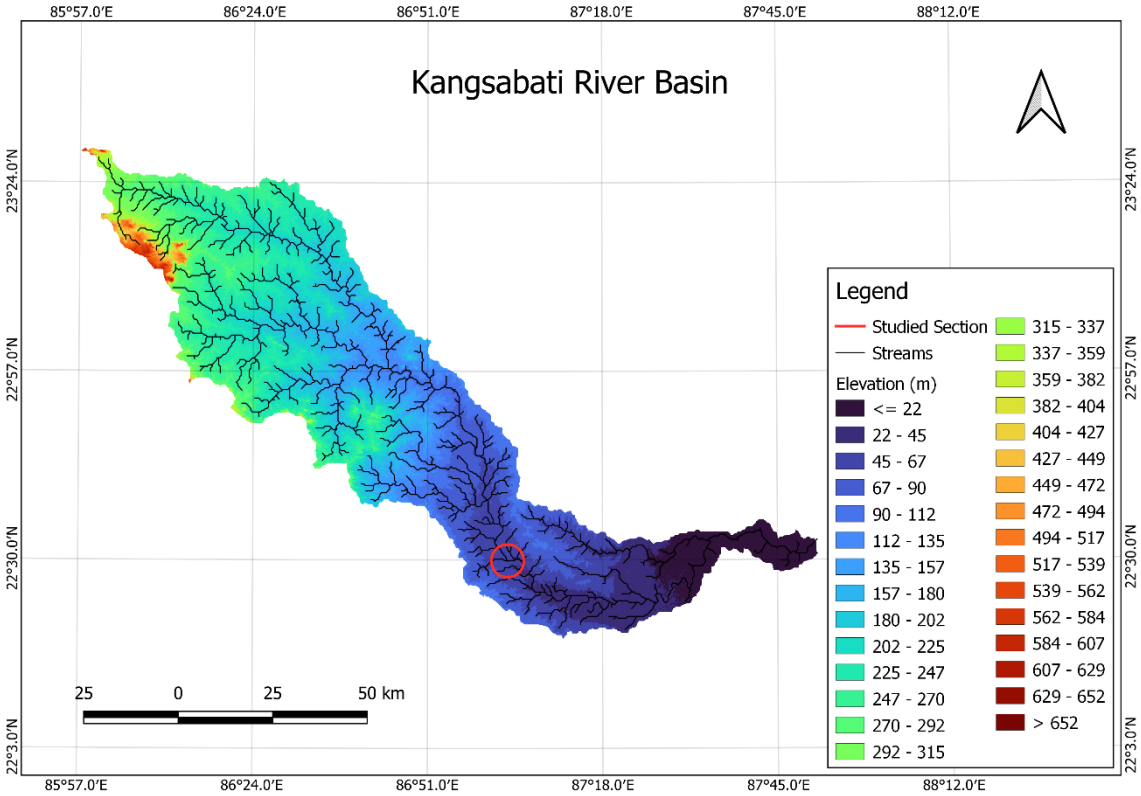

Figure 3.5: Kangsabati River Basin

3.3 Lithological Survey

The lithological investigation has been carried out to ascertain the subsurface strata of the river bed within the study area. Lithology of the Main Well and the three Observation Wells have been discussed along with the slim-bores which were drilled at selected locations for the gallery. Along the river Kangsabati, slim bores of 50 mm diameter up to 20 m depth were drilled in the selected locations. The borehole module of Starter 5.8 software has been used to visualize the borehole lithology created from drilling logs. Depth of the drilled slim bores ranges from 6.5 to 13 m. Lithologs obtained in 7 locations to show vertical transitions for the present study along with their lateral persistence.

The positions of the all the wells and slim-bore are shown in the map in Figure 3.6. The infiltration gallery is proposed to laid at the positions from B1 (position of collector well) to both at upstream towards B U/S and downstream towards B D/S.

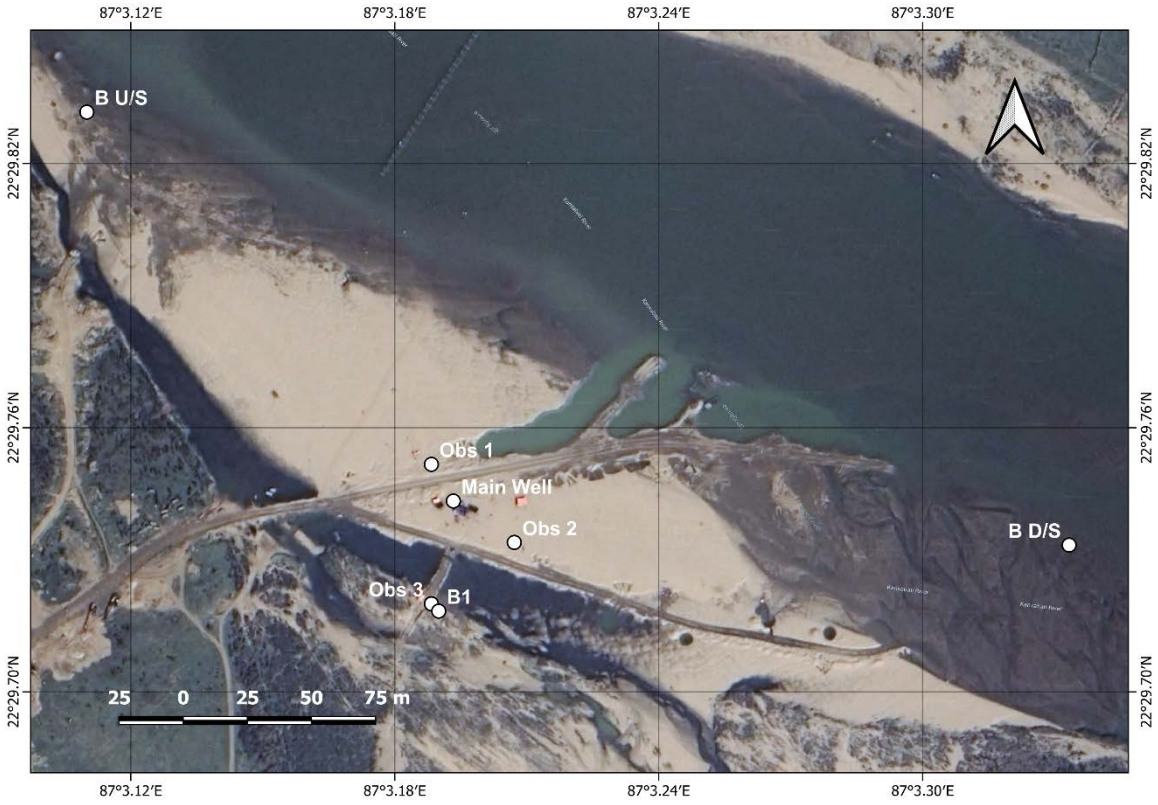

Figure 3.6: Position of Wells

3.3.1 Lithology of Main Well

The bore-hole column deposits (4-6 m) constitute coarse grained, moderately to well sort dark yellowish ochre siliciclastic sand with organic debris. The sediment dominantly consists of small clast by volume (30%). The quartz clasts are monocrystalline and dominantly angular to sub-angular shaped and feldspar clasts are tabular in shape. Clasts are variable in size. This is also texturally immature, smaller clasts are rounded in the shape of the detrital grains and contain 30% of the matrix.

3.3.2 Lithology of Observation Well 1

The bore-hole column deposits (6-8 m) constitute very coarse grained, poorly sorted dark yellowish coloured siliciclastic gravel with a muddy matrix. The sediment dominantly consists of large clast by volume (30%). The sediment is polymictic, as it contains pebbles of quartz, feldspar, chlorite and lithic fragments of muscovite, biotite, paragneiss, granite, granitic gneiss, chloritic schist. The quartz clasts are monocrystalline and polycrystalline and dominantly angular to sub-angular shaped and feldspar clasts are tabular in shape. The other clasts are tabular, elliptical or spherical in shape. Other constituents are rare but few cherts and heavy minerals also have been found. Clasts are variable in size. Due to variation in grain size, the sediment is poorly sorted.

This is also texturally immature i.e. there is poorly sorting, smaller clasts are rounded in the shape of the detrital grains and contain 30% of the matrix. In every successive bed system variation in clast composition between the successive beds reflects a contribution from crystalline rocks, like meta-sediments, paragneiss, gneissic granite, granite etc.

3.3.3 Lithology of Observation Well 2

The bore-hole column deposits (0-1 m) constitute very coarse grained, poorly sorted dark yellowish coloured siliciclastic gravel with a muddy matrix. The sediment dominantly consists of large clast by volume (30%). The sediment is polymictic, as it contains pebbles of quartz, feldspar, chlorite and lithic fragments of muscovite, biotite, magnetite, granite, granitic gneiss, chloritic schist. The clasts are tabular, elliptical or spherical in shape. Other constituents are rare but few cherts and heavy minerals also have been found. Clasts are variable in size. Due to variation in grain size, the sediment is poorly sorted.

This is also texturally immature i.e. there is poorly sorting, smaller mud clasts are rounded in the shape of the detrital grains and contain 40% of the matrix.

3.3.4 Lithology of Observation Well 3

The bore-hole column deposits (0-10 m) constitute several successive beds. The 1st bed (0-1.5 m) is fine to medium grained, moderately sorted yellowish coloured siliciclastic sand. The 2nd bed (1.5-3 m) constitutes coarse grained, poorly sorted dark yellowish coloured siliciclastic sand with a muddy matrix. Sediment dominantly consists of large clast by volume (30%). The sediment is polymictic, as it contains pebbles of quartz, feldspar, chlorite and lithic fragments of muscovite, biotite, paragneiss, granite, granitic gneiss, chloritic schist. The quartz clasts are monocrystalline and polycrystalline and dominantly angular to sub-angular shaped and feldspar clasts are tabular in shape. The other clasts are tabular, elliptical or spherical in shape. Other constituents are rare but few cherts and heavy minerals also have been found. Clasts are variable in size. Due to variation in grain size, the sediment is poorly sorted.

The 3rd bed (3-4.5m) constitutes clayey to medium grained, poorly sorted dark grey coloured siliciclastic sand enriched with organic matter and small mud clasts. The clasts are angular, tabular, elliptical or spherical in shape. Clasts are variable in size. Due to variation in grain size, the sediment is poorly sorted.

The 4th bed (4.5-6 m) constitutes fine to medium grained, moderately sorted yellowish coloured siliciclastic sand exhibiting very few small quartz clasts. The quartz clasts are monocrystalline and polycrystalline and dominantly angular to sub-angular shaped and feldspar clasts are tabular in shape. The other clasts are tabular, elliptical or spherical in shape. Other constituents are rare but few cherts and heavy minerals also

have been found. Clasts are variable in size. Due to variation in grain size, the sediment is poorly sorted.

The 5th (6- 8 m) and 6th beds (8-10 m) constitute coarse grained, moderately sorted yellowish coloured siliciclastic sand. The sediment dominantly consists of large clast by volume (30%). The sediment is polymictic, as it contains pebbles of quartz, feldspar, chlorite and lithic fragments of muscovite, biotite, paragneiss, granite, granitic gneiss, chloritic schist. The quartz clasts are monocrystalline and polycrystalline and dominantly angular to sub-angular shaped and feldspar clasts are tabular in shape.

Figure 3.7: In-situ Borehole Sample for Main Well

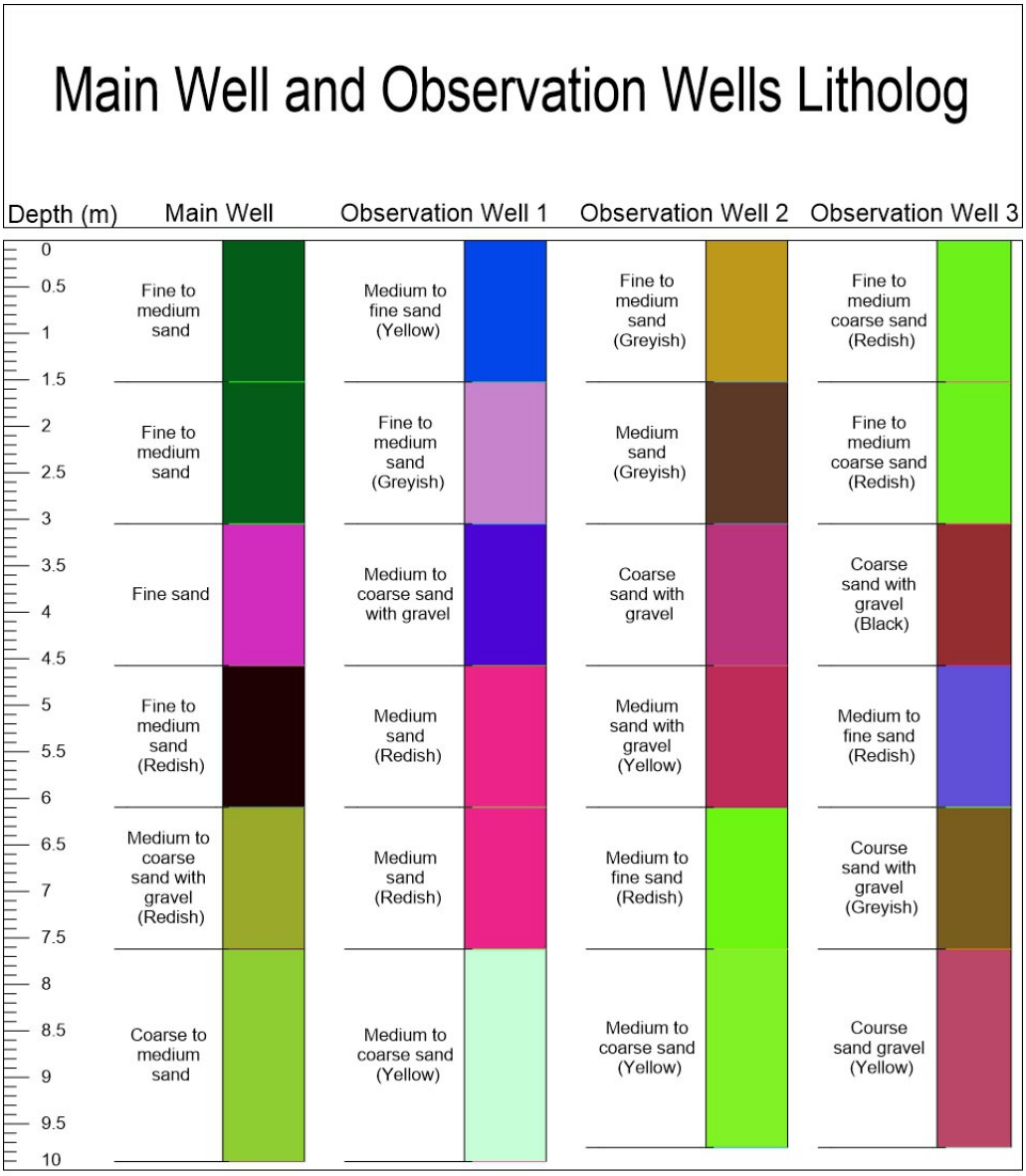

Figure 3.8: Lithological Details of Main Well & Observation Wells

3.3.5 Lithology of Slim-bore Upstream (B U/S)

The bore-hole column deposits (0-9 m) constitute several successive beds. The 1st bed (0-3 m) is coarse grained, poorly sorted dark brownish siliciclastic sand. The sediment consists of organic debris. The sediment contains quartz, feldspar, lithic fragments of muscovite, biotite, magnetite and heavy minerals. The quartz clasts are monocrystalline and polycrystalline and dominantly angular to sub-angular shaped and feldspar clasts are tabular in shape.

The 2nd bed (3-4.5 m) constitutes coarse grained, poorly sorted yellowish siliciclastic sand. The sediment dominantly consists of small clast by volume (30%). The sediment is polymictic, as it contains pebbles of quartz, feldspar, chlorite and lithic fragments of muscovite, biotite, paragneiss, granite, granitic gneiss, magnetite, heavy minerals, ferruginous globules. The quartz clasts are monocrystalline and polycrystalline

and dominantly angular to sub-angular shaped and feldspar clasts are tabular in shape. The other clasts are tabular, elliptical or spherical in shape. Clasts are variable in size. Due to variation in grain size, the sediment is poorly sorted.

The 3rd bed (4.5-6 m) constitutes very coarse grained, poorly sorted dark yellowish siliciclastic sand enriched with muddy matrix and mud clasts. The quartz clasts are monocrystalline and dominantly angular to sub-angular shaped and feldspar clasts are tabular in shape.

The 4th bed (6-8 m) constitutes very coarse grained, matrix supported poorly sorted yellow ochre coloured siliciclastic gravel enrich with profuse amounts of quartz clasts. The sediment dominantly consists of large clasts by volume (30%). The sediment is polymictic, as it contains pebbles of quartz, feldspar and lithic fragments of muscovite, biotite, paragneiss, granite, granitic gneiss. The quartz clasts are monocrystalline and polycrystalline and dominantly angular to sub-angular shaped and feldspar clasts are tabular in shape.

The 5th bed (8-9 m) constitutes coarse grained, poorly sorted dark brown siliciclastic gravel. The sediment dominantly consists of large clasts by volume (30%). The sediment is polymictic, as it contains pebbles of quartz, feldspar and lithic fragments of muscovite, biotite, paragneiss, granite, granitic gneiss, chlorite, chloritic schist. Other constituents are rare but few cherts and heavy minerals also have been found. The quartz clasts are monocrystalline and polycrystalline and dominantly angular to sub-angular shaped and feldspar clasts are tabular in shape.

In every successive bed system variation in clast composition between the successive beds reflects a contribution from crystalline rocks, like meta-sediments, paragneiss, gneissic granite, granite, chlorite and chloritic schist etc.

3.3.6 Lithology of Slim-bore Downstream (B D/S)

The bore-hole column deposits (0-9 m) constitute several successive beds. The 1st bed and 2nd bed (0-4.5 m) are medium grained, poorly sorted whitish siliciclastic sand. The sediment consists of rock fragments. The sediment contains quartz, feldspar, lithic fragments of muscovite, biotite, magnetite and heavy minerals. The quartz clasts are monocrystalline and polycrystalline and dominantly angular to sub-angular shaped and feldspar clasts are tabular in shape.

The 3rd bed (4.5-6 m) constitutes coarse grained, poorly sorted whitish siliciclastic sand. The sediment dominantly consists of small mud clast by volume (30%). The sediment is polymictic, as it contains pebbles of quartz, feldspar and lithic fragments of muscovite, biotite, paragneiss, granite, granitic gneiss, magnetite, heavy minerals, ferruginous globules. The quartz clasts are monocrystalline and polycrystalline and dominantly angular to sub-angular shaped and feldspar clasts are tabular in shape. The other clasts are tabular, elliptical or spherical in shape. Clasts are variable in size. Due to variation in grain size, the sediment is poorly sorted.

The 4th (6-8 m) and 5th beds (8-9 m) constitute very coarse grained, poorly sorted dark brown siliciclastic gravel enriched with profuse amounts of quartz clasts. The quartz clasts are monocrystalline and polycrystalline and dominantly angular to sub-angular shaped and feldspar clasts are tabular in shape.

In every successive bed system variation in clast composition between the successive beds reflects a contribution from crystalline rocks, like metasediments, paragneiss, gneissic granite, granite etc. The clast composition is variable, indicating contribution to the sediment budget from both the felsic igneous and metasedimentary sources.

Note: The lithology of Slim-bore B1 is analogous to the lithology of Observation Well 3, as they are very close to each other. However few variation of constituents are always there in the bed aquifer. The lithological details of the Slim-bores are shown in Figure 3.9.

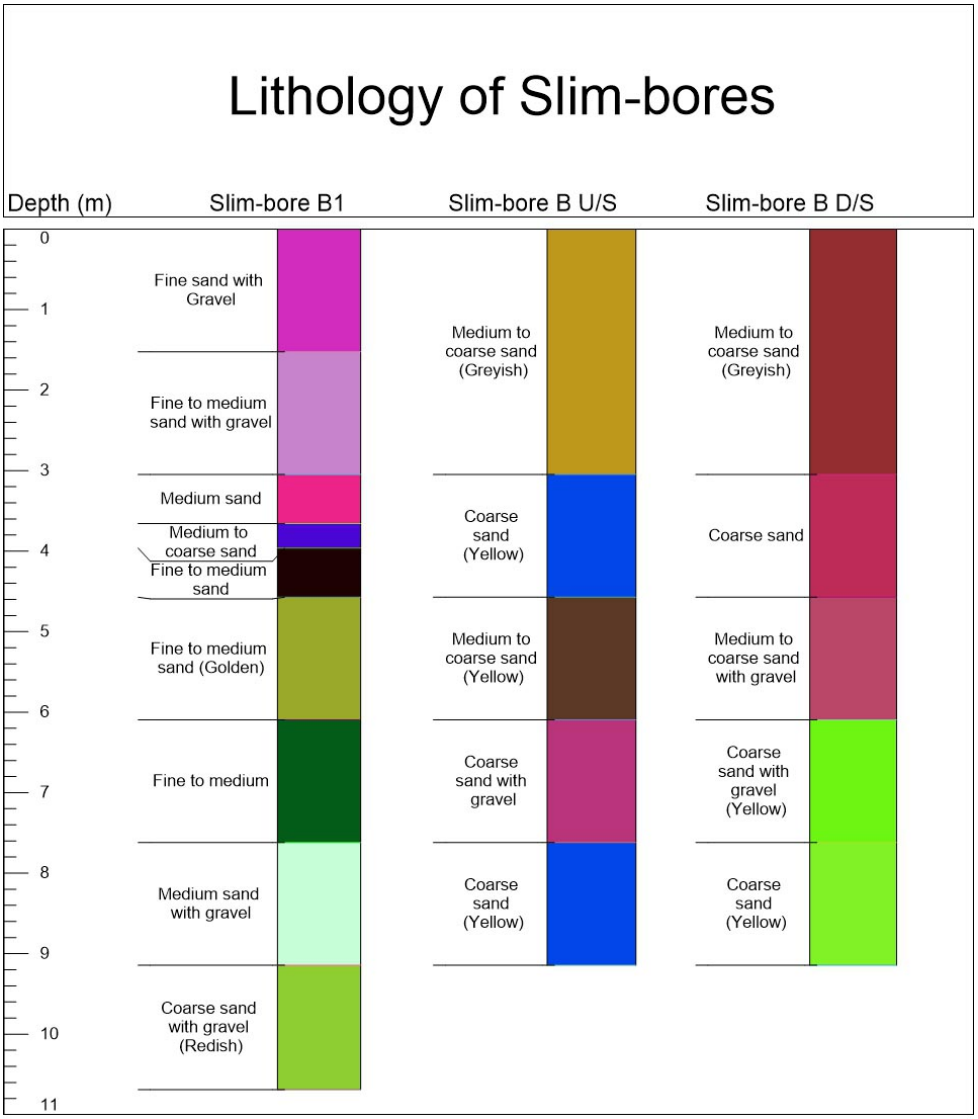

Figure 3.9: Lithological Details of Slim-bores

Chapter 4 Conceptualization of Groundwater Hydraulics and Subsurface Water intake structure Design

4.1 Hydrological Cycle

Water occurs on the earth in all its three states viz. liquid, solid and gaseous, and in various degree of motion. Evaporation of water from water bodies such as oceans and lakes, formations and movements of clouds, rain and snowfall, streamflow and groundwater movement are some examples of the dynamic aspects of water. The various aspects of water related to the earth can be explained in terms of a cycle known as the Hydrological cycle.

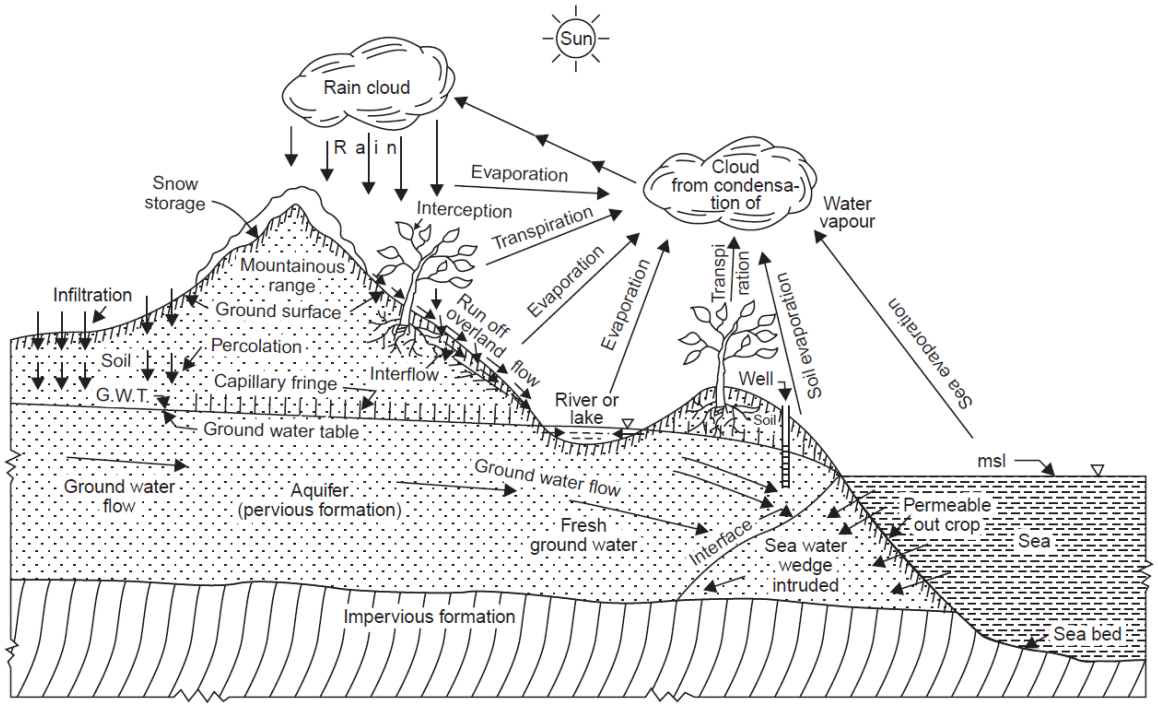

Figure 4.1: Schematic illustration of the hydrological cycle (source: Raghunath 2006)

The hydrological cycle is the basic purification mechanism for water on Earth as any water constituents are left behind during the phase change from liquid water to water vapour. For billions of years, this process supplied the land surface with freshwater, which was and is the basis for life. The precipitated water dissolved minerals on its way through the hydrological compartments to the oceans and thereby gradually increased ocean salinity. Reliable and adequate supply of clean freshwater is essential to the survival of humankind as well as to the maintenance of terrestrial biotic systems worldwide. However, the rapidly growing human population increasingly stresses available water resources (Ferguson and Maxwell 2012).

4.2 Water-Budget Equation

A water-budget, hydrologic budget or water balance is a measurement of continuity of the flow of water, which holds true for any time interval and apply to any size area ranging from local-scale areas to regional-scale areas or from any drainage area to the earth as a whole. The hydrologists usually must consider an open system, for which the quantification of the hydrologic cycle for that system becomes a mass balance equation in which the change of storage of water (dS/dt) with respect to time within that system is equal to the inputs (I) to the system minus the outputs (O) from the system.

Considering an open system, the water budget equation can be expressed for the surface water system and the groundwater system in units of volume per unit time separately, or for a given time period and area, in depth.

Surface Water System Hydrologic Budget

$$P + Qin - Qout + Qg - Es - Ts - I = \Delta Ss \qquad \textbf{Eqn 4.1}$$

where, P is the precipitation, Q_{in} is the surface water flow into the system, Q_{out} is the surface water flow out of the system, Q_g is the groundwater flow into the stream, E_s is the surface evaporation, T_s is the transpiration, I is the infiltration and ΔS_s is the change in water storage of the surface water system.

Groundwater System Hydrologic Budget

$$I + Gn - Gout - Qg - Eg - Tg = \Delta Sg \qquad \textbf{Eqn 4.2}$$

where, G_{in} is the groundwater flow into the system, G_{out} is the groundwater flow out of the system and ΔS_g is the change in groundwater storage. The evaporation, E_g and the transpiration T_g can be significant if the water table is near the ground surface.

System Hydrologic Budget

The system hydrologic budget is developed by adding the above two budgets together:

$$P - (Qout - Qin) - (Es + Eg) - (Ts + Tg) - (Gout - Gin) = \Delta(Ss + Sg) \qquad \textbf{Eqn 4.3}$$

Using net mass exchanges, Eqn 4.3 can be expressed as

$$P - Q - G - E - T = \Delta S \qquad \textbf{Eqn 4.4}$$

Hydrologic budgets can be used for numerous studies related to groundwater including

- Estimating groundwater exchange with lakes.
- Estimating surface water and groundwater interaction.
- Computing recharge from a well-hydrograph data.

4.3 Water Demand

A water-supply system must satisfy the water demand of the population being served and the fire flows needed to protect life and property, while providing due consideration to the proximity of the service area to the source(s) of water. The water demand at the end of the design life is usually the basis for system design, and so water-demand forecasting is generally required.

There are a variety of methods that are used to forecast water demand, and the appropriate method depends on the particular situation. Most forecasting methods can be categorized as per-capita models, extrapolation models, disaggregation models, multiple-regression models, and land-use models. Brief descriptions of these models are given below.

- Per-capita Models: These models simply estimate the average consumption per capita (i.e., per person) and multiply this per-capita consumption by a projected population at the end of the design life to estimate the average total demand. In some cases, a trend is also applied to the per-capita consumption. Per-capita models produce satisfactory results as long as the population forecast is accurate, and the consumer mix does not change substantially.
- Extrapolation Models: Extrapolation models plot the annual or monthly water consumption as a function of time or population and then extrapolate this relationship into the future. This approach can be applied separately to various water-use components, such as residential and non-residential use.
- Disaggregation Models: Water use is disaggregated into basic segments such as single-family residential, multifamily residential, institutional, commercial, industrial, and public facilities. The consumption per unit within each segment is estimated and multiplied by the projected number of units at the end of the design period.
- Multiple-Regression Models: These empirical models relate the water demand to a variety of independent variables such as population, number of households or dwelling units, household income, lot sizes, land use, employment, and various weather variables.
- Land-Use Models: These models base their water-use forecasts on the projected uses of residential, commercial, industrial, and public lands within the service area. Water-use projections are developed for each land-use segment.

The development of water-demand forecast models involves highly specialized activities and usually require close coordination with the local planning department. The per-capita model which is majorly used in India to illustrate the methodology for developing and applying a water-demand forecast model.

4.3.1 Estimation of Per Capita Demand

Estimation of the water demand using a per-capita model requires prediction of population, development, and per-capita water usage in the service area at the end of the design period. The average water demand from various sectors of the population is usually taken as equal to the predicted population in that sector multiplied by the per-capita demand in that sector.

There are usually several categories (sectors) of water demand within any populated area, and these sources of demand can be broadly grouped into residential, commercial, industrial, and public. Residential water use is associated with houses and apartments where people live; commercial water use is associated with retail businesses, offices, hotels, and restaurants; industrial water use is associated with manufacturing and processing operations; and public water use includes governmental facilities that use water. Large industrial requirements are typically satisfied by sources other than the public water supply.

The recommended values for domestic and non-domestic purposes as per IS 1172:1993 are given below:

Table 4.1: Recommended per capita water demand for domestic and non-domestic purposes (source: IS 1172:1993)

Sl. No.	Classification of towns/cities	Recommended minimum water supply levels (lpcd)
1	For communities with population up to 20000 and without flushing system a) Water supply through stand post. b) Water supply through house service connection.	 40 70-100
2	For communities with population 20000 to 100,000 together with full flushing system.	100-150
3	For communities with population above 100000 together with full flushing system.	150-200

Note: As per Ministry of Housing and Urban Affairs, GOI, 135 litre per capita per day (lpcd) has been suggested as the benchmark for urban water supply. For rural areas, a minimum service delivery of 55 lpcd has been fixed under Jal Jeevan Mission, which may be enhanced to higher level by states.

Table 4.2: Typical Distribution of per capita water demand in a city

Sl. No.	Use	Demand (lpcd)
1	Domestic Water Demand	200
2	Industrial water demand	50
3	Civic or public use	10
4	Waste, theft etc.	55
5	Commercial use	20
	Total	335 lpcd

Note: The total per capita demand can range between 100 to 360 lpcd. The various other factors affecting the per capita demand are needed to be considered as per the study area.

4.3.2 Population Forecasting

Water supply scheme involves huge and costly structures which cannot be easily replaced or increased in their capacity. Therefore they are purposely made larger, so that it can satisfy the need of a community for a reasonable period of time (design period). The design period for the underground intake structures as recommended by the GOI manual is 30 years. Therefore population forecasting plays an important role towards the serviceability of the intake structures to run smoothly for the upcoming years.

Various methods of population forecasting based on laws of probability and with assumption that the factors which are responsible for population increase in the past will continue in the future with the same intensity.

- **Arithmetic increase method:** In this method, per decade increasing population is assumed to be constant. It is generally suited for old and settled communities. The average increase in population is calculated from the previously available census data.
- **Geometric increase method:** In this method, the percentage increase in growth rate is assumed to be constant. And the increase is compounded over the existing population every decade. This method is also known as uniform increase method and it is suitable for new younger cities expanding at a very fast rate.
- **Incremental increase method:** This method is basically an extension of arithmetic method of analysis where no assumption is made in the per decade growth rate. To estimate the future population, the average increment over the increase is calculated, and the rate is progressively increased or decreased depending upon whether the average increment over the increase is positive or negative.
- **Decreasing rate of growth method:** This method is applicable for the communities where the growth is showing a downward trend as population is approaching its saturation value. In this method the average decrease in percentage increase is

calculated and subtracted from latest percentage increase for each successive decade.

- **Simple graphical method:** In this method, graph is plotted between the population and the corresponding year for the available census data. The obtained graph can be extended to get the population of the required year. This method is approximate and the accuracy is depended on the skill and experience of the person dragging the curve.

Population forecasting is not limited to these methods only. There are some other advanced and more detailed method of population forecasting like comparative graph method, master planning method or zoning method, ratio method or apportionment method and logistic curve method.

4.3.2.1 Logistic Curve Method

In an ideal environment, populations grow at an exponential rate. The growth curve of these populations is smooth and becomes increases steeply over time. However, exponential growth is not possible because of factors such as limitations in food, competition for other resources, disease etc. Populations eventually reach the carrying capacity or saturation capacity of the environment, causing the growth rate to slow nearly to zero. This produces an S-shaped curve of population growth known as the logistic curve.

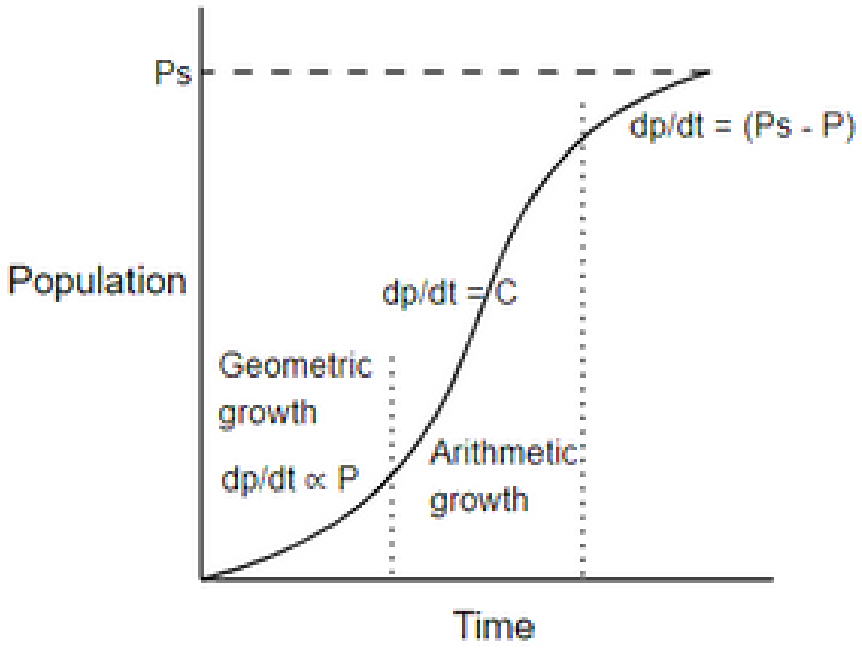

Figure 4.2: Logistic Curve of Population Growth

As discussed, this method uses the logistic curve of population growth. Therefore, it uses the equation of the logistic curve to directly predict the population. Equation of the logistic curve is given as

$$P = \frac{P_s}{1 + me^{nt}} \qquad \text{Eqn 4.5}$$

where, $m = \frac{P_s - P_0}{P_0}$

$$n = \frac{2.303}{t_1} \log\left(\frac{P_0(P_s - P_1)}{P_1(P_s - P_0)}\right)$$

$$P_s = \frac{2P_0P_1P_2 - P_1^2(P_0 + P_2)}{P_0P_2 - P_1^2}$$

P_0 = Population at t_0 year

P_1 = Population at t_1 years

P_2 = Population at t_2 years

$t_2 = 2t_1$

4.4 Groundwater & Hydraulic Properties

Groundwater is the water found underground in the cracks and spaces in soil, sand and rock. It is stored in and moves slowly through geologic formations of soil, sand and rocks called aquifers. It is derived from precipitation and recharge from surface water. It is the water that has infiltrated into the earth directly from precipitation, recharge from streams and other natural water bodies and artificial recharge due to action of man.

All earth materials, from soils to rocks have pore spaces. Although these pores are completely saturated with water below the water table, from the groundwater utilization aspect only such material through which water moves easily and hence can be extracted with ease are significant. An aquifer is a saturated formation of earth material which not only stores water but yield it in sufficient quantity. Thus, an aquifer transmits water relatively easily due to its high permeability. Unconsolidated deposits of sand and gravel form good aquifers.

4.4.1 Specific Yield

The volume of water, expressed as a percentage of the total volume of the saturated aquifer, that can be drained by gravity is called the specific yield S_y and the volume of water retained by molecular and surface tension forces, against the force of gravity, expressed as a percentage of the total volume of the saturated aquifer, is called specific retention S_r and corresponds to field capacity.

$$\text{Porosity (n)} = \text{Specific yield } (S_y) + \text{Specific retention } (S_r) \qquad \text{Eqn 4.6}$$

Specific yield is the water removed from unit volume of aquifer by pumping or drainage and is expressed as percentage volume of aquifer. Specific yield depends upon

grain size, shape and distribution of pores and compaction of the formation. The variation of porosity with S_y and S_r is shown in Figure 4.3.

4.4.2 Storage Coefficient

Storage coefficient (or Storativity) of an aquifer is the volume of water discharged from a unit prism, i.e., a vertical column of aquifer standing on a unit area ($1m^2$) as water level (piezometric level in confined aquifer—artesian conditions) falls by a unit depth (1m). For unconfined aquifers (water table conditions) the storage coefficient is the same as specific yield. The storage coefficient for confined aquifers ranges from 0.00005 to 0.005 and for water table aquifers 0.05 to 0.30.

Under artesian conditions, when the piezometric surface is lowered by pumping, water is released from storage by the compression of the water bearing material (aquifer) and by expansion of the water itself'. Thus, the coefficient of storage is a function of the elasticity of water and the aquifer skeleton and is given by (Jacob, 1950) as

$$S = \gamma_w \, b \, (\alpha + n\beta) \qquad \textbf{Eqn 4.7}$$

where, S= coefficient of storage, fraction; It = porosity of aquifer, fraction; b= saturated thickness of aquifer (m); γ_w = units weight of water (9810 N/m^3); $\beta = \frac{1}{K_w}$, reciprocal of the bulk modulus of elasticity of water $K_w = 2.1 \times 10^9$ N/m^2; and $\alpha = \frac{1}{E_s}$, reciprocal of the bulk modulus of elasticity of aquifer skeleton.

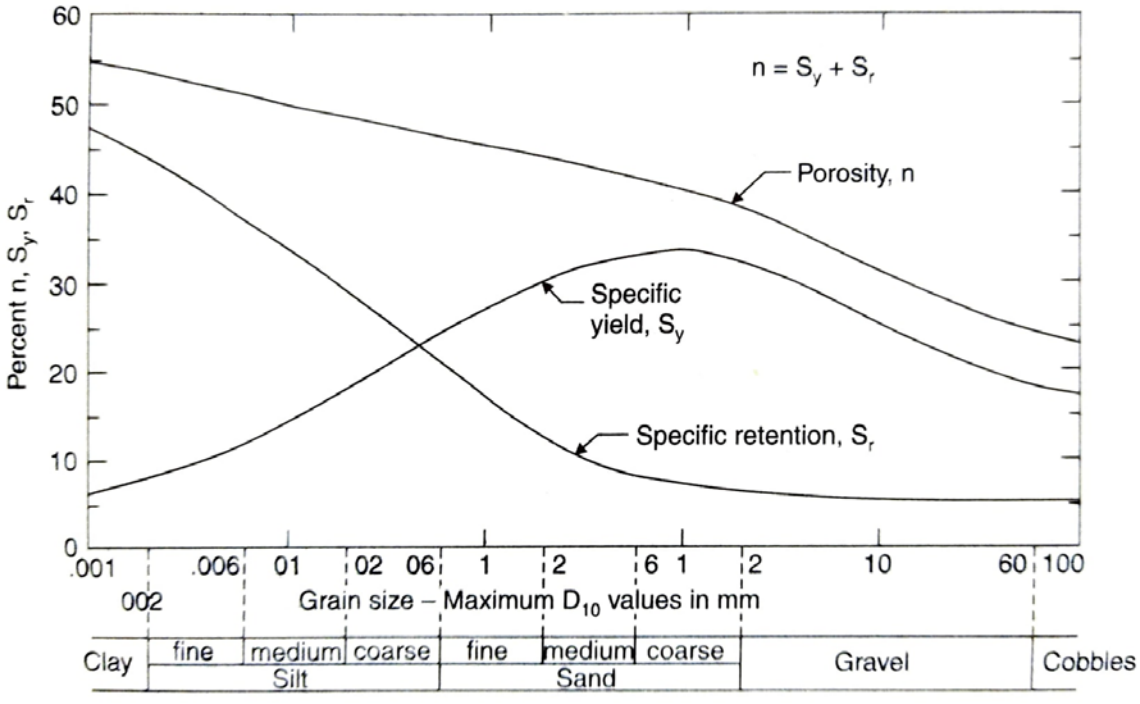

Figure 4.3: Variations of n, S_y and S_r with grain size

4.4.3 Transmissivity

The coefficient of transmissivity (T) is the discharge through unit width of aquifer for the fully saturated depth under a unit hydraulic gradient and is usually expressed as 1lpd/m or m^2/sec. It is the product of field permeability (K) and saturated thickness of the aquifer (b); $T = Kb$ and has the dimensions L^2/T.

Permeability (K) is the ability of a formation to transmit water through it pores when subjected to a difference in bead. It can be defined as the flow per unit cross-sectional area of the formation when subjected to a unit hydraulic head per unit length of flow (i.e. per unit hydraulic gradient) and has the dimension of velocity, i.e, L/T.

For a soil sample the permeability is different for all three axes defined as Kx, Ky, Kz. If the aquifer is isotropic with respect to permeability, i.e, Kx = Ky = Kz = K

From Darcy's law, $u = -K_x \frac{\partial h}{\partial x}$, $v = -K_y \frac{\partial h}{\partial y}$, $w = -K_w \frac{\partial h}{\partial w}$

Permeability can be related to storage coefficient as, for anisotropic aquifer.

$$K_x \frac{\partial^2 h}{\partial x^2} + K_y \frac{\partial^2 h}{\partial y^2} + K_z \frac{\partial^2 h}{\partial z^2} = (\alpha + n\beta)\gamma \frac{\partial h}{\partial t} \qquad \textbf{Eqn 4.8}$$

$$K\left(\frac{\partial^2 h}{\partial x^2} + \frac{\partial^2 h}{\partial y^2} + \frac{\partial^2 h}{\partial z^2}\right) = (\alpha + n\beta)\gamma \frac{\partial h}{\partial t}$$

Or,
$$\frac{\partial^2 h}{\partial x^2} + \frac{\partial^2 h}{\partial y^2} + \frac{\partial^2 h}{\partial z^2} = (\alpha + n\beta)\frac{\gamma b}{Kb}\frac{\partial h}{\partial t}$$

Defining the coefficient of storage as, $S = \gamma_w b (\alpha + n\beta)$

Transmissivity of the aquifer, $T = Kb$ and $\nabla^2 h = \frac{\partial^2 h}{\partial x^2} + \frac{\partial^2 h}{\partial y^2} + \frac{\partial^2 h}{\partial z^2}$

$$\therefore \nabla^2 h = \frac{S}{T}\frac{\partial h}{\partial t} \qquad \textbf{Eqn 4.9}$$

which is the equation for the piezometric head for unsteady flow in a saturated, confined, isotropic aquifer. For steady flow, the equation becomes

$$\nabla^2 h = 0 \qquad \textbf{Eqn 4.10}$$

The coefficient of storage (S) is defined as the volume of water released from storage from a vertical column of aquifer of unit cross-sectional area under a unit decline of piezometric head. The first term ($\alpha\gamma b$) gives the fraction attributable to the compressibility of the aquifer skeleton and the second term ($n\beta\gamma b$) that attributable to the expansibility of water. In water table aquifers the coefficient of storage is given by (Hantush, 1964)

$$S = S_y + (\alpha + n\beta)\gamma b \qquad \textbf{Eqn 4.11}$$

4.4.4 Radius of Influence

The Radius of Influence is defined as the maximum distance at which the drawdowns can be detected. Generally static water table can be considered as horizontal. After the pumping operation is done, due to the radial flow into the well through the aquifer the water table assumes a conical shape called cone of depression. The areal extent of the cone of depression is called the areal influence and its radial extent is the radius of influence.

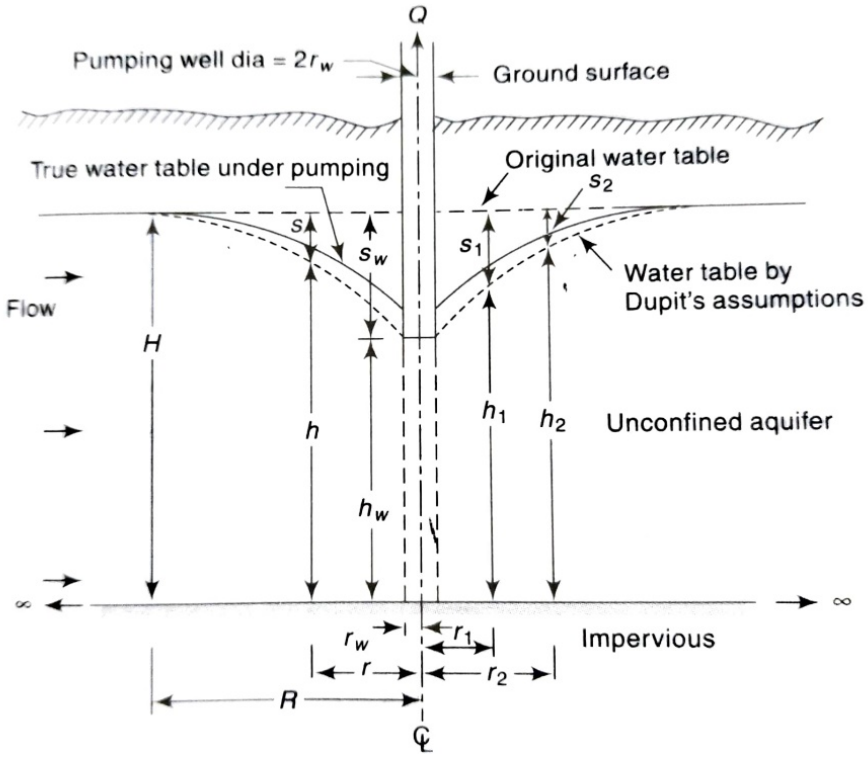

Figure 4.4: Radial flow to a well in an unconfined aquifer

For the well, considered in Figure 4.4, at any radial distance r, the velocity of radial flow V_r into the well is

$$V_r = K\frac{dh}{dr}$$

for steady flow, by continuity

$$Q = (2\pi rh)V_r = 2\pi rKh\frac{dh}{dr}$$

$$\text{or,} \quad \frac{Q}{2\pi K}\frac{dr}{r} = h\,dh$$

on integrating between limits r_w and R where the water table depth are h_w and H,

$$Q = \frac{\pi K(H^2 - h_w^2)}{\ln\frac{R}{r_w}}$$

now, as the drawdown is very small for practical cases as compared to the thickness of aquifer, and T = KH, we have

$$Q = \frac{2\pi T s_w}{\ln \frac{R}{r_w}} \qquad \textbf{Eqn 4.12}$$

4.4.5 Neuman's method for Drawdown

The response of an unconfined aquifer to pumping is complicated. Once a cone of depression forms, it naturally decreases the aquifer thickness and transmissivity because the upper boundary of the aquifer is the water table. Also, the way in which water comes out of storage in the aquifer changes with time. At early time, when the well is first turned on, water is released from storage due to compression of the matrix and expansion of the water.

As Pumping continues, water comes from the slow gravity drainage of water from pores as the water table falls near the well. The pattern of drawdown depends on the vertical and horizontal hydraulic conductivity and the thickness of the aquifer. Once this delayed drainage begins, drawdown data deviate from the Theis curve. Flow in the aquifer is mainly radial, and drawdown versus time data again fall on a Theis-type curve. The storativity of the aquifer now is the same as the specific yield (S_y). The specific yield is the ratio of the volume of water that drains from a rock or sediment by gravity to the volume of the rock or soil.

Methods for determining hydraulic parameters in an unconfined aquifer were first introduced by Boulton (1954, 1955, 1963). Since then they have been improved through the efforts of numerous investigators. In this section, we examine three solutions that differ from each other as a function of where in the aquifer the drawdown is calculated (Figure 4.5).

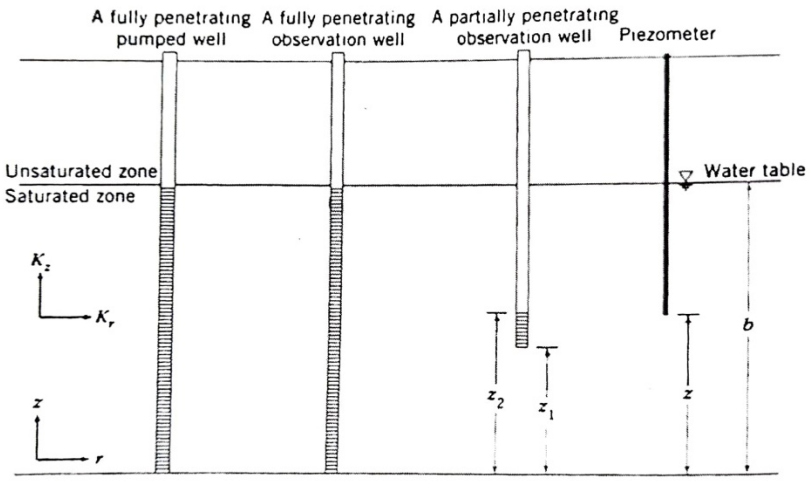

Figure 4.5: A fully penetrating pumping well along with observation wells in unconfined aquifer.

For fully penetrating pumping and observation wells in an unconfined aquifer (Figure 4.5), drawdown is given as

$$s = \frac{Q}{4\pi T} W(u_A, u_B, \beta) \qquad \textbf{Eqn 4.13}$$

where $W(u_A, u_B, \beta)$ is the well function for the unconfined aquifer, s is the drawdown, Q is the pumping rate, and T is the transmissivity (Neuman, 1975). The dimensionless parameters u_A, u_B, β are defined as

$$\frac{1}{u_A} = \frac{Tt}{Sr^2} \quad \text{(For early-time data)}$$

$$\frac{1}{u_B} = \frac{Tt}{S_y r^2} \quad \text{(For later data)}$$

$$\beta = \frac{K_z r^2}{K_r b^2}$$

where b is the initial saturated thickness, K_r is the hydraulic conductivity in the radial horizontal direction, and K_z is the vertical hydraulic conductivity.

When drawdown is calculated for a piezometer in an unconfined aquifer that is being pumped at a constant rate by a fully penetrating well, the solution depends on where in the aquifer the piezometer is completed. Close to the well, head changes vertically because there is a downward flow component. This analytical solution is

$$s = \frac{Q}{4\pi T} W(u_A, u_B, \beta, z_D)$$

where $z_D = z/b$, z is the coordinate of the piezometer and b is the thickness of the aquifer. The drawdown in an observation well is the average of the analytical solution along with the screen is expressed as,

$$W(u_A, u_B, \beta, z_{D1}, z_{D2}) = \frac{Q}{4\pi T} \frac{1}{z_{D2} - z_{D1}} \int_{z_{D1}}^{z_{D2}} W(u_A, u_B, \beta, z_D) dz_D \qquad \textbf{Eqn 4.14}$$

Evaluation of Neuman's analytical solution requires a large amount of computational time. To improve the efficiency and accuracy of the calculation it is further simplified into the Straight Line Method.

4.4.5.1 The Straight Line Method

Neuman illustrated this method, which is a simpler version to determine the hydraulic parameters of an unconfined aquifer by straight line fits to early and late time drawdown data. The method is summarized as,

1. Plot values of drawdown versus time on semi-log graph paper (Figure 4.6).

2. From the late-time segment of the s-log(t) curve, the transmissivity and specific yield of an unconfined aquifer are determined as,

$$T = \frac{2.3Q}{4\pi\Delta s} \qquad \textbf{Eqn 4.15}$$

$$S_y = \frac{2.25Tt_{0y}}{r^2} \qquad \textbf{Eqn 4.16}$$

3. From the early-time segment of the s-log(t) curve, the transmissivity and Storativity (same as specific yield for early time segment) of an unconfined aquifer are determined as,

$$\mathrm{T} = \frac{2.3\mathrm{Q}}{4\pi\Delta\mathrm{s}} \qquad \textbf{Eqn 4.15}$$

$$S = \frac{2.25Tt_{0s}}{r^2} \qquad \textbf{Eqn 4.17}$$

where, Δs = Differential drawdown,

r = Radial distance from Main Well,

t_{0y}, t_{0s} = Time at zero drawdown.

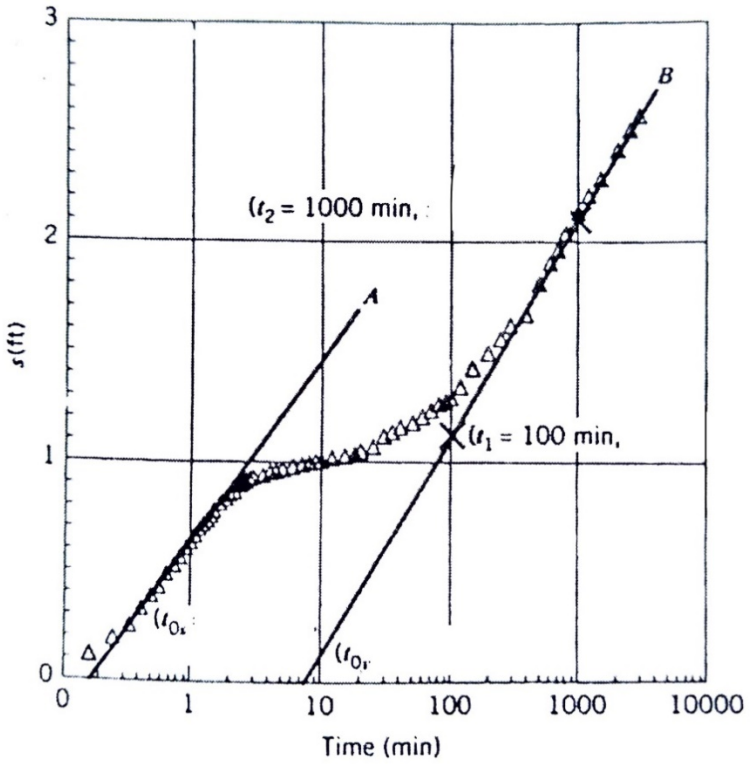

Figure 4.6: Drawdown vs Time plotted on semi log scale

Figure 4.6 shows the three types of drawdown responses. At an early time, the aquifer behaves as though it is confined with data falling along a straight line. At some intermediate time, it deviates from this straight line due to delayed gravity drainage. At a late time, data again follow a straight line as the aquifer exhibits a Theis-type response with S equivalent to S_y.

4.4.6 Theis Recovery

A well is pumped at a constant rate Q, the pumping is stopped after a time t_1 and it is desired to compute the residual drawdown s after a time t′ since pumping stopped. The recovery of piezometric head can be determined by considering a negative discharge for the time t′.

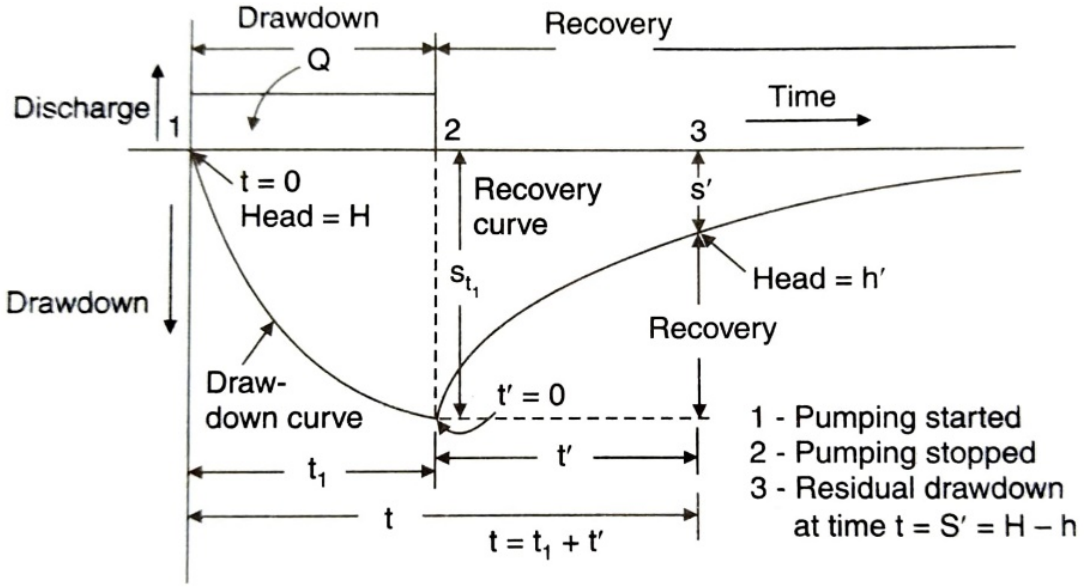

Figure 4.7: Drawdown and Recovery of GWL in the vicinity of a pumping well.

For small r and large t′, and the residual drawdown s after time $t_1 + t' = t$ since pumping started is obtained as,

$$s = \frac{2.3Q}{4\pi T}\log_{10}\frac{2.25Tt}{r^2S} - \frac{2.3Q}{4\pi T}\log_{10}\frac{2.25Tt'}{r^2S}$$

$$\text{or,} \qquad s = \frac{2.3Q}{4\pi T}\log_{10}\left(\frac{t}{t'}\right)$$

In Theis recovery method, the residual drawdowns in a pumped well or a nearby observation well are measured at different time intervals after pumping is stopped. From a semi-log plot of s vs t/t', the transmissivity T can be obtained as

$$T = \frac{2.3Q}{4\pi\Delta s} \qquad \textbf{Eqn 4.18}$$

where, Δs is the residual drawdown per log cycle of time t/t'.

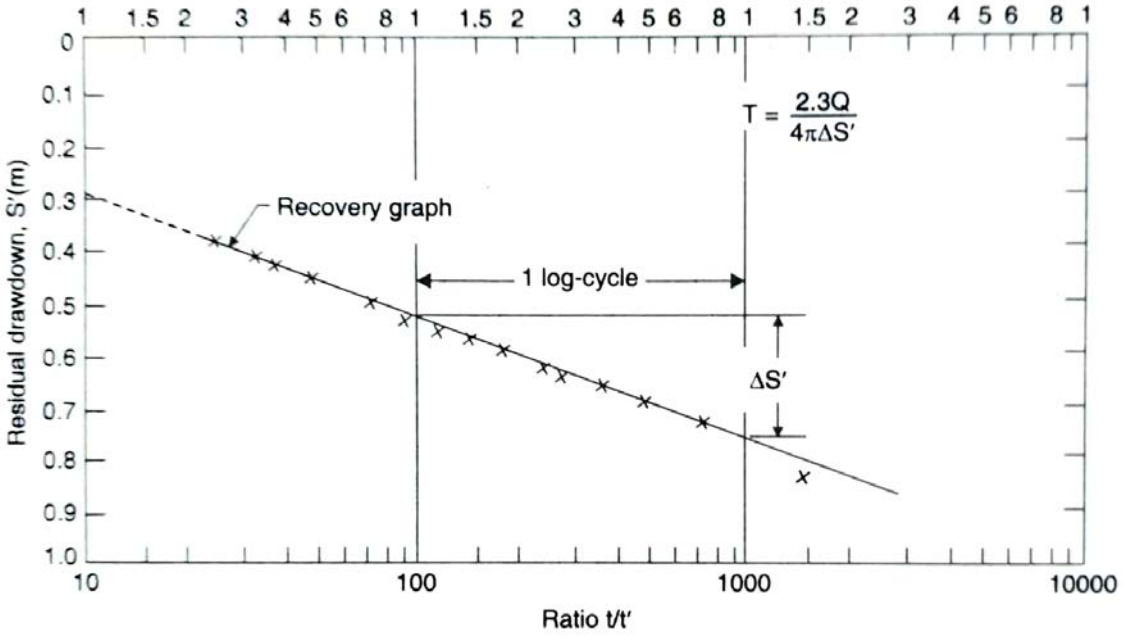

Figure 4.8: Time-drawdown Curve: Theis Recovery

The storage coefficient S can be determined from the value of drawdown at the time the pumping was stopped. S can also be determined from the time-drawdown plot of the pumping data. If s_t is the observed drawdown, when pumping stopped then S can be calculated using,

$$s = \frac{2.3Q}{4\pi T} log_{10} \frac{2.25Tt_1}{r^2 S} \qquad \textbf{Eqn 4.19}$$

4.5 Infiltration Galleries

Infiltration galleries are horizontal perforated or porous pipes which open joints, surrounded by a gravel filter envelop laid in a permeable aquifer with a high water table and a continuous recharge with a perennial flow. Infiltration galleries are usually laid parallel to river beds at depths of 3m to 6m for intercepting and collecting groundwater by gravity flow or across the river bed [18]. Infiltration galleries are used to encourage and accelerate the process of groundwater recharge by allowing water to naturally infiltrate the river bed material. Gallery systems harvest river water through a network of collection pipes installed under or beside the river bed. The horizontal pipes may be vitrified clay, brick, or concrete of 0.5 to 1.5m diameter, set in a trench across the aquifer well below the lowest permeable water table, and packed in granite chips around the concrete pipes to fine gravel against the aquifer material, so that clear water percolates with low entrance velocities.

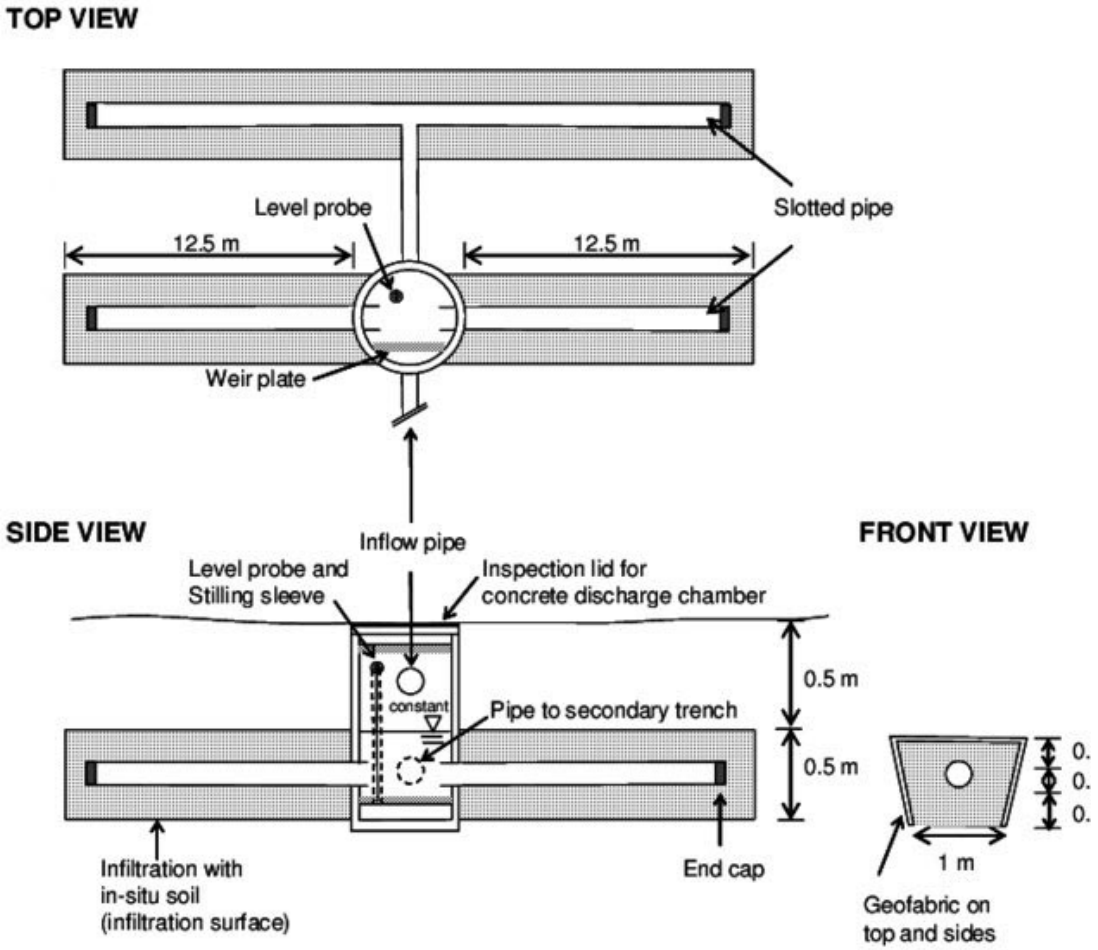

Figure 4.9: Infiltration Gallery

4.5.1 The Role of Infiltration Galleries

Infiltration galleries should be seen as one of a number of techniques available for diverting/abstracting river water. Natural filtration is one of the main benefits of an infiltration intake and is used to reduce water quality variance. Galleries can eliminate the need for fish protection screens, and therefore the issues with screen cleaning of surface intakes.

Infiltration galleries may not be appropriate for every situation encountered. For example, local conditions may inhibit their use if the infiltration capacity of the ground is low, if the risk of high energy storm events is high or, if the river system is highly unstable and significant remedial works will be required to divert the course of the river over the galleries.

4.5.2 Principles of Infiltration Galleries

The availability of groundwater is heavily dependent upon soil structure and in particular, the volume of voids. Gravels and coarse sands will allow water to flow through the voids relatively easily in comparison to fine grained soils such as silts and clays. The ease in which water can pass through the soil structure is expressed in terms of permeability.

Highly permeable and fully saturated soils are the aquifers. An aquiclude is a term used to describe saturated soils with a low permeability. Aquifers can also be unconfined or confined. An unconfined aquifer is exposed to the atmosphere whilst a confined aquifer is overlain with a relatively impermeable stratum.

Infiltration gallery systems are a form of river intake structure used to collect and distribute river water from alluvial/shallow aquifers. As the system is usually housed below the water table, it can also be considered a direct recharge system. The governing principals, used in the design gallery systems, are similar to those used for the design of drainage systems. In essence, the proficient designer will seek to effectively and efficiently facilitate the movement of water through the soil structure, without compromising the surrounding environment.

For an infiltration gallery system to be effective, the surface water body must be close enough to the structure and have a surface area large enough to allow processes such as infiltration and seepage to occur. The size of the required recharge area (A) is dictated by the hydraulic properties of the soil, namely its permeability (k), and the required discharge (Q), as stipulated by Darcy's law.

$$Q = Aki$$

4.5.3 Advantages and Challenges of Infiltration Galleries

The main advantages of infiltration gallery systems are as follows:

- Natural infiltration can significantly improve water quality.
- Whole-life costs may be less than alternative intake types.
- Correctly designed and well maintained systems can have less of a detrimental impact on the local environment than more conventional intake systems.

The main challenges with infiltration gallery systems are as follows:

- Gallery performance is dependent on the properties of the soil in which they are constructed.
- Ground investigations are required to determine the design parameters.
- Whilst the hydraulic conductivity of the ground may be good, transmissivity may be poor if the aquifers saturated depth is low.
- The introduction of water into the soil may induce geotechnical problems.

- Poorly designed systems can experience a significant reduction in yield if the filter pack becomes blinded through ingress of silt.
- Gallery systems require regular maintenance to sustain design performance.
- Specialist trenching machines may be required to reduce ground pressures during construction.
- The presence of clay can present many technical difficulties and hinder gallery performance.
- Mobilisation and demobilisation costs can be high.

4.6 Design of Infiltration Gallery

Designing of an Infiltration Gallery mainly includes the parameters of the gallery in order to physically execute and its construction. This includes the length of the gallery, strainer length, depth etc. The design methodology will be discussed further.

4.6.1 Design as per CPHEEO

As per the CPHEEO Manual on Water Supply Treatment (1999) (page 66), GOI, expression for the flow rate into an infiltration gallery under equilibrium condition is,

$$Q = KL\left(\frac{H^2 - h^2}{2R}\right) \quad \Rightarrow \quad L = \frac{1}{K}\left(\frac{2RQ}{H^2 - h^2}\right) \qquad \textbf{Eqn 4.20}$$

where, Q = rate of flow in m^3/day

K = permeability constant in m/d

L = length of the infiltration gallery in m

H = initial depth of water level in m

h = final depth of water level in m

R = radius of influence in m

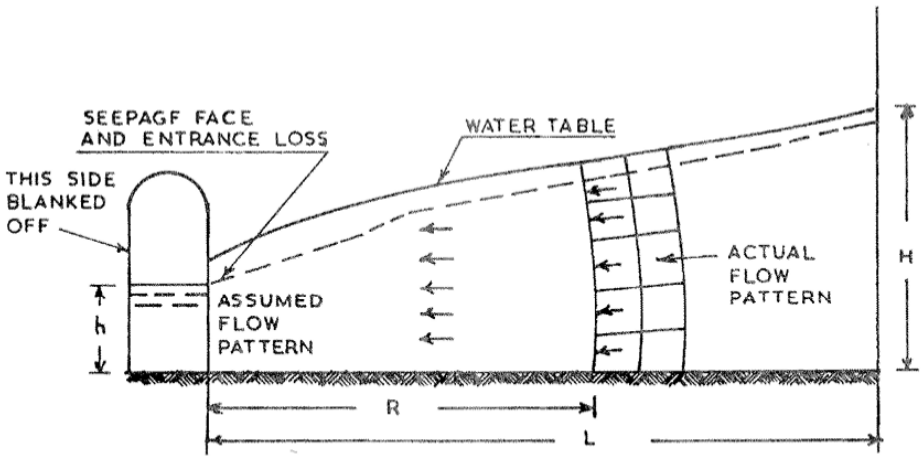

Figure 4.10: Infiltration Gallery under equilibrium condition (source: CPHEEO Manual)

4.6.2 Ferris Drain Function

Ferris (1950) developed a drain function relating aquifer parameters and the drawdown data to estimate the yield of the infiltration gallery. The drawdown pattern away from the gallery is given by Ferris as,

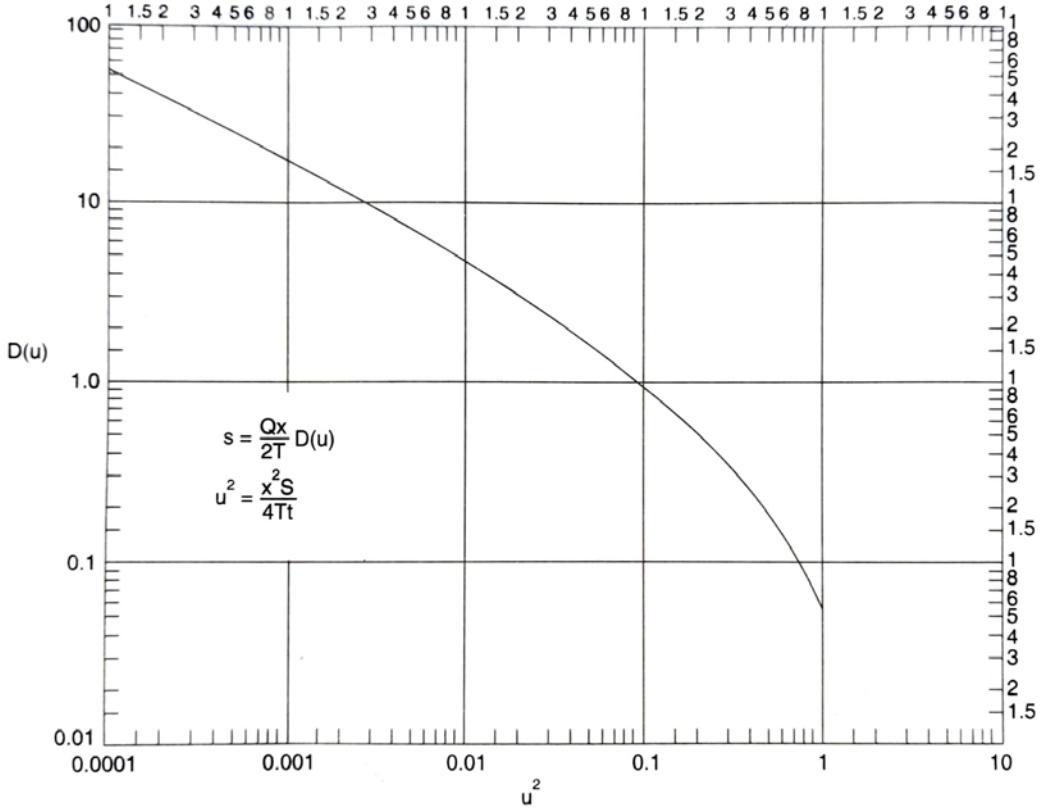

Figure 4.11: Ferris Drain Function

For the drain function D(u), the allowable drawdown is given as,

$$s = \frac{Qx}{2T} D(u) \qquad \textbf{Eqn 4.21}$$

$$\text{and,} \quad u^2 = \frac{x^2 S}{4Tt} \qquad \textbf{Eqn 4.22}$$

where,x = distance from drain to the point of observation.

s = allowable drawdown

S = storativity

T = transmissivity

t = time to attain allowable drawdown

Values of $D(u)$ for respective u^2 can be obtained from Figure 4.11 as well as Table 4.3.

Table 4.3: Values of D(u) and u^2 for drain function

u^{2*}	$D(u)^*$	$u^{2‡}$	$D(u)‡$
0.0025	10.32	1×10^{-7}	1783
0.0036	8.468	2×10^{-7}	1261
0.0049	7.109	4×10^{-7}	891.1
0.0064	6.130	7×10^{-7}	673.2
0.0081	5.331	1×10^{-6}	563.1
0.010	4.714	2×10^{-6}	398.0
0.013	4.008	4×10^{-6}	281.1
0.016	3.532	7×10^{-6}	212.1
0.020	3.079	1×10^{-5}	177.4
0.025	2.657	2×10^{-5}	125.2
0.030	2.354	4×10^{-5}	88.2
0.035	2.109	7×10^{-5}	66.42
0.040	1.943	1×10^{-4}	55.42
0.050	1.658	2×10^{-4}	38.92
0.060	1.441	4×10^{-4}	27.20
0.070	1.282	7×10^{-4}	20.36
0.090	1.049	1×10^{-3}	16.90
0.110	0.8810	2×10^{-3}	11.67
0.130	0.7598	4×10^{-3}	7.99
0.160	0.6284	7×10^{-3}	5.84
0.190	0.5324	1×10^{-2}	4.698
0.230	0.4384		
0.280	0.3517		
0.330	0.2895		
0.380	0.2434		
0.440	0.2008		
0.500	0.1837		
0.580	0.1345		
0.660	0.1094		
0.760	0.0864		
0.900	0.0623		
1.000	0.0507		

4.6.3 Scour Depth

Scouring is a natural phenomenon caused by the flow of water in rivers and streams. Scouring occurs naturally as part of morphological changes of river and as also as a result of man-made structures as well. Major floods produce large amount of scour and can cause dramatic changes in the plan cross section and depths of the streams.

The mean scour depth below the Highest Flood Level (HFL) for natural channels flowing over scouring bed can be calculated theoretically from following Eqn 4.23 as given in IRC: 78-2014:

$$d_{sm} = 1.34\left(\frac{D_b^2}{K_{sf}}\right)^{\frac{1}{3}} \qquad \textbf{Eqn 4.23}$$

where, D_b = Design discharge for substructure/foundation per meter width of the effective waterway.

Maximum flood discharge can be calculated using Dickens Formula (1865),

$$Q_p = C_D A^{3/4} \quad \textbf{Eqn 4.24}$$

where, C_D = Dickens constants = 6 (can be assumed for the study)

A = Catchment area of the river basin.

K_{sf} = Silt factor for a representative sample of bed material obtained up to the level anticipated deepest scour.

The value of D_b may be determined by dividing the design discharge for foundation by lower of theoretical and actual effective linear waterway as given in IRC: 5:2015.

K_{sf} is given by the expression

$$K_{sf} = 1.76\sqrt{d_m} \quad \textbf{Eqn 4.25}$$

where, d_m being the weighted mean diameter in millimetre.

The values of K_{sf}, d_m for various grades of sandy bed are given in Table 4.4.

Table 4.4: Values of silt factor (source: IRC 78:2014)

Type of Bed Material	d_m	K_{sf}
Coarse silt	0.04	0.35
Silt/Fine sand	0.081-0.158	0.5-0.7
Medium sand	0.223-0.505	0.85-1.25
Coarse sand	0.725	1.5
Fine bajri and sand	0.988	1.75
Heavy sand	1.29-2.00	2.0-2.42

4.6.4 Gravel Pack

In many practical cases, the aquifer material is so fine that selection of screen openings on the basis of its size and uniformity coefficient would yield openings so small that the entrance velocity would be unacceptably high. Under these circumstances, gravel packs or (equivalently) filter packs are placed in the annular region between the screen and the perimeter of the gallery. In this context, the term gravel pack refers to any filtering media that is placed around the well screen and is not limited to a coarse gravel material as the name implies. Fine to medium sand is commonly used as gravel-pack material. Gravel packs in unconsolidated formations are usually justified when $C_u < 3$ and $D_{10} < 0.25$ mm. The gravel pack does not exclude fine silt and clay particles, and

where these occur in significant amounts in a formation it is usually best to use blank casing sections (i.e., no screen or gravel pack).

4.6.4.1 Gravel Pack Material

The specifications of the gravel pack are determined primarily by the aquifer matrix, and criteria for selecting the gravel pack and corresponding screen slot size are given in the below Table 4.5. Typically, a gravel pack should have a uniformity coefficient between 1 and 2.5, with a median grain size between six and nine times the median grain size of the aquifer material. The corresponding slot size of the screen opening should be between the 5 and 10 percentile grain sizes of the gravel pack, with the 10-percentile size usually being preferable to minimize entrance losses. The maximum grain size of a gravel pack should generally be around 10 mm. Gravel packs usually consist of quartz-grained material that is sieved and washed to remove the finer material such as silt and clay. The grains of the gravel-pack material must be well rounded, to maximize the porosity; angular grains will tend to lock into adjacent grains, reducing the openings through which water and fine aquifer material can move.

Table 4.5: Criteria for Gravel Pack Selection (source: USBR 1995, Chin 2013)

Uniformity coefficient of Aquifer Matrix	Gravel-Pack Criteria	Screen slot size
<2.5	1. C_u between 1 and 2.5, with the 50% size not greater than six times the 50% size of the aquifer (preferable criteria).	5%–10% passing size of the gravel pack
	2. If C_u between 2.5 and 5, with the 50% size not greater than nine times the 50% size of the aquifer (alternative criteria).	
2.5-5	1. C_u between 1 and 2.5, with the 50% size not greater than nine times the 50% size of the aquifer (preferable criteria).	5%–10% passing size of the gravel pack
	2. If C_u between 2.5 and 5, with the 50% size not greater than twelve times the 50% size of the aquifer (alternative criteria).	
>5	Multiply the 30% passing size of the aquifer by 6 and 9 and locate the points on the grain-size distribution graph on the same horizontal line. Through these points draw two parallel lines representing materials with $C_u \leq 2.5$. Select gravel pack material that falls between the two lines.	5%–10% passing size of the gravel pack

4.6.4.2 Thickness of Gravel Pack

The thickness of the gravel pack is typically in the range of 8–23 cm (Todd and Mays, 2005). The thickness of the gravel pack should not be less than 8 cm to ensure that a continuous pack will surround the entire screen (Boonstra, 1998). It is also difficult to develop a system through a gravel pack much thicker than 20 cm, since the seepage velocities induced during the development procedure must be able to penetrate the gravel pack to repair the damage done by drilling, break down any residual drilling fluid on the borehole wall, and remove finer particles near the borehole (USBR, 1995).

4.6.4.3 Design of Gravel Pack

An artificial gravel pack is desired when $C_u < 3$, then

D_{30} (Gravel pack material) $=$ 4 to 6 times D_{30} of aquifer material.

With these points for D_{30} for gravel pack material, smooth curves can be drawn such that C_u for the gravel pack material is 2.5. The slot size can be kept at D_{10} of the gravel pack material.

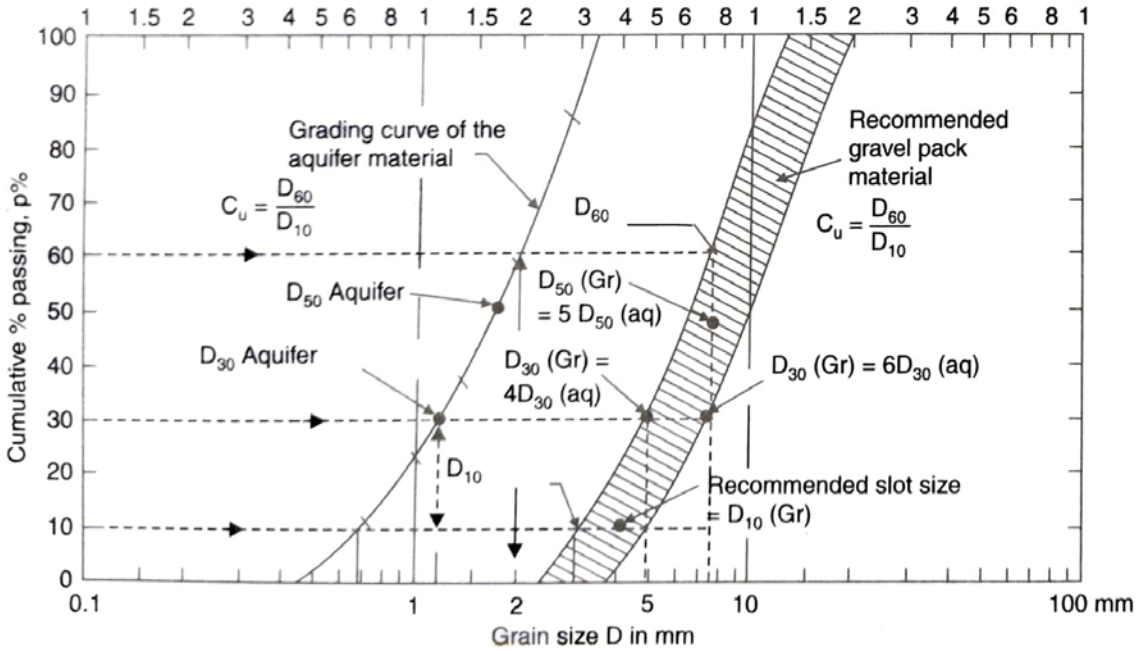

Figure 4.12: Design of Gravel Pack (source: Raghunath 2007)

Chapter 5 Methodology

Methodologies to achieve the different properties and to design the systems of the study objectives are discussed in this chapter. Various activities that are carried out in this study are shown in the flowchart.

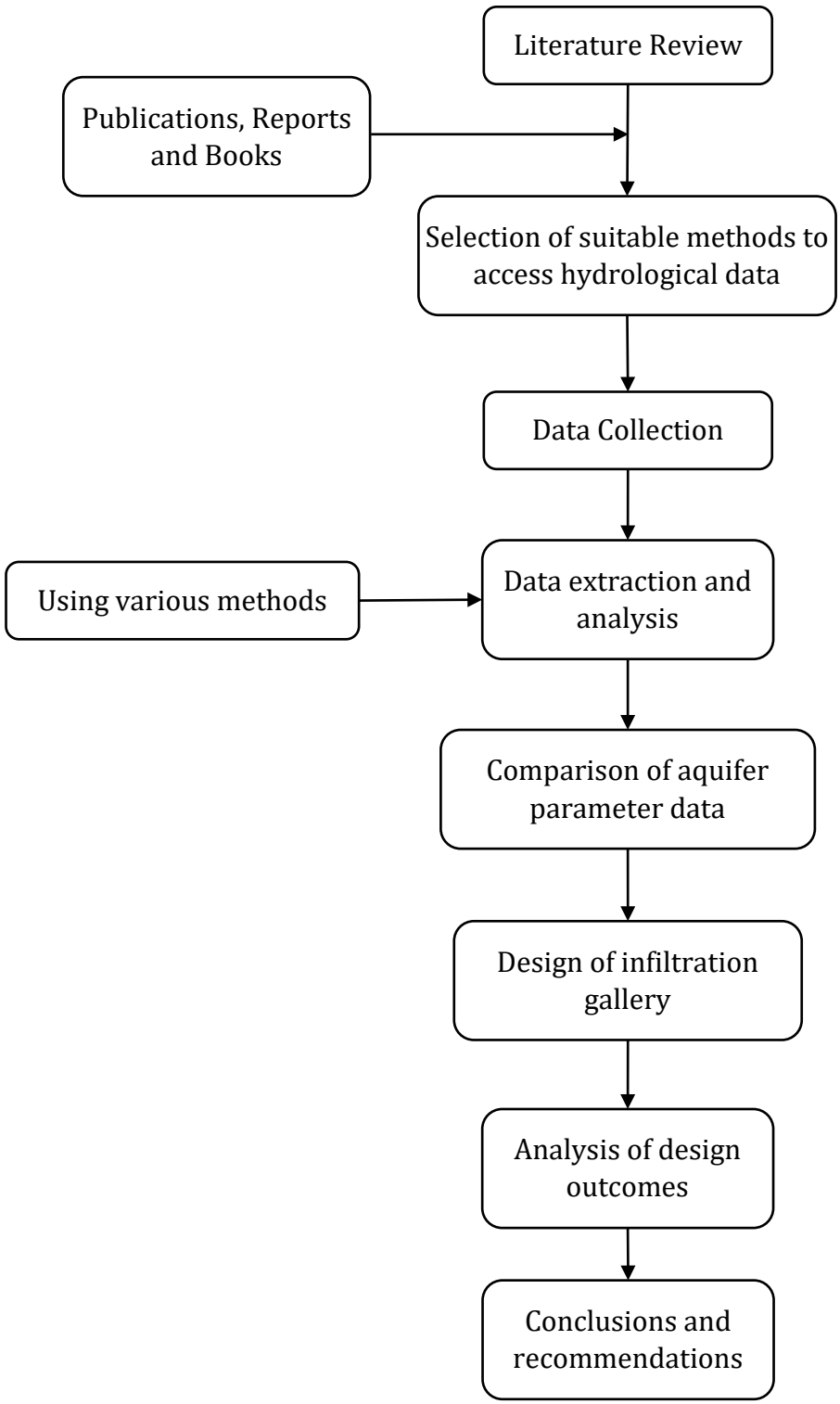

Figure 5.1: Flowchart of Methodology

The Jhargram District is suffering from water scarcity for a long time due to relatively low annual precipitation and moreover due to its high altitude and slope. The district falls under the rocky layered zone. Along with these type of geographic features, over exploitation of ground water and globalization over the plainer areas had made the condition even worse. During summer, water bodies dried up, therefore groundwater is the only available option for domestic, irrigation and various other uses. To reduce the groundwater exploitation, an infiltration gallery may be proposed under the Kangsabati river bed to continue the supply to a limited area throughout the summer season.

5.1 Literature Review

A literature review has been carried out to get the appropriate methods to find the related parameters and to design the infiltration gallery. Proper mapping of the study area has to be done. The studies reviewed has helped to collect proper field data and performing field test and lab test in order to find out the aquifer parameters and others. These studies have provided a general outline of proper mapping, designing and widen the disciplines of research and analysis.

5.2 Mapping of the Study Area

5.2.1 Steps for Contour Mapping in QGIS 3.22.7

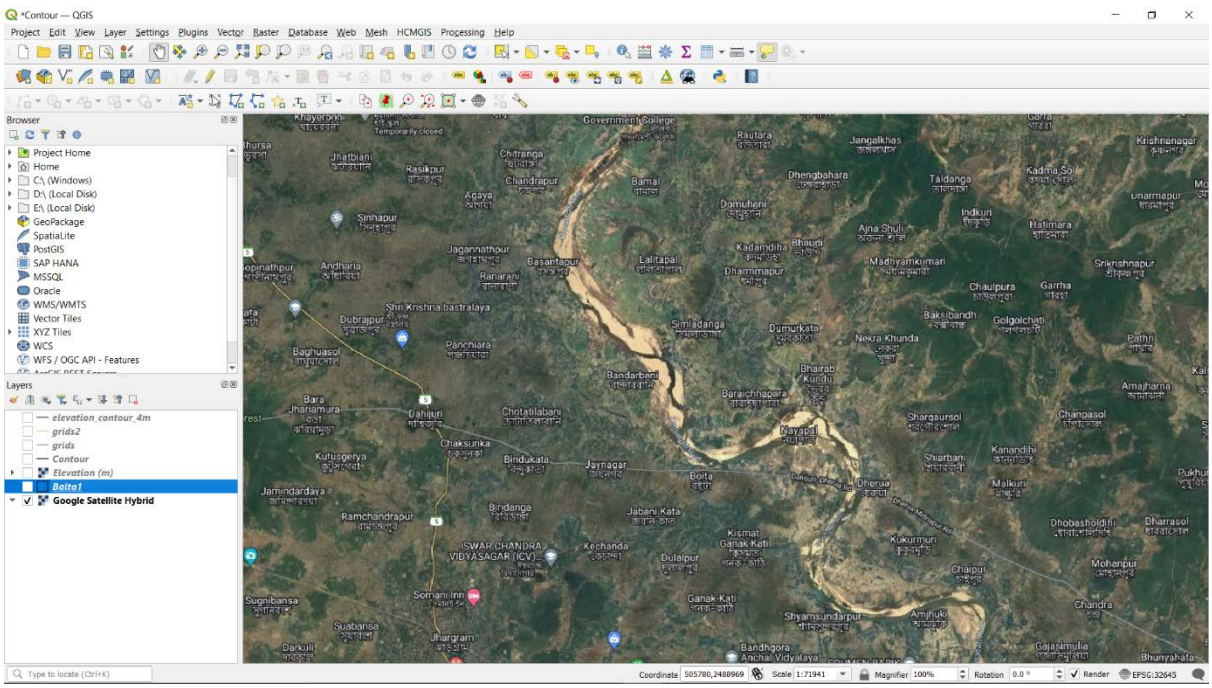

Figure 5.2: Study Map of the Jhargram region

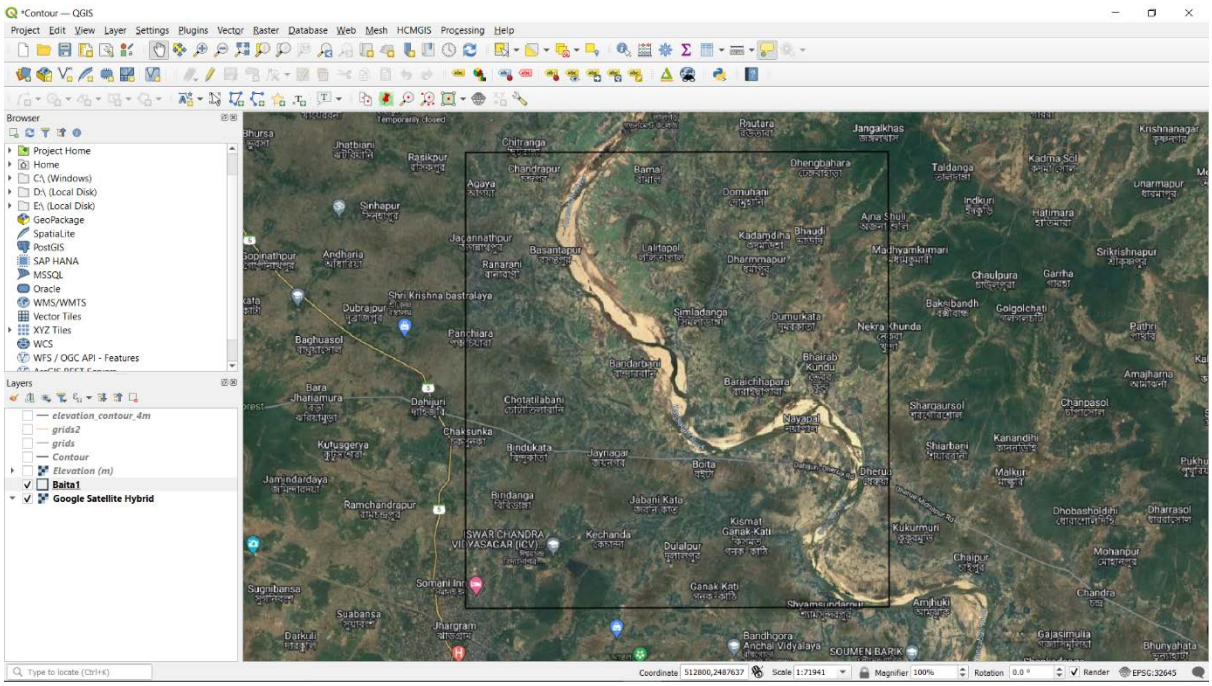

Figure 5.3: Localization of the Study Area

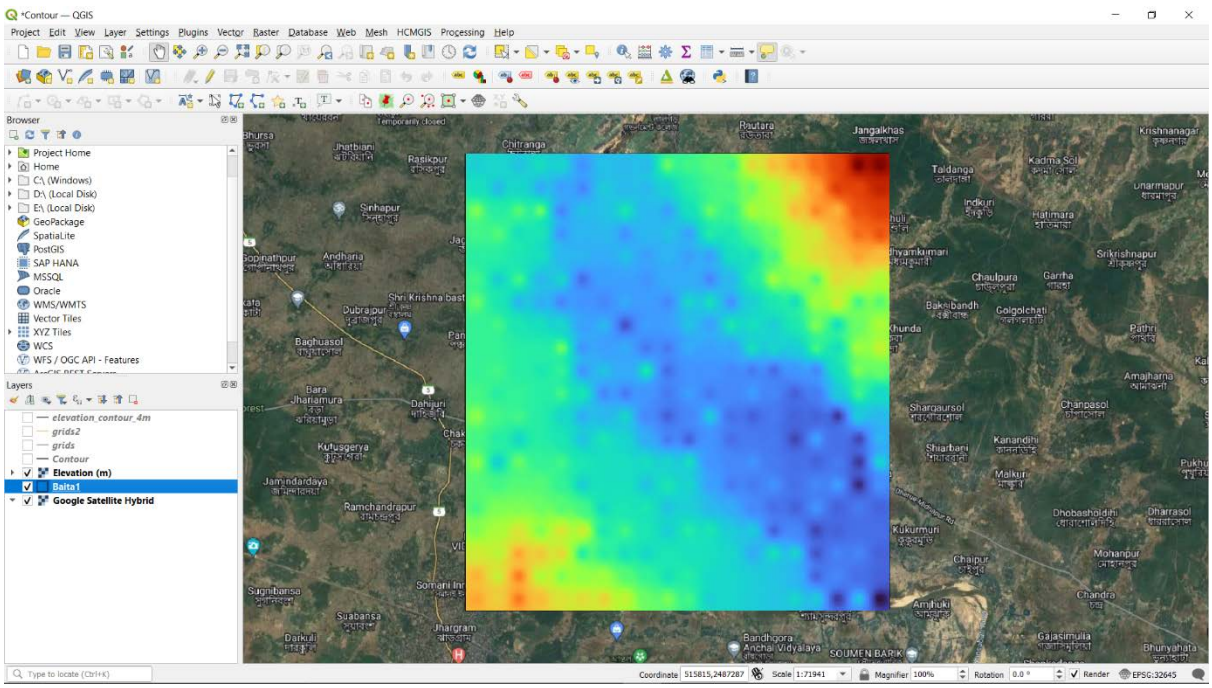

Figure 5.4: Importing the STRM DEM Data

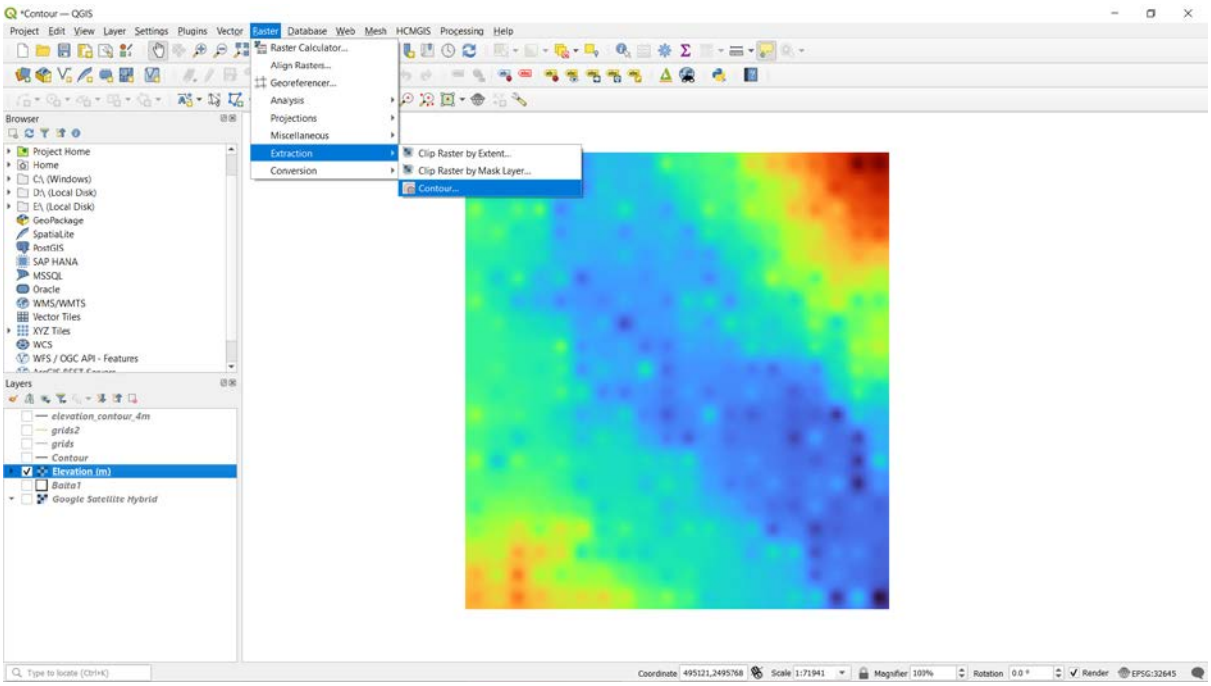

Figure 5.5: Generation of Contours

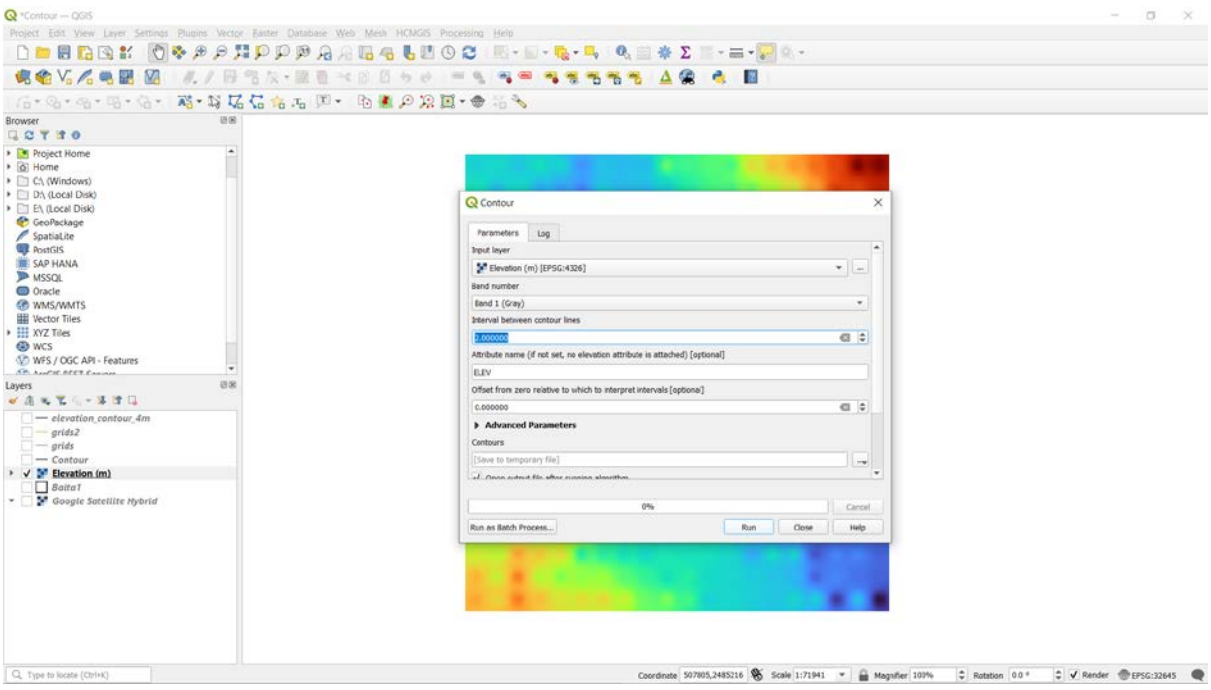

Figure 5.6: Setup for Contour Lines

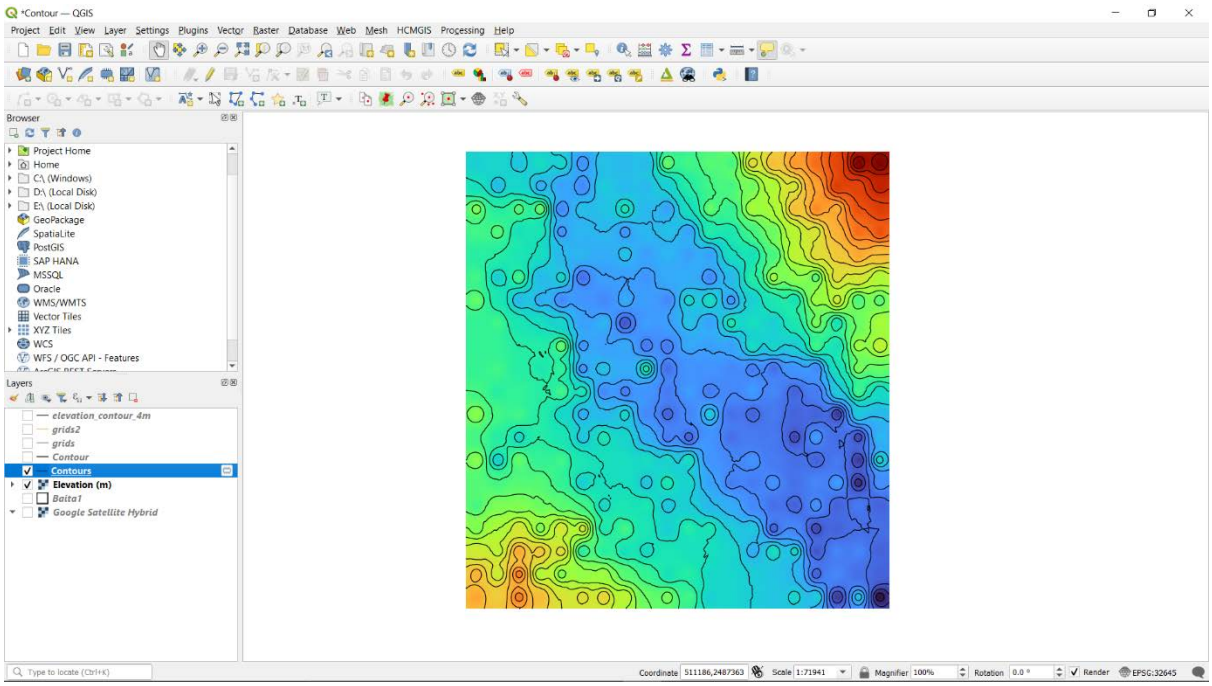

Figure 5.7: Contour Lines of the Study Area

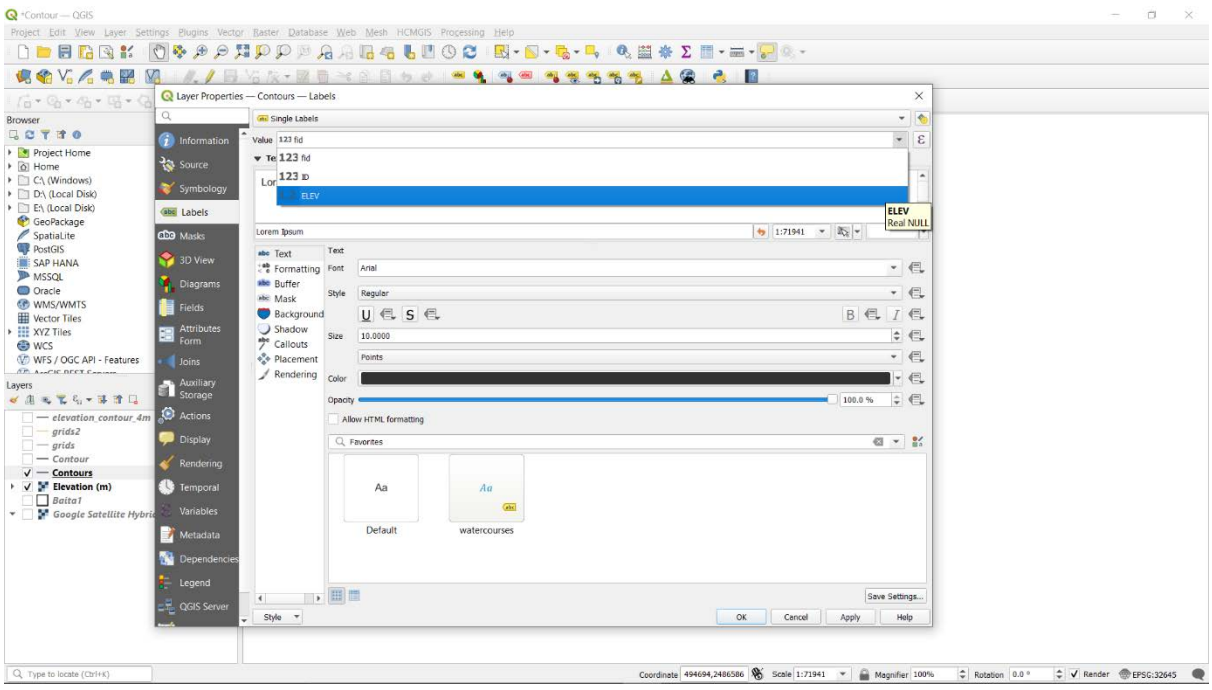

Figure 5.8: Setup for Contour Annotations

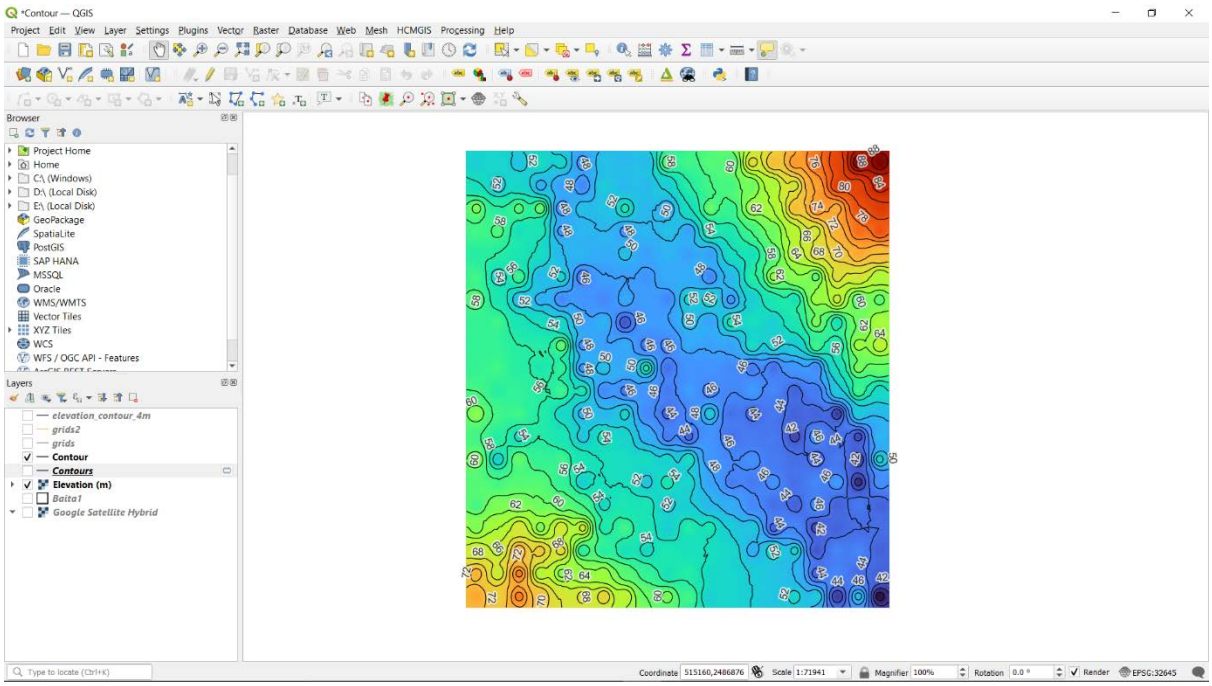

Figure 5.9: Finalized Contour Map of the Study Area

5.2.2 Steps for Lithology of Bore-holes in Strater 5.8

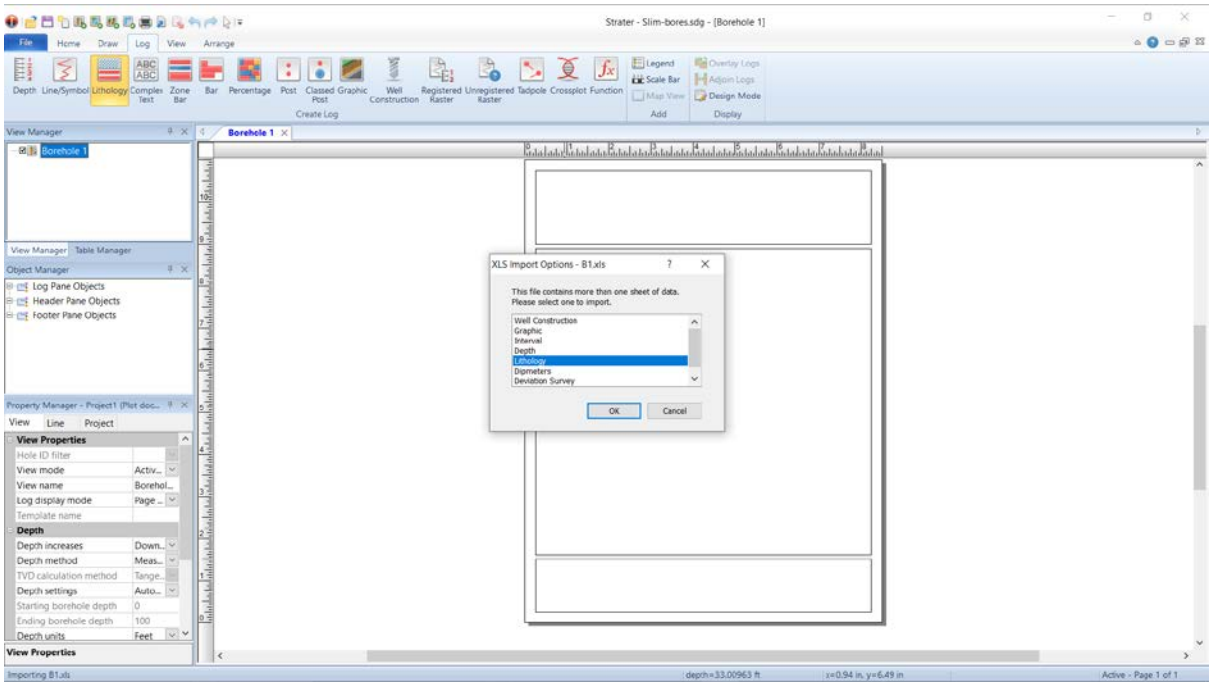

Figure 5.10: Importing of Litholog Data

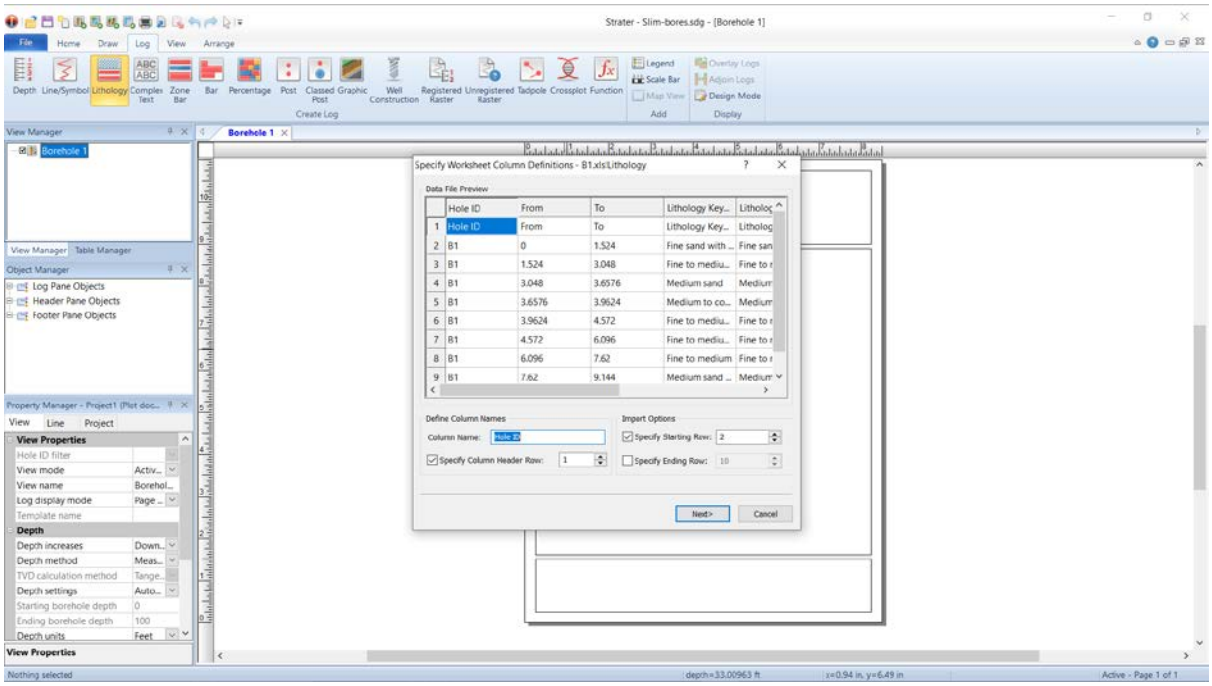

Figure 5.11: Setup for Litholog Data Import

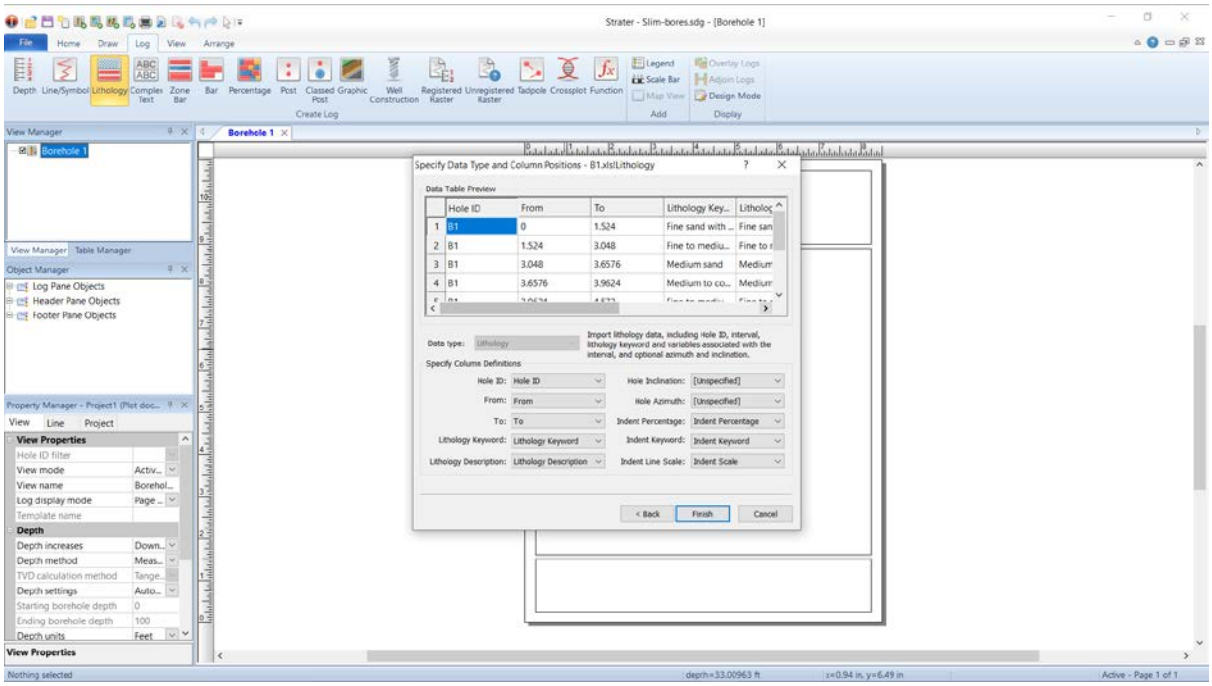

Figure 5.12: Data-set for Lithological Map

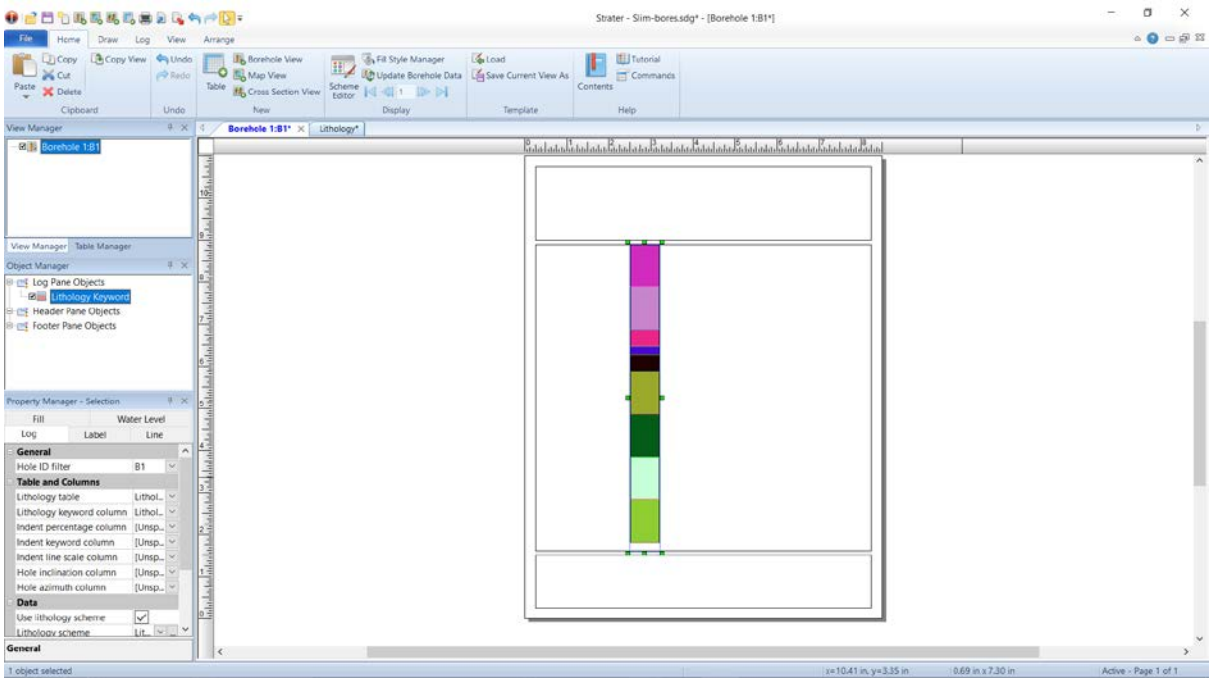

Figure 5.13: Litholog of Slim-bore B1

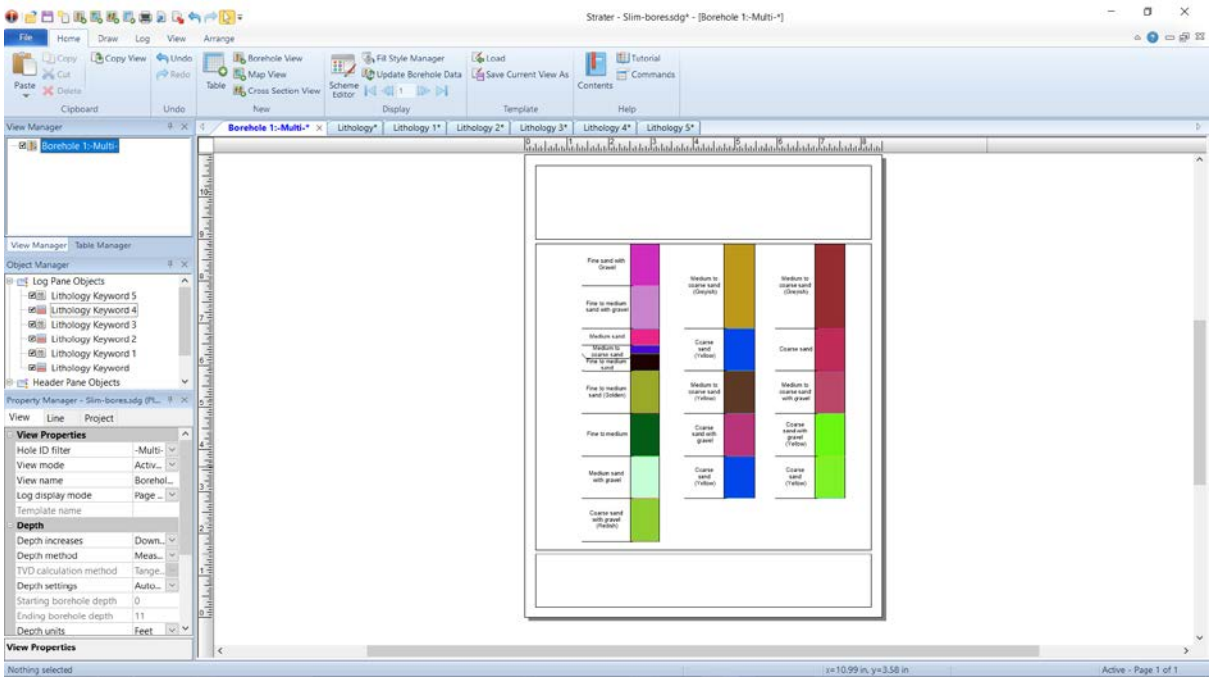

Figure 5.14: Litholog of all Slim-bores

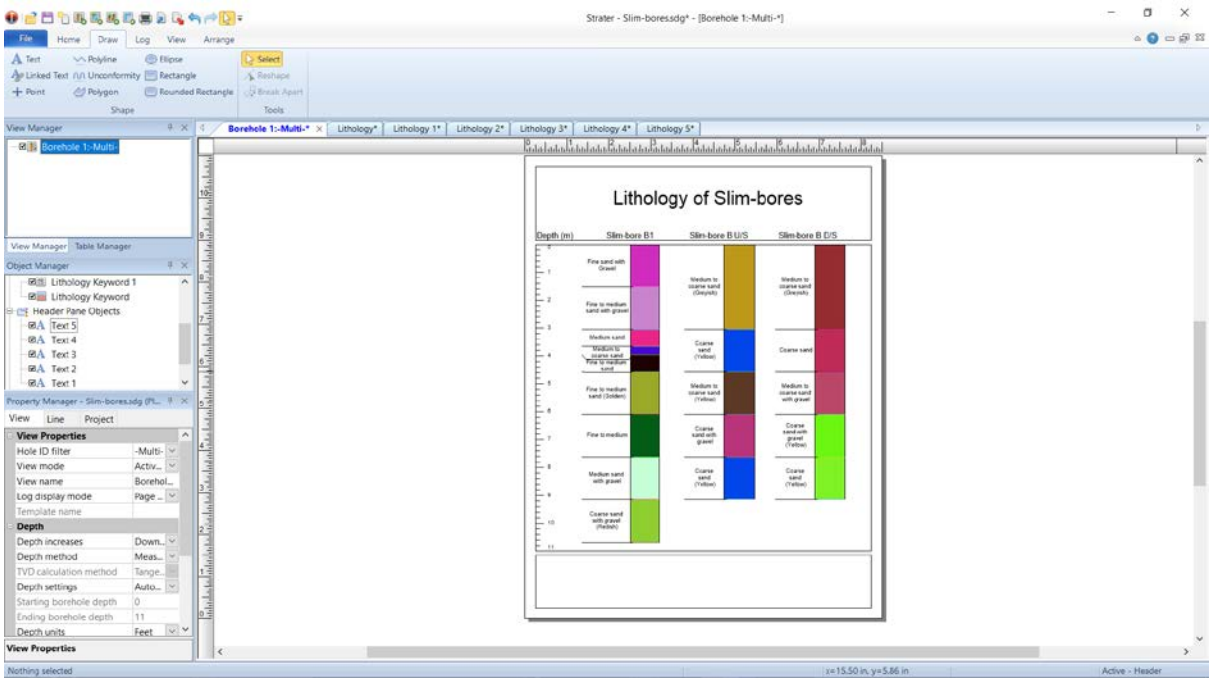

Figure 5.15: Annotations and Finalization of Lithological Details

5.3 Data Collection

In order to extract various hydrogeological parameters, pumping test was done which was intended to carry out for 72 hours. Since the stable drawdown has been achieved in 67 hours, pumping has been stopped and a recuperation test has been started thereafter. During the constant discharges, the drawdowns were noted in the pumping well and three observation wells. The readings were taken at one-minute intervals only for the period of the first one hour followed by two minutes' intervals for the next half an hour duration. Gradually depending upon the rate of change of drawdown, intervals were increased from five minutes to two hours.

After achieving saturation drawdown, instant recuperation test has been started and continuous monitoring of the augmentation of the water table with respect to time in the main as well as in the three observation wells have been done. After continuous six hours of monitoring, it was observed that almost the original level of the water table was regained. Accordingly, the water level data as obtained from the main, as well as the observation wells.

For lithological investigations, the samples were collected which were further dried in the laboratory to perform the mechanical sieve analysis to check whether the artificial gravel pack is needed, and if needed then the followed analysis and design.

5.4 Data Analysis

As discussed in the previous chapter, values of drawdown versus with varying time are plotted on semi-log graph paper. At an early time, the aquifer behaves as though it is confined with data falling along a straight line. At some intermediate time, it deviates from this straight line due to delayed gravity drainage. At a late time, data again follow a straight line as the aquifer exhibits a Theis-type response with S equivalent to S_y.

5.4.1 Aquifer Properties

The transmissivity and specific yield of the aquifer are determined using Neuman's Straight line method by fitting a straight line through the late-time data. The early-time response provides another estimate of transmissivity, and a confined storativity value for the aquifer can be obtained.

The transmissivity (T) of the aquifer has been determined using Eqn 4.15

$$T = \frac{2.3Q}{4\pi\Delta s}$$

The specific yield (S_y) has been determined using Eqn 4.16

$$S_y = \frac{2.25Tt_{0y}}{r^2}$$

The confined storativity (S) has been determined using Eqn 4.17

$$S = \frac{2.25Tt_{0s}}{r^2}$$

The Radius of Influence (R) can be given by the following Eqn 4.12

$$Q = \frac{2\pi Ts_w}{\ln\frac{R}{r_w}}$$

At the end of the pumping test when the pump is stopped, the water level in pumping and observation wells will begin to rise. This is referred to as recovery of groundwater level, while measurements of drawdown below the original static water level (prior to pumping) during this recovery period are known as residual drawdowns.

Aquifer properties can be calculated using the recovery data, to compare and corelate the properties that has been calculated using the drawdown data.

Using the Theis recovery method, the transmissivity can be calculated using Eqn 4.18

$$T = \frac{2.3Q}{4\pi\Delta s}$$

Storage coefficient can be obtained using Eqn 4.19

$$s = \frac{2.3Q}{4\pi T}\log_{10}\frac{2.25Tt_1}{r^2S}$$

The mechanical sieve analysis was done for the borehole samples to find out the Coefficient of Uniformity and the standard dimensions e.g. D_{10}, D_{30}, D_{60} etc.

5.4.2 Projected Drawdown

The projected drawdown after withdrawing the supply demand can be calculated using the Eqn 4.12.

$$Q = \frac{2\pi T s_w}{\ln\frac{R}{r_w}}$$

For a particular well, keeping all the parameters constant except Q = Discharge, and s_w = Drawdown, we have,

$$\frac{Q_1}{Q_2} = \frac{s_1}{s_2} \qquad \textbf{Eqn 5.1}$$

Using the above equation, the projected drawdown for the particular well can be calculated at the end of the withdrawal.

5.5 Water Demand

The total water demand of the target area is to be calculated with the help of the population and the per capita demand. The target area i.e. Jhargram Municipality is to be supplied with domestic demand only. The daily demand of the area can be obtained from the Table 4.1.

5% of the demand can be considered for public use.

15% of the demand can be considered as losses.

The population forecasting is important in order to design a structure for a period of 30 years. Forecasting can be done with previous Census data of the target area by the method of Logistic curve. Equation of the logistic curve is given in Eqn 4.5

$$P = \frac{P_s}{1 + me^{nt}}$$

where, $m = \frac{P_s - P_0}{P_0}$

$$n = \frac{2.303}{t_1}\log\left(\frac{P_0(P_s - P_1)}{P_1(P_s - P_0)}\right)$$

$$P_s = \frac{2P_0P_1P_2 - P_1^2(P_0+P_2)}{P_0P_2 - P_1^2}$$

P_0 = Population at t_0 year

P_1 = Population at t_1 years

P_2 = Population at t_2 years

$t_2 = 2t_1$

5.6 Design of Infiltration Gallery Components

5.6.1 Length of the Infiltration Gallery

The length of the gallery can be estimated using two different methods as discussed in the previous chapter.

The length of the gallery as per CPHEEO Manual on Water Supply Treatment (1999) (page 66), GOI, can be calculated using Eqn 4.20,

$$L = \frac{1}{K}\left(\frac{2RQ}{H^2 - h^2}\right)$$

On the other hand, Ferris Drain Function can also be used to calculate the same and also it provides a better comparison.

In the design, u^2 can be calculated using Eqn 4.22

$$u^2 = \frac{x^2 S}{4Tt}$$

For the calculated u^2, corresponding $D(u)$ can be obtained from Table 4.3.

Further the discharge can be calculated using Eqn 4.21

$$s = \frac{Qx}{2T}D(u)$$

The length of the infiltration gallery $= \frac{\text{Total water Demand}}{\text{Discharge per unit length of gallery}}$

5.6.2 Scour Depth

The mean scour depth below the Highest Flood Level (HFL) for natural channels flowing over scouring bed can be calculated theoretically from Eqn 4.23

$$d_{sm} = 1.34\left(\frac{D_b^2}{K_{sf}}\right)^{\frac{1}{3}}$$

K_{sf} is given by Eqn 4.25

$$K_{sf} = 1.76\sqrt{d_m}$$

The maximum depth of scour below the highest flood level for the protection required $= 2d_{sm}$

5.7 Gravel Pack Design

Artificial gravel pack is required when the aquifer material is homogeneous with a uniformity coefficient (C_u) of less than 3 and an effective grain size (D_{10}) of less than 0.25 mm (Raghunath, 2007). The pack-aquifer ratio (ratio of the 30 or 50% size of the gravel-pack material to 30 or 50% size of the aquifer material) should be 4:1 if the aquifer material is fine and uniform. However, if aquifer material is coarse and non-uniform, the pack-aquifer ratio should be 6:1. The gravel-pack material should have a uniformity coefficient (C_u) of less than 2.5. The design procedure for selecting the gravel material is to determine the point D_{30} of the gravel pack which is equal to 4 to 6 times the D_{30} of the aquifer material obtained from the sieve analysis of the aquifer material samples and then drawing a smooth curve through this point (corresponding to D_{30} of the gravel pack) representing a material with a uniformity coefficient of 2.5 or less. This is the gradation of the gravel pack to be used (Raghunath, 2007). The slot size of the well screen is selected as D_{10} of the gravel-pack material to avoid segregation of fine particles near the screen openings. The width of screen slots ranges from 1.5 to 4 mm and the length ranges from 5 to 12.5 cm. A pack-aquifer ratio of 5 (i.e., ratio of 50% size of the gravel-pack material and 50% size of the aquifer material) has been successfully used in water wells (Raghunath, 2007).

Chapter 6 Collection and Preparation of Data

6.1 Pumping Test Data

Pumping test was done which was intended to carry out for 72 hours. Since the stable drawdown has been achieved in 67 hours, pumping has been stopped and a recuperation test has been started thereafter. During the constant discharges at the Main Well (Pumping Well), the drawdowns were noted in the pumping well and three observation wells.

Table 6.1: Pumping Test Data for Main Well

Sl no.	Time	Interval(min)	Time since pumping began (min)	Water Level (m)	Static Water Level (m)	Drawdown (m)
1	16:53	1	1	0.530	0.43	0.100
2	16:54	1	2	0.980	0.43	0.550
3	16:55	1	3	0.990	0.43	0.560
4	16:56	1	4	1.000	0.43	0.570
5	16:57	1	5	1.000	0.43	0.570
6	16:58	1	6	1.000	0.43	0.570
7	16:59	1	7	1.005	0.43	0.575
8	17:00	1	8	1.010	0.43	0.580
9	17:01	1	9	1.015	0.43	0.585
10	17:02	1	10	1.020	0.43	0.590
11	17:03	1	11	1.020	0.43	0.590
12	17:04	1	12	1.020	0.43	0.590
13	17:05	1	13	1.020	0.43	0.590
14	17:06	1	14	1.020	0.43	0.590
15	17:07	1	15	1.020	0.43	0.590
16	17:08	1	16	1.025	0.43	0.595
17	17:09	1	17	1.025	0.43	0.595
18	17:10	1	18	1.025	0.43	0.595
19	17:11	1	19	1.025	0.43	0.595
20	17:12	1	20	1.030	0.43	0.600
21	17:13	1	21	1.030	0.43	0.600
22	17:14	1	22	1.030	0.43	0.600
23	17:15	1	23	1.035	0.43	0.605
24	17:16	1	24	1.035	0.43	0.605
25	17:17	1	25	1.030	0.43	0.600
26	17:18	1	26	1.035	0.43	0.605
27	17:19	1	27	1.035	0.43	0.605
28	17:20	1	28	1.035	0.43	0.605
29	17:21	1	29	1.035	0.43	0.605

Sl no.	Time	Interval(min)	Time since pumping began (min)	Water Level (m)	Static Water Level (m)	Drawdown (m)
30	17.22	1	30	1.035	0.43	0.605
31	17:23	1	31	1.035	0.43	0.605
32	17:24	1	32	1.040	0.43	0.610
33	17:25	1	33	1.040	0.43	0.610
34	17:26	1	34	1.040	0.43	0.610
35	17:27	1	35	1.050	0.43	0.620
36	17:28	1	36	1.050	0.43	0.620
37	17:29	1	37	1.050	0.43	0.620
38	17:30	1	38	1.055	0.43	0.625
39	17:31	1	39	1.050	0.43	0.620
40	17:32	1	40	1.050	0.43	0.620
41	17:51	19	59	1.055	0.43	0.625
42	17:56	5	64	1.060	0.43	0.630
43	18:02	6	70	1.065	0.43	0.635
44	18:15	13	83	1.065	0.43	0.635
45	18:24	9	92	1.070	0.43	0.640
46	18:39	15	107	1.070	0.43	0.640
47	18:56	17	124	1.075	0.43	0.645
48	19:00	4	128	1.075	0.43	0.645
49	19:20	20	148	1.080	0.43	0.650
50	19:34	14	162	1.080	0.43	0.650
51	19:45	11	173	1.079	0.43	0.649
52	20:00	15	188	1.080	0.43	0.650
53	21:00	60	248	1.075	0.43	0.645
54	22:00	60	308	1.075	0.43	0.645
55	23:00	60	368	1.072	0.43	0.642
56	00:00	60	428	1.072	0.43	0.642
57	01:00	60	488	1.074	0.43	0.644
58	02:00	60	548	1.075	0.43	0.645
59	03:00	60	608	1.075	0.43	0.645
60	04:00	60	668	1.075	0.43	0.645
61	05:00	60	728	1.077	0.43	0.647
62	06:00	60	788	1.077	0.43	0.647
63	07:00	60	848	1.080	0.43	0.650
64	08:00	60	908	1.084	0.43	0.654
65	09:00	60	968	1.085	0.43	0.655
66	09:20	20	988	1.085	0.43	0.655
67	10:00	40	1028	1.085	0.43	0.655
68	11:00	60	1088	1.085	0.43	0.655
69	11:20	20	1108	1.090	0.43	0.660
70	12:00	40	1148	1.090	0.43	0.660

Sl no.	Time	Interval(min)	Time since pumping began (min)	Water Level (m)	Static Water Level (m)	Drawdown (m)
71	13:00	60	1208	1.090	0.43	0.660
72	14:00	60	1268	1.085	0.43	0.655
73	15:05	65	1333	1.090	0.43	0.660
74	16:00	55	1388	1.085	0.43	0.655
75	17:00	60	1448	1.085	0.43	0.655
76	17:30	30	1478	1.085	0.43	0.655
77	18:30	60	1538	1.085	0.43	0.655
78	20:30	120	1658	1.088	0.43	0.658
79	22:30	120	1778	1.090	0.43	0.660
80	00:30	120	1898	1.090	0.43	0.660
81	02:30	120	2018	1.090	0.43	0.660
82	04:30	120	2138	1.090	0.43	0.660
83	06:30	120	2258	1.090	0.43	0.660
84	08:30	120	2378	1.090	0.43	0.660
85	10:30	120	2498	1.100	0.43	0.670
86	11:30	60	2558	1.110	0.43	0.680
87	12:30	60	2618	1.140	0.43	0.710
88	12:57	27	2645	1.150	0.43	0.720
89	13:14	17	2662	1.160	0.43	0.730
90	13:34	20	2682	1.170	0.43	0.740
91	13:44	10	2692	1.175	0.43	0.745
92	14:05	21	2713	1.190	0.43	0.760
93	14:28	23	2736	1.210	0.43	0.780
94	14:56	28	2764	1.230	0.43	0.800
95	15:24	28	2792	1.250	0.43	0.820
96	16:55	91	2883	1.285	0.43	0.855
97	17:55	60	2943	1.310	0.43	0.880
98	19:30	95	3038	1.340	0.43	0.910
99	20:30	60	3098	1.375	0.43	0.945
100	21:30	60	3158	1.390	0.43	0.960
101	22:30	60	3218	1.410	0.43	0.980
102	23:30	60	3278	1.425	0.43	0.995
103	01:00	90	3368	1.450	0.43	1.020
104	02:30	90	3458	1.485	0.43	1.055
105	04:00	90	3548	1.505	0.43	1.075
106	05:30	90	3638	1.520	0.43	1.090
107	07:00	90	3728	1.525	0.43	1.095
108	08:30	90	3818	1.530	0.43	1.100
109	10:00	90	3908	1.535	0.43	1.105
110	11:27	87	3995	1.540	0.43	1.110
111	11:50	23	4018	1.550	0.43	1.120

Table 6.2: Pumping Test data for Observation Well 1

Sl no.	Time	Interval(min)	Time since pumping began (min)	Water Level (m)	Static Water Level (m)	Drawdown (m)
1	16:53	1	1	0.660	0.656	0.004
2	16:54	1	2	0.662	0.656	0.006
3	16:55	1	3	0.664	0.656	0.008
4	16:56	1	4	0.666	0.656	0.010
5	16:57	1	5	0.667	0.656	0.011
6	16:58	1	6	0.667	0.656	0.011
7	16:59	1	7	0.668	0.656	0.012
8	17:00	1	8	0.669	0.656	0.013
9	17:01	1	9	0.670	0.656	0.014
10	17:02	1	10	0.672	0.656	0.016
11	17:03	1	11	0.672	0.656	0.016
12	17:04	1	12	0.672	0.656	0.016
13	17:06	2	14	0.673	0.656	0.017
14	17:08	2	16	0.674	0.656	0.018
15	17:10	2	18	0.674	0.656	0.018
16	17:12	2	20	0.675	0.656	0.019
17	17:14	2	22	0.676	0.656	0.020
18	17:16	2	24	0.678	0.656	0.022
19	17:18	2	26	0.680	0.656	0.024
20	17:20	2	28	0.680	0.656	0.024
21	17:22	2	30	0.681	0.656	0.025
22	17:24	2	32	0.682	0.656	0.026
23	17:26	2	34	0.683	0.656	0.027
24	17:28	2	36	0.683	0.656	0.027
25	17:30	2	38	0.684	0.656	0.028
26	17:32	2	40	0.685	0.656	0.029
27	17:35	3	43	0.686	0.656	0.030
28	17:38	3	46	0.686	0.656	0.030
29	17:41	3	49	0.686	0.656	0.030
30	17:45	4	53	0.687	0.656	0.031
31	17:50	5	58	0.687	0.656	0.031
32	17:55	5	63	0.688	0.656	0.032
33	18:00	5	68	0.689	0.656	0.033
34	18:05	5	73	0.691	0.656	0.035
35	18:10	5	78	0.691	0.656	0.035
36	18:15	5	83	0.692	0.656	0.036
37	18:20	5	88	0.693	0.656	0.037
38	18:25	5	93	0.694	0.656	0.038
39	18:30	5	98	0.695	0.656	0.039

Sl no.	Time	Interval(min)	Time since pumping began (min)	Water Level (m)	Static Water Level (m)	Drawdown (m)
40	18:40	10	108	0.700	0.656	0.044
41	18:50	10	118	0.704	0.656	0.048
42	19:00	10	128	0.708	0.656	0.050
43	19:30	30	158	0.710	0.656	0.054
44	20:04	34	192	0.711	0.656	0.055
45	21:05	61	253	0.712	0.656	0.056
46	22:00	55	308	0.713	0.656	0.057
47	23:00	60	368	0.714	0.656	0.058
48	00:10	70	438	0.717	0.656	0.061
49	01:10	60	498	0.722	0.656	0.066
50	02:10	60	558	0.726	0.656	0.070
51	03:10	60	618	0.728	0.656	0.072
52	04:10	60	678	0.730	0.656	0.074
53	05:10	60	738	0.731	0.656	0.075
54	06:10	60	798	0.734	0.656	0.078
55	07:10	60	858	0.737	0.656	0.081
56	08:10	60	918	0.739	0.656	0.083
57	09:10	60	978	0.739	0.656	0.083
58	09:20	10	988	0.740	0.656	0.084
59	10:00	40	1028	0.742	0.656	0.086
60	11:36	96	1124	0.742	0.656	0.086
61	12:02	26	1150	0.742	0.656	0.086
62	12:52	50	1200	0.743	0.656	0.087
63	14:08	76	1276	0.744	0.656	0.088
64	15:05	57	1333	0.746	0.656	0.090
65	16:25	80	1413	0.746	0.656	0.090
66	17:30	65	1478	0.748	0.656	0.092
67	18:30	60	1538	0.748	0.656	0.092
68	20:30	120	1658	0.750	0.656	0.094
69	22:30	120	1778	0.754	0.656	0.098
70	00:30	120	1898	0.756	0.656	0.100
71	02:30	120	2018	0.758	0.656	0.102
72	04:30	120	2138	0.761	0.656	0.105
73	06:30	120	2258	0.766	0.656	0.110
74	08:30	120	2378	0.771	0.656	0.115
75	10:30	120	2498	0.774	0.656	0.118
76	11:20	50	2548	0.775	0.656	0.119
77	11:57	37	2585	0.776	0.656	0.120
78	12:06	9	2594	0.776	0.656	0.120
79	12:16	10	2604	0.777	0.656	0.121
80	12:27	11	2615	0.777	0.656	0.121

Sl no.	Time	Interval(min)	Time since pumping began (min)	Water Level (m)	Static Water Level (m)	Drawdown (m)
81	12:39	12	2627	0.781	0.656	0.125
82	12:55	16	2643	0.786	0.656	0.130
83	13:08	13	2656	0.787	0.656	0.131
84	13:20	12	2668	0.787	0.656	0.131
85	13:32	12	2680	0.787	0.656	0.131
86	13:45	13	2693	0.787	0.656	0.131
87	14:00	15	2708	0.787	0.656	0.131
88	14:15	15	2723	0.789	0.656	0.133
89	14:30	15	2738	0.792	0.656	0.136
90	14:45	15	2753	0.792	0.656	0.136
91	15:00	15	2768	0.792	0.656	0.136
92	15:30	30	2798	0.797	0.656	0.141
93	16:00	30	2828	0.801	0.656	0.145
94	16:30	30	2858	0.801	0.656	0.145
95	17:00	30	2888	0.802	0.656	0.146
96	17:30	30	2918	0.802	0.656	0.146
97	18:00	30	2948	0.802	0.656	0.146
98	18:30	30	2978	0.802	0.656	0.146
99	19:30	60	3038	0.801	0.656	0.145
100	20:30	60	3098	0.804	0.656	0.148
101	21:30	60	3158	0.804	0.656	0.148
102	22:30	60	3218	0.805	0.656	0.149
103	23:30	60	3278	0.806	0.656	0.150
104	01:00	90	3368	0.807	0.656	0.151
105	02:30	90	3458	0.806	0.656	0.150
106	04:00	90	3548	0.808	0.656	0.152
107	05:30	90	3638	0.808	0.656	0.152
108	07:00	90	3728	0.808	0.656	0.152
109	08:30	90	3818	0.808	0.656	0.152
110	10:00	90	3908	0.808	0.656	0.152
111	11:27	87	3995	0.808	0.656	0.152
112	11:50	23	4018	0.808	0.656	0.152

Table 6.3: Pumping Test data for Observation Well 2

Sl no.	Time	Interval(min)	Time since pumping began (min)	Water Level (m)	Static Water Level (m)	Drawdown (m)
1	16:53	1	1	0.625	0.62	0.005
2	16:54	1	2	0.627	0.62	0.007
3	16:55	1	3	0.628	0.62	0.008
4	16:56	1	4	0.630	0.62	0.010

Sl no.	Time	Interval(min)	Time since pumping began (min)	Water Level (m)	Static Water Level (m)	Drawdown (m)
5	16:57	1	5	0.631	0.62	0.011
6	16:58	1	6	0.633	0.62	0.013
7	16:59	1	7	0.635	0.62	0.015
8	17:00	1	8	0.635	0.62	0.015
9	17:01	1	9	0.637	0.62	0.017
10	17:02	1	10	0.637	0.62	0.017
11	17:03	1	11	0.638	0.62	0.018
12	17:04	1	12	0.639	0.62	0.019
13	17:05	1	13	0.640	0.62	0.020
14	17:06	1	14	0.643	0.62	0.023
15	17:07	1	15	0.643	0.62	0.023
16	17:08	1	16	0.645	0.62	0.025
17	17:09	1	17	0.645	0.62	0.025
18	17:10	1	18	0.647	0.62	0.027
19	17:11	1	19	0.647	0.62	0.027
20	17:12	1	20	0.647	0.62	0.027
21	17:13	1	21	0.648	0.62	0.028
22	17:14	1	22	0.648	0.62	0.028
23	17:15	1	23	0.648	0.62	0.028
24	17:16	1	24	0.649	0.62	0.029
25	17:17	1	25	0.650	0.62	0.030
26	17:18	1	26	0.651	0.62	0.031
27	17:19	1	27	0.651	0.62	0.031
28	17:20	1	28	0.651	0.62	0.031
29	17:21	1	29	0.652	0.62	0.032
30	17:22	1	30	0.652	0.62	0.032
31	17:23	1	31	0.651	0.62	0.031
32	17:24	1	32	0.651	0.62	0.031
33	17:25	1	33	0.652	0.62	0.032
34	17:26	1	34	0.652	0.62	0.032
35	17:27	1	35	0.652	0.62	0.032
36	17:28	1	36	0.652	0.62	0.032
37	17:29	1	37	0.652	0.62	0.032
38	17:30	1	38	0.652	0.62	0.032
39	17:31	1	39	0.653	0.62	0.033
40	17:32	1	40	0.653	0.62	0.033
41	17:33	1	41	0.653	0.62	0.033
42	17:34	1	42	0.652	0.62	0.032
43	17:35	1	43	0.654	0.62	0.034
44	17:36	1	44	0.654	0.62	0.034
45	17:37	1	45	0.654	0.62	0.034

Sl no.	Time	Interval(min)	Time since pumping began (min)	Water Level (m)	Static Water Level (m)	Drawdown (m)
46	17:38	1	46	0.653	0.62	0.033
47	17:44	6	52	0.654	0.62	0.034
48	17:47	3	55	0.655	0.62	0.035
49	17:50	3	58	0.655	0.62	0.035
50	17:55	5	63	0.657	0.62	0.037
51	18:00	5	68	0.659	0.62	0.039
52	18:10	10	78	0.660	0.62	0.040
53	18:20	10	88	0.661	0.62	0.041
54	18:30	10	98	0.662	0.62	0.042
55	18:40	10	108	0.662	0.62	0.042
56	18:55	15	123	0.664	0.62	0.044
57	19:10	15	138	0.666	0.62	0.046
58	19:25	15	153	0.668	0.62	0.048
59	19:40	15	168	0.670	0.62	0.050
60	19:50	10	178	0.670	0.62	0.050
61	20:00	10	188	0.670	0.62	0.050
62	21:00	60	248	0.670	0.62	0.050
63	22:00	60	308	0.670	0.62	0.050
64	23:00	60	368	0.670	0.62	0.050
65	00:00	60	428	0.671	0.62	0.051
66	01:00	60	488	0.672	0.62	0.052
67	02:00	60	548	0.672	0.62	0.052
68	03:00	60	608	0.675	0.62	0.055
69	04:00	60	668	0.680	0.62	0.060
70	05:00	60	728	0.683	0.62	0.063
71	06:00	60	788	0.684	0.62	0.064
72	07:00	60	848	0.687	0.62	0.067
73	08:00	60	908	0.690	0.62	0.070
74	09:00	60	968	0.690	0.62	0.070
75	10:00	60	1028	0.693	0.62	0.073
76	11:00	60	1088	0.695	0.62	0.075
77	12:00	60	1148	0.695	0.62	0.075
78	12:50	50	1198	0.697	0.62	0.077
79	14:00	70	1268	0.699	0.62	0.079
80	15:00	60	1328	0.699	0.62	0.079
81	16:30	90	1418	0.702	0.62	0.082
82	17:30	60	1478	0.705	0.62	0.085
83	18:30	60	1538	0.706	0.62	0.086
84	20:30	120	1658	0.707	0.62	0.087
85	23:00	150	1808	0.709	0.62	0.089
86	00:30	90	1898	0.712	0.62	0.092

Sl no.	Time	Interval(min)	Time since pumping began (min)	Water Level (m)	Static Water Level (m)	Drawdown (m)
87	02:30	120	2018	0.712	0.62	0.092
88	04:30	120	2138	0.715	0.62	0.095
89	06:30	120	2258	0.720	0.62	0.100
90	08:30	120	2378	0.720	0.62	0.100
91	10:30	120	2498	0.721	0.62	0.101
92	11:35	65	2563	0.721	0.62	0.101
93	12:00	25	2588	0.721	0.62	0.101
94	12:01	1	2589	0.723	0.62	0.103
95	12:02	1	2590	0.723	0.62	0.103
96	12:03	1	2591	0.720	0.62	0.100
97	12:06	3	2594	0.722	0.62	0.102
98	12:09	3	2597	0.722	0.62	0.102
99	12:16	7	2604	0.724	0.62	0.104
100	12:22	6	2610	0.722	0.62	0.102
101	12:28	6	2616	0.722	0.62	0.102
102	12:36	8	2624	0.725	0.62	0.105
103	12:45	9	2633	0.726	0.62	0.106
104	12:55	10	2643	0.727	0.62	0.107
105	13:05	10	2653	0.728	0.62	0.108
106	13:15	10	2663	0.730	0.62	0.110
107	13:30	15	2678	0.730	0.62	0.110
108	14:30	60	2738	0.729	0.62	0.109
109	15:00	30	2768	0.735	0.62	0.115
110	15:30	30	2798	0.735	0.62	0.115
111	16:00	30	2828	0.737	0.62	0.117
112	16:30	30	2858	0.737	0.62	0.117
113	16:55	25	2883	0.738	0.62	0.118
114	17:45	50	2933	0.739	0.62	0.119
115	18:05	20	2953	0.739	0.62	0.119
116	19:30	85	3038	0.740	0.62	0.120
117	20:30	60	3098	0.740	0.62	0.120
118	21:30	60	3158	0.739	0.62	0.119
119	22:30	60	3218	0.739	0.62	0.119
120	23:30	60	3278	0.740	0.62	0.120
121	01:00	90	3368	0.740	0.62	0.120
122	02:30	90	3458	0.741	0.62	0.121
123	04:00	90	3548	0.741	0.62	0.121
124	05:30	90	3638	0.743	0.62	0.123
125	07:00	90	3728	0.745	0.62	0.125
126	08:30	90	3818	0.745	0.62	0.125
127	10:00	90	3908	0.745	0.62	0.125

Sl no.	Time	Interval(min)	Time since pumping began (min)	Water Level (m)	Static Water Level (m)	Drawdown (m)
128	11:30	90	3998	0.745	0.62	0.125
129	11:50	20	4018	0.745	0.62	0.125

Table 6.4: Pumping Test data for Observation Well 3

Sl no.	Time	Interval(min)	Time since pumping began (min)	Water Level (m)	Static Water Level (m)	Drawdown (m)
1	16:55	1	1	0.203	0.194	0.009
2	16:56	1	2	0.204	0.194	0.010
3	16:57	1	3	0.204	0.194	0.010
4	16:58	1	4	0.205	0.194	0.011
5	16:59	1	5	0.206	0.194	0.012
6	17:00	1	6	0.206	0.194	0.012
7	17:01	1	7	0.206	0.194	0.012
8	17:02	1	8	0.206	0.194	0.012
9	17:03	1	9	0.209	0.194	0.015
10	17:04	1	10	0.211	0.194	0.017
11	17:05	1	11	0.212	0.194	0.018
12	17:06	1	12	0.213	0.194	0.019
13	17:07	1	13	0.213	0.194	0.019
14	17:08	1	14	0.213	0.194	0.019
15	17:10	2	16	0.214	0.194	0.020
16	17:11	1	17	0.215	0.194	0.021
17	17:12	1	18	0.215	0.194	0.021
18	17:13	1	19	0.215	0.194	0.021
19	17:14	1	20	0.216	0.194	0.022
20	17:15	1	21	0.217	0.194	0.023
21	17:16	1	22	0.216	0.194	0.022
22	17:17	1	23	0.217	0.194	0.023
23	17:18	1	24	0.219	0.194	0.025
24	17:19	1	25	0.218	0.194	0.024
25	17:20	1	26	0.218	0.194	0.024
26	17:21	1	27	0.219	0.194	0.025
27	17:22	1	28	0.219	0.194	0.025
28	17:23	1	29	0.221	0.194	0.027
29	17:24	1	30	0.221	0.194	0.027
30	17:25	1	31	0.219	0.194	0.025
31	17:26	1	32	0.221	0.194	0.027
32	17:27	1	33	0.220	0.194	0.026
33	17:28	1	34	0.220	0.194	0.026
34	17:29	1	35	0.221	0.194	0.027

Sl no.	Time	Interval(min)	Time since pumping began (min)	Water Level (m)	Static Water Level (m)	Drawdown (m)
35	17:30	1	36	0.220	0.194	0.026
36	17:31	1	37	0.221	0.194	0.027
37	17:32	1	38	0.222	0.194	0.028
38	17:35	3	41	0.221	0.194	0.027
39	17:38	3	44	0.221	0.194	0.027
40	17:41	3	47	0.220	0.194	0.026
41	17:44	3	50	0.221	0.194	0.027
42	17:47	3	53	0.222	0.194	0.028
43	17:52	5	58	0.222	0.194	0.028
44	17:57	5	63	0.224	0.194	0.030
45	18:02	5	68	0.225	0.194	0.031
46	18:07	5	73	0.225	0.194	0.031
47	18:12	5	78	0.226	0.194	0.032
48	18:17	5	83	0.226	0.194	0.032
49	18:27	10	93	0.226	0.194	0.032
50	18:37	10	103	0.226	0.194	0.032
51	18:47	10	113	0.227	0.194	0.033
52	19:02	15	128	0.229	0.194	0.035
53	19:17	15	143	0.231	0.194	0.037
54	19:32	15	158	0.231	0.194	0.037
55	19:47	15	173	0.232	0.194	0.038
56	20:00	13	186	0.232	0.194	0.038
57	21:00	60	246	0.232	0.194	0.038
58	22:00	60	306	0.232	0.194	0.038
59	23:00	60	366	0.232	0.194	0.038
60	00:00	60	426	0.232	0.194	0.038
61	01:00	60	486	0.236	0.194	0.042
62	02:00	60	546	0.239	0.194	0.045
63	03:00	60	606	0.246	0.194	0.052
64	04:00	60	666	0.249	0.194	0.055
65	05:00	60	726	0.250	0.194	0.056
66	06:00	60	786	0.250	0.194	0.056
67	07:00	60	846	0.251	0.194	0.057
68	08:00	60	906	0.252	0.194	0.058
69	09:00	60	966	0.253	0.194	0.059
70	10:00	60	1026	0.256	0.194	0.062
71	11:00	60	1086	0.260	0.194	0.066
72	12:00	60	1146	0.262	0.194	0.068
73	13:00	60	1206	0.263	0.194	0.069
74	14:00	60	1266	0.266	0.194	0.072
75	15:00	60	1326	0.269	0.194	0.075

Sl no.	Time	Interval(min)	Time since pumping began (min)	Water Level (m)	Static Water Level (m)	Drawdown (m)
76	16:30	90	1416	0.268	0.194	0.074
77	17:55	85	1501	0.269	0.194	0.075
78	18:46	51	1552	0.272	0.194	0.078
79	20:30	104	1656	0.274	0.194	0.080
80	22:30	120	1776	0.276	0.194	0.082
81	00:30	120	1896	0.279	0.194	0.085
82	02:30	120	2016	0.281	0.194	0.087
83	04:30	120	2136	0.282	0.194	0.088
84	06:30	120	2256	0.283	0.194	0.089
85	08:30	120	2376	0.283	0.194	0.089
86	10:30	120	2496	0.284	0.194	0.090
87	12:08	98	2594	0.285	0.194	0.091
88	12:09	1	2595	0.286	0.194	0.092
89	12:10	1	2596	0.286	0.194	0.092
90	12:11	1	2597	0.286	0.194	0.092
91	12:12	1	2598	0.286	0.194	0.092
92	12:13	1	2599	0.286	0.194	0.092
93	12:14	1	2600	0.286	0.194	0.092
94	12:15	1	2601	0.286	0.194	0.092
95	12:16	1	2602	0.286	0.194	0.092
96	12:17	1	2603	0.286	0.194	0.092
97	12:18	1	2604	0.286	0.194	0.092
98	12:19	1	2605	0.286	0.194	0.092
99	12:20	1	2606	0.286	0.194	0.092
100	12:25	5	2611	0.286	0.194	0.092
101	12:30	5	2616	0.286	0.194	0.092
102	12:35	5	2621	0.286	0.194	0.092
103	12:40	5	2626	0.286	0.194	0.092
104	12:50	10	2636	0.286	0.194	0.092
105	13:00	10	2646	0.286	0.194	0.092
106	13:15	15	2661	0.286	0.194	0.092
107	13:30	15	2676	0.285	0.194	0.091
108	13:45	15	2691	0.285	0.194	0.091
109	14:00	15	2706	0.286	0.194	0.092
110	14:15	15	2721	0.286	0.194	0.092
111	14:30	15	2736	0.287	0.194	0.093
112	15:00	30	2766	0.287	0.194	0.093
113	15:30	30	2796	0.287	0.194	0.093
114	16:00	30	2826	0.287	0.194	0.093
115	19:30	210	3036	0.288	0.194	0.094
116	20:30	60	3096	0.288	0.194	0.094

Sl no.	Time	Interval(min)	Time since pumping began (min)	Water Level (m)	Static Water Level (m)	Drawdown (m)
117	21:30	60	3156	0.288	0.194	0.094
118	22:30	60	3216	0.288	0.194	0.094
119	23:30	60	3276	0.288	0.194	0.094
120	01:00	90	3366	0.289	0.194	0.095
121	02:30	90	3456	0.289	0.194	0.095
122	04:00	90	3546	0.289	0.194	0.095
123	05:30	90	3636	0.289	0.194	0.095
124	07:00	90	3726	0.289	0.194	0.095
125	08:30	90	3816	0.289	0.194	0.095
126	10:00	90	3906	0.289	0.194	0.095
127	11:43	103	4009	0.289	0.194	0.095
128	11:50	9	4018	0.289	0.194	0.095

6.2 Mechanical Sieve Analysis Data

Mechanical sieve analysis is done with the bore well samples, which is further used to determine the grain size (D) and other parameters like Coefficient of Uniformity to design the artificial gravel pack.

Figure 6.1: Performing Sieve Analysis at University Laboratory

6.2.1 Sieve Analysis of Main Well

Table 6.5: Sieve Analysis Data for Main Well

Sample Weight: 1000gms				Pan Weight: 371.67gms
Sieve Size (mm)	Weight Retained (gms)	Cumulative Weight Retained (gms)	% of Cum. Wt. Retained	% Finer
11.200	0.000	0.000	0.000	100.000
4.000	31.060	31.060	3.114	96.886
2.300	155.650	186.710	18.719	81.281
1.700	46.100	232.810	23.341	76.659
1.000	50.570	283.380	28.410	71.590
0.600	231.440	514.820	51.614	48.386
0.425	156.250	671.070	67.279	32.721
0.355	4.440	675.510	67.724	32.276
0.300	320.080	995.590	99.814	0.186
0.180	0.500	996.090	99.864	0.136
0.125	1.360	997.450	100.000	0.000
Pan	0.000	997.450	100.000	0.000
Calculation				
$D_{10} = 0.317$ mm, $D_{30} = 0.351$ mm, $D_{50} = 0.628$ mm, $D_{60} = 0.800$ mm				
Coefficient of Uniformity (C_u) $= 2.526$				

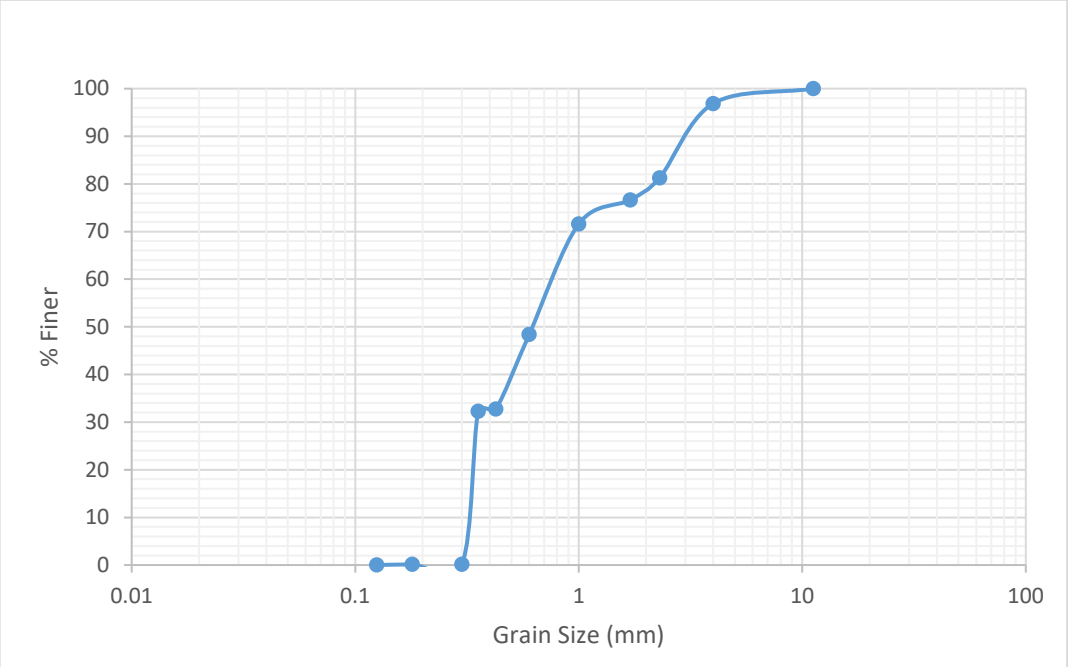

Figure 6.2: Grain Size Distribution Curve for Main Well

6.2.2 Sieve Analysis of Observation Well 1

Table 6.6: Sieve Analysis Data for Observation Well 1

Sample Weight: 1000gms				Pan Weight: 371.67gms
Sieve Size (mm)	Weight Retained (gms)	Cumulative Weight Retained (gms)	% of Cum. Wt. Retained	% Finer
25.000	0.000	0.000	0.000	100.000
19.000	42.300	42.300	4.241	95.759
11.200	149.480	191.780	19.226	80.774
4.000	108.250	300.030	30.078	69.922
2.300	94.330	394.360	39.534	60.466
1.700	50.900	445.260	44.637	55.363
1.000	98.760	544.020	54.538	45.462
0.600	231.820	775.840	77.778	22.222
0.425	105.470	881.310	88.351	11.649
0.355	3.400	884.710	88.692	11.308
0.300	110.450	995.160	99.764	0.236
0.180	2.350	997.510	100.000	0.000
Pan	0.000	997.510	100.000	0.000
Calculation				
$D_{10} = 0.349$ mm, $D_{30} = 0.734$ mm, $D_{50} = 1.321$ mm, $D_{60} = 2.245$ mm				
Coefficient of Uniformity (C_u) $= 6.443$				

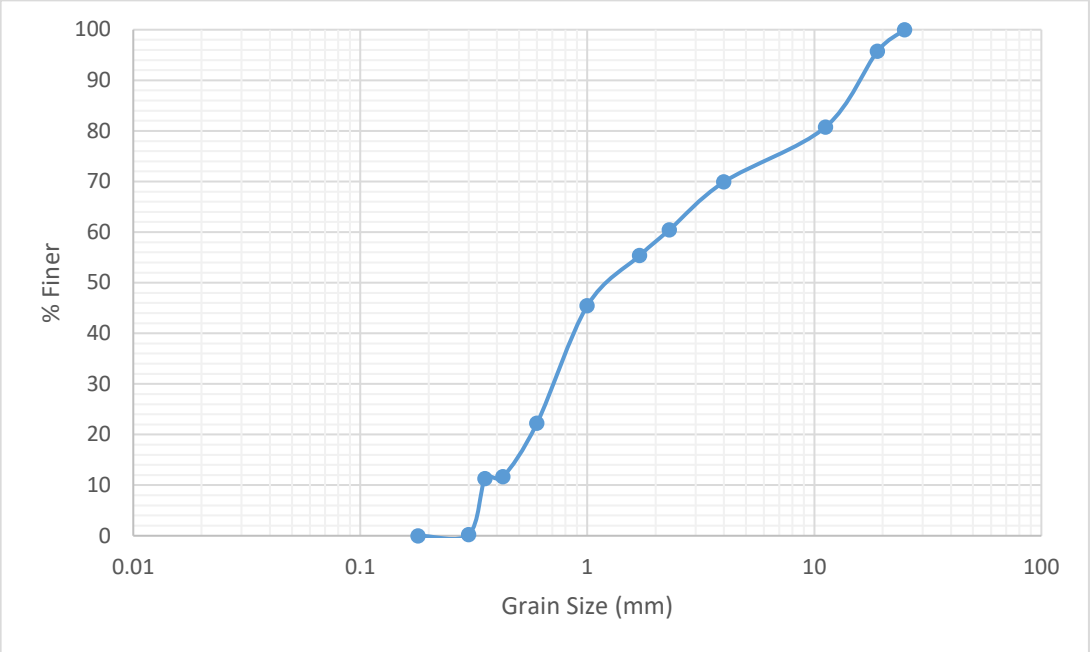

Figure 6.3: Grain Size Distribution Curve for Observation Well 1

6.2.3 Sieve Analysis of Observation Well 2

Table 6.7: Sieve Analysis Data for Observation Well 2

Sample Weight: 1000gms				Pan Weight: 371.67gms
Sieve Size (mm)	Weight Retained (gms)	Cumulative Weight Retained (gms)	% of Cum. Wt. Retained	% Finer
25.000	0.000	0.000	0.000	100.000
19.000	125.150	125.150	12.529	87.471
11.200	66.220	191.370	19.158	80.842
4.000	147.200	338.570	33.894	66.106
2.300	127.650	466.220	46.673	53.327
1.700	64.010	530.230	53.081	46.919
1.000	126.400	656.630	65.735	34.265
0.600	211.410	868.040	86.900	13.100
0.425	57.040	925.080	92.610	7.390
0.355	1.180	926.260	92.728	7.272
0.300	70.240	996.500	99.760	0.240
0.180	2.400	998.900	100.000	0.000
Pan	0.000	998.900	100.000	0.000
Calculation				
$D_{10} = 0.505$ mm, $D_{30} = 0.919$ mm, $D_{50} = 1.989$ mm, $D_{60} = 3.188$ mm				
Coefficient of Uniformity (C_u) $= 6.313$				

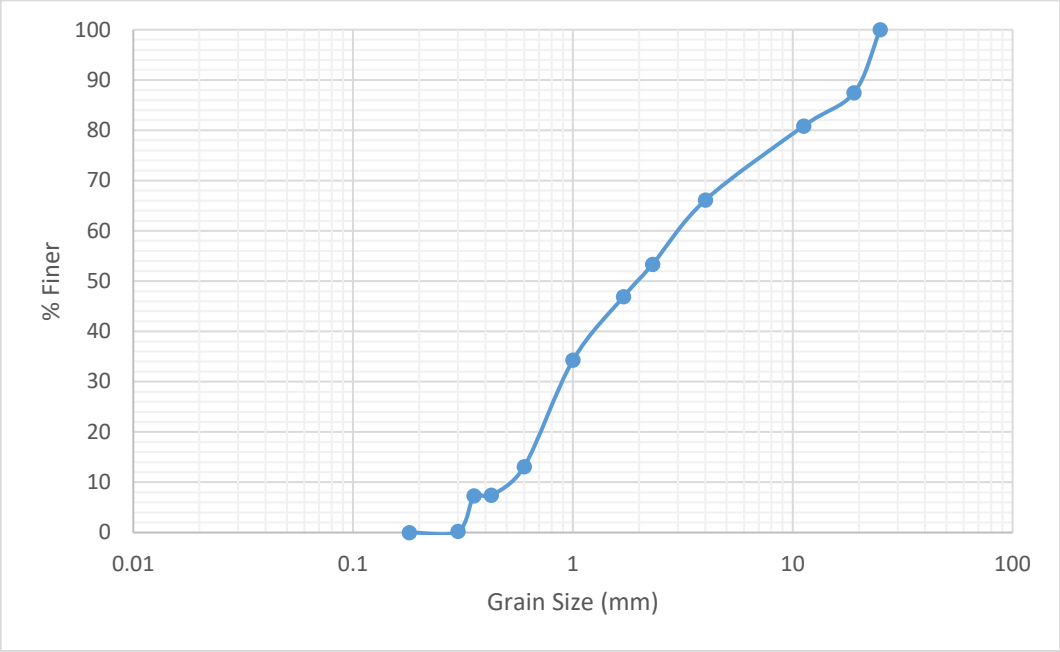

Figure 6.4: Grain Size Distribution Curve for Observation Well 2

6.2.4 Sieve Analysis of Observation Well 3

Table 6.8: Sieve Analysis Data for Observation Well 3

Sample Weight: 1000gms				Pan Weight: 371.67gms
Sieve Size (mm)	Weight Retained (gms)	Cumulative Weight Retained (gms)	% of Cum. Wt. Retained	% Finer
25.000	0.000	0.000	0.000	100.000
19.000	128.260	128.260	12.891	87.109
11.200	163.240	291.500	29.298	70.702
4.000	171.300	462.800	46.515	53.485
2.300	79.400	542.200	54.495	45.505
1.700	39.750	581.950	58.490	41.510
1.000	65.930	647.880	65.117	34.883
0.600	135.680	783.560	78.754	21.246
0.425	60.400	843.960	84.824	15.176
0.355	3.240	847.200	85.150	14.850
0.300	144.250	991.450	99.648	0.352
0.180	1.400	992.850	99.789	0.211
0.125	2.100	994.950	100.000	0.000
Calculation				
$D_{10} = 0.337$ mm, $D_{30} = 0.857$ mm, $D_{50} = 3.258$ mm, $D_{60} = 6.724$ mm				
Coefficient of Uniformity (C_u) = 19.978				

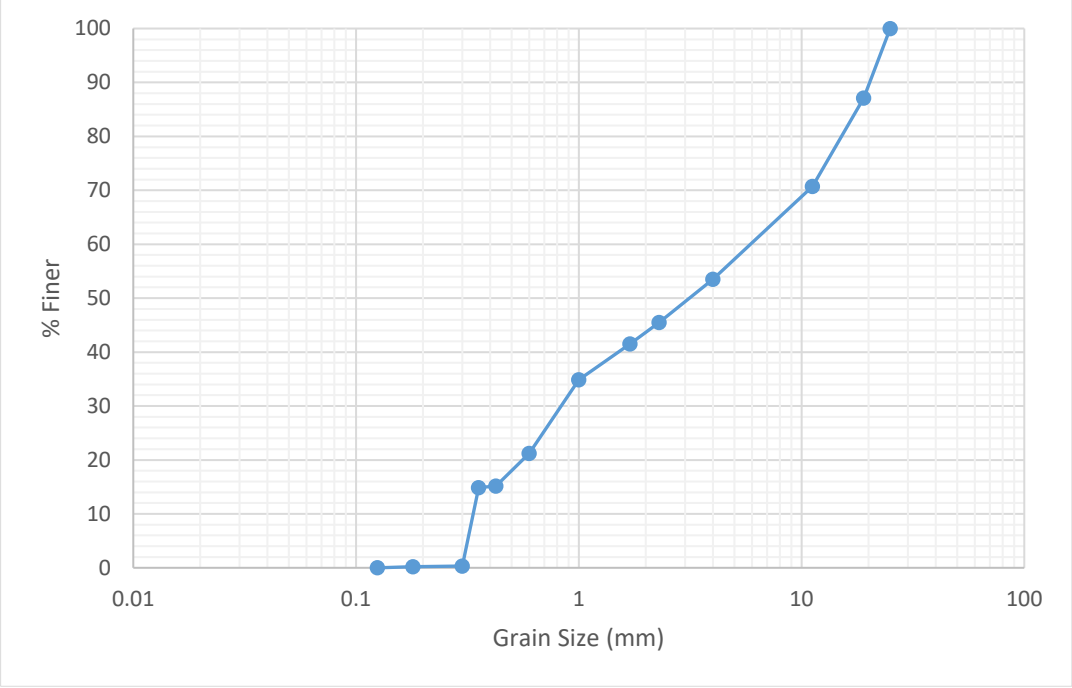

Figure 6.5: Grain Size Distribution Curve for Observation Well 3

6.2.5 Sieve Analysis of Slim-bore Upstream

Table 6.9: Sieve Analysis Data for Slim Bore Upstream

Sample Weight: 1000gms				Pan Weight: 371.67gms
Sieve Size (mm)	Weight Retained (gms)	Cumulative Weight Retained (gms)	% of Cum. Wt. Retained	% Finer
19.000	0.000	0.000	0.000	100.000
11.200	137.440	137.440	13.785	86.215
4.000	111.250	248.690	24.944	75.056
2.300	117.110	365.800	36.690	63.310
1.700	71.200	437.000	43.831	56.169
1.000	153.140	590.140	59.191	40.809
0.600	224.090	814.230	81.667	18.333
0.425	71.120	885.350	88.801	11.199
0.355	2.040	887.390	89.005	10.995
0.300	104.280	991.670	99.464	0.536
0.180	5.340	997.010	100.000	0.000
Pan	0.000	997.010	100.000	0.000
Calculation				
$D_{10} = 0.350$ mm, $D_{30} = 0.808$ mm, $D_{50} = 1.419$ mm, $D_{60} = 2.022$ mm				
Coefficient of Uniformity (C_u) = 5.781				

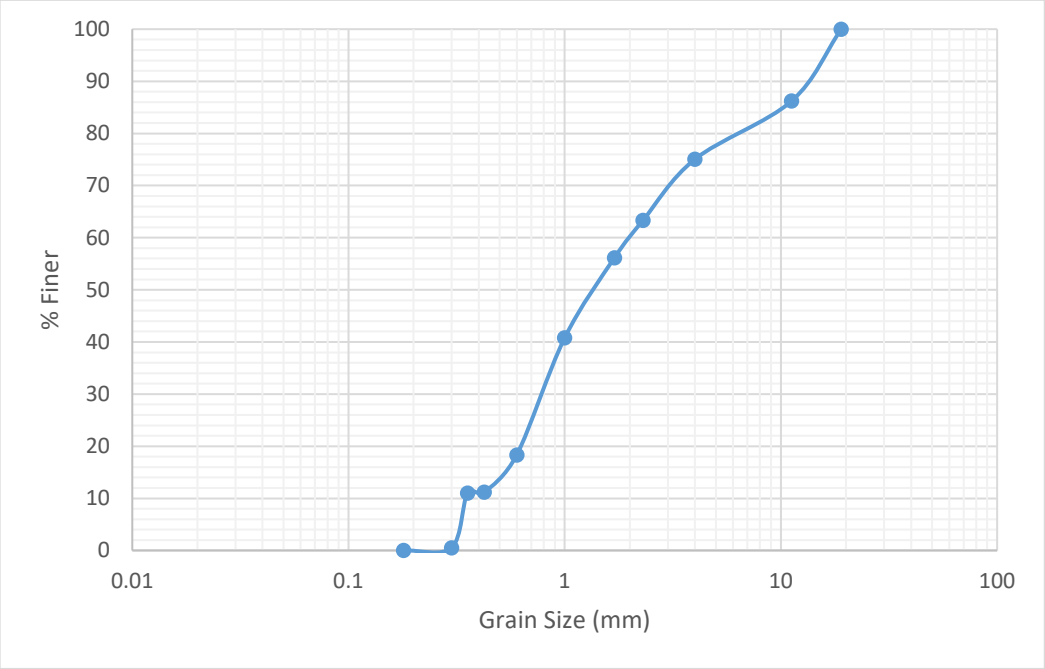

Figure 6.6: Grain Size Distribution Curve for Slim Bore Upstream

6.2.6 Sieve Analysis of Slim-bore Downstream

Table 6.10: Sieve Analysis Data for Slim Bore Downstream

Sample Weight: 1000gms				Pan Weight: 371.67gms
Sieve Size (mm)	Weight Retained (gms)	Cumulative Weight Retained (gms)	% of Cum. Wt. Retained	% Finer
25.000	0.000	0.000	0.000	100.000
19.000	18.200	18.200	1.825	98.175
11.200	114.620	132.820	13.322	86.678
4.000	133.500	266.320	26.712	73.288
2.300	109.800	376.120	37.725	62.275
1.700	66.170	442.290	44.362	55.638
1.000	127.800	570.090	57.180	42.820
0.600	225.680	795.770	79.816	20.184
0.425	87.980	883.750	88.640	11.360
0.355	2.420	886.170	88.883	11.117
0.300	109.540	995.710	99.870	0.130
0.180	1.100	996.810	99.980	0.020
0.125	0.200	997.010	100.000	0.000
Pan	0.000	997.010	100.000	0.000
Calculation				
$D_{10} = 0.349$ mm, $D_{30} = 0.773$ mm, $D_{50} = 1.392$ mm, $D_{60} = 2.094$ mm				
Coefficient of Uniformity (C_u) = 5.994				

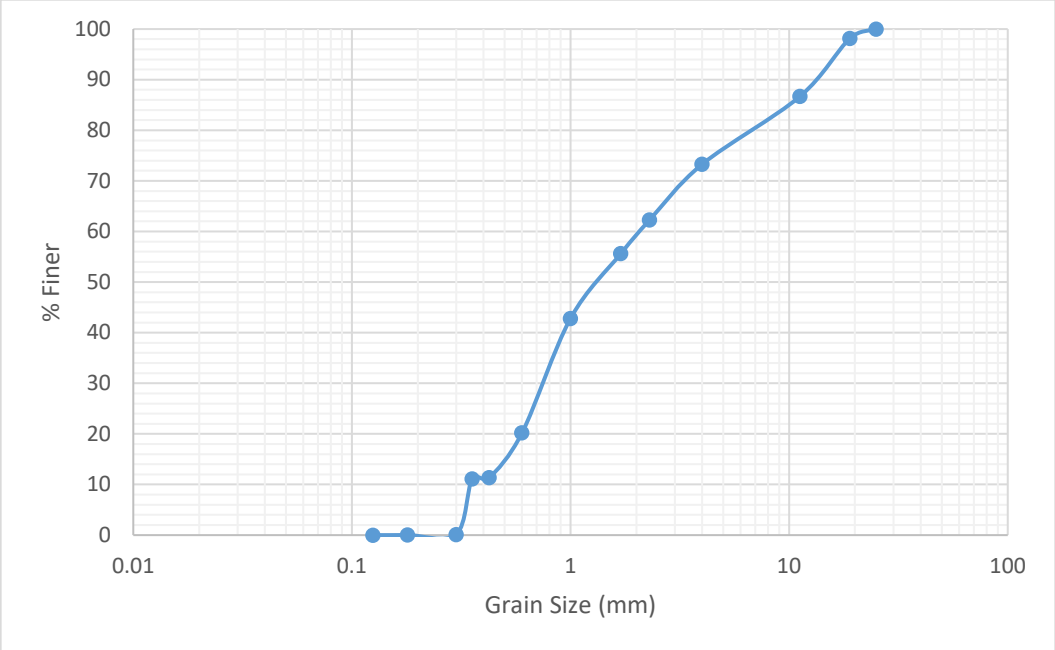

Figure 6.7: Grain Size Distribution Curve for Slim Bore Downstream

Chapter 7 Results & Discussions

The study is being carried out by collecting data and performing the required operations to design suitable infiltration gallery to provide sufficient yield to meet the water demand.

7.1 Water Demand

For designing the infiltration gallery system for a period of 30 years, the total per capita demand and the population for the next 30 years is to be calculated. As discussed in the previous chapter, the per capita demand for Jhargram Municipality is given in Table 7.1.

Table 7.1: Per capita demand of Jhargram Municipality

Sl No.	Use	Demand (lpcd)
1	Domestic Use	150
2	Commercial Use	25
3	Public Use	10
4	Theft	10
5	Losses	30
	Total	225 lpcd

7.1.1 Population Forecasting

The Population of Jhargram Municipality has been collected from the past census data of the country (source: Office of the Registrar General & Census Commissioner, India) is given in Table 7.2.

Table 7.2: Population of Jhargram Municipality

Year	Population
1971	19237
1981	25502
1991	42094
2001	53145
2011	61682

The method of Logistic Curve has been used to forecast the data for next 30 years i.e. 2051. The equation of logistic curve used as given in Eqn 4.5

$$P = \frac{P_s}{1 + me^{nt}}$$

where, P_0 = Population at 1971 = 19237

P_1 = Population at 1991 = 42094

P_2 = Population at 2011 = 61682

t_1 = 20 years

t_2 = 40 years

$$\Longrightarrow P_s = \frac{2P_0P_1P_2 - P_1^2(P_0 + P_2)}{P_0P_2 - P_1^2}$$

$$\Rightarrow P_s = \frac{(2 \times 19237 \times 42094 \times 61682) - 42094^2\ (19237 + 61682)}{19237 \times 61682 - 42094^2}$$

$$\therefore P_s = 74293$$

$$\Rightarrow m = \frac{P_s - P_0}{P_0} = \frac{74293 - 19237}{19237} = 2.862$$

$$\Rightarrow n = \frac{2.303}{t_1}\log\left(\frac{P_0(P_s - P_1)}{P_1(P_s - P_0)}\right) = \frac{2.303}{20}\log\left(\frac{19237(74293 - 42094)}{42094(74293 - 19237)}\right) = -0.066$$

For estimating the population of the year 2051, we will have $t = (2051 - 1971) = 80$ years.

$$\therefore P = \frac{P_s}{1 + me^{nt}} = \frac{74293}{1 + 2.862\ e^{(-0.066 \times 80)}} = 73226$$

The decadal population has been calculated and shown in Table 7.3.

Table 7.3: Population forecasting of Jhargram Municipality

Year	Population
1971	19237
1981	25502
1991	42094
2001	53145
2011	61682
2022	67612
2031	70448
2051	73226

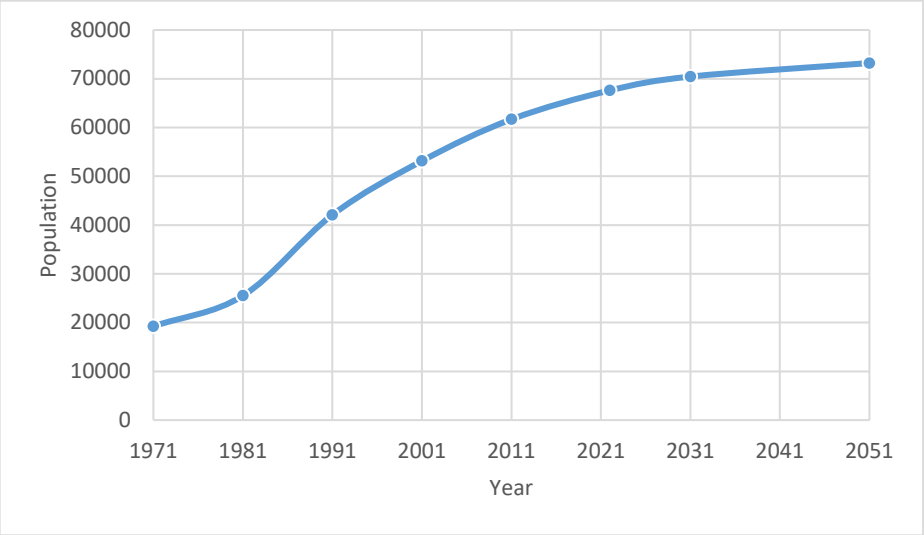

Figure 7.1: Logistic Variation of Population of Jhargram Municipality

Therefore the total design demand of the infiltration gallery is

$$\text{Per capita demand per day} \times \text{Total Population} = 225 \text{ lpcd} \times 73226$$

$$= 16.5 \text{ MLD (Million Litres per Day)}$$

7.2 Analysis of Pumping Test Data

As per the pumping data collected for the Main Well (Table 6.1), the corresponding variation with time has been shown below,

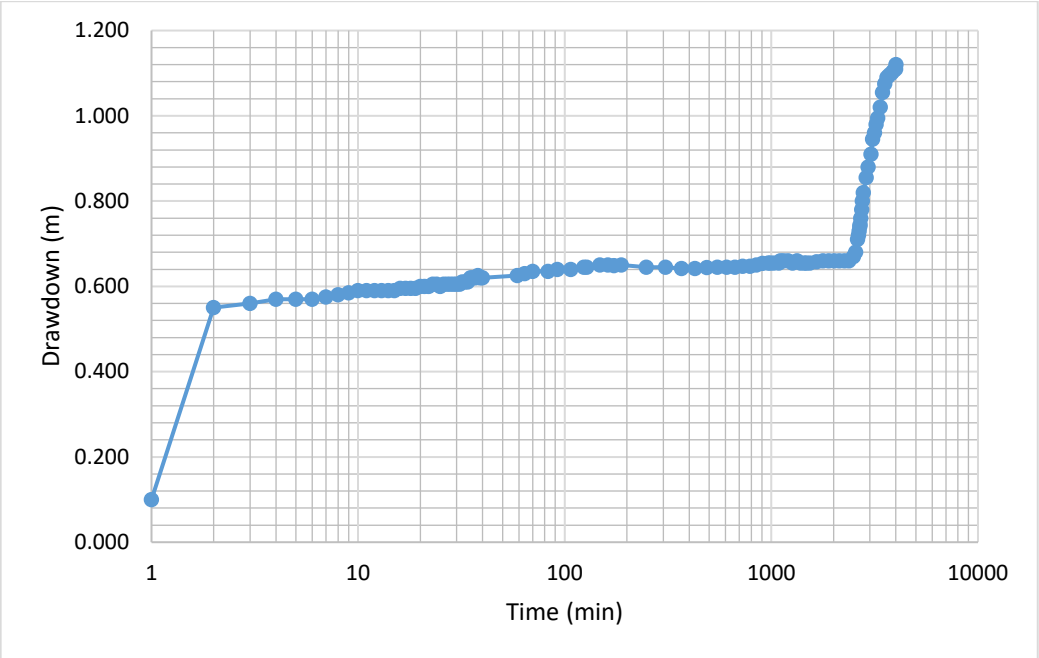

Figure 7.2: Variation of Drawdown vs Time for Main well Pumping Test

As discussed in the earlier chapters about the study area, where the positions of the main well and the observation wells have been shown. Below table shows the depth of static water level in the wells and their positions with respect to the main well.

Table 7.4: Position and Static Water level of Wells

Well Id.	Distance from Main Well (m)	Duration of monitoring (hrs)	Depth of water from Datum (Bed level) / Static Water level (m)	Pump Discharge (m3/hr)
Main Well	-	67	0.430	60
Obs Well 1	20	67	0.656	60
Obs Well 2	30	67	0.620	60
Obs Well 3	40	67	0.194	60

7.2.1 Determination of Aquifer Parameters

Neuman's Straight-Line Method has been used to determine the hydraulic parameters. The transmissivity and specific yield of the aquifer are determined by fitting a straight line through the late-time data. The early-time response provides another estimate of transmissivity, and a confined storativity value for the aquifer can be obtained.

7.2.1.1 Analysis of Observation Well 1

The drawdown variation obtained at observation well 1 following the pumping test with a constant discharge of 60m^3/hr at the Main Well is given as per Table 6.2.

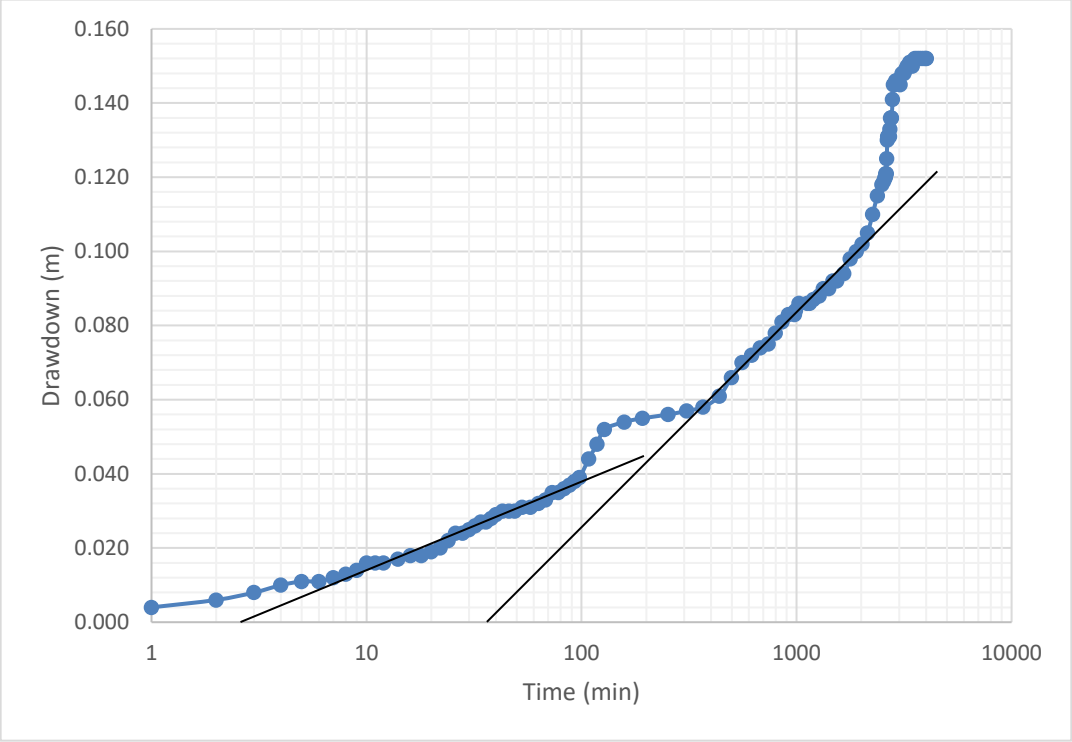

Figure 7.3: Variation of Drawdown vs Time for Observation Well 1

Straight-line fitted through the data as shown in the plot for the calculation of hydraulic parameters.

⇒ Transmissivity of the aquifer can be determined using Eqn 4.15

$$T = \frac{2.3Q}{4\pi\Delta s}$$

where, $Q = 60\ m^3/hr$

$\Delta s = (0.092 - 0.024) = 0.068$ m (from Figure 7.3)

$$\therefore T = \frac{2.3(60 \times 24)}{4 \times \pi \times 0.068} = 3875.89\ m^2/day \approx 3875\ m^2/day$$

⇒ Specific yield of the aquifer can be determined using Eqn 4.16

$$S_y = \frac{2.25Tt_{0y}}{r^2}$$

where, $t_{0y} = 24$ mins (from Figure 7.3)

$r = 20$ m (from Table 7.4)

$$\therefore S_y = \frac{2.25 \times 3875 \times \left(24 \times \frac{1}{1440}\right)}{20^2} = 0.3633$$

⇒ The Confined storativity can be determined using Eqn 4.17

$$S = \frac{2.25Tt_{0s}}{r^2}$$

where, $t_{0s} = 2$ mins (from Figure 7.3)

$$\therefore S = \frac{2.25 \times 3875 \times \left(2 \times \frac{1}{1440}\right)}{20^2} = 0.03$$

⇒ The Radius of Influence can be determined using Eqn 4.12

$$Q = \frac{2\pi Ts_w}{\ln\frac{R}{r_w}}$$

where, s_w = Drawdown at the end of pumping test $= 0.152$ m

$r_w = r = 20$ m (from Figure 7.3)

$$\therefore 60 \times 24 = \frac{2 \times \pi \times 3875 \times 0.152}{\ln\left(\frac{R}{20}\right)}$$

$$\rightarrow R \approx 260\ m$$

7.2.1.2 Analysis of Observation Well 2

The drawdown variation obtained at observation well 2 following the pumping test with a constant discharge of $60 m^3/hr$ at the Main Well as per Table 6.3.

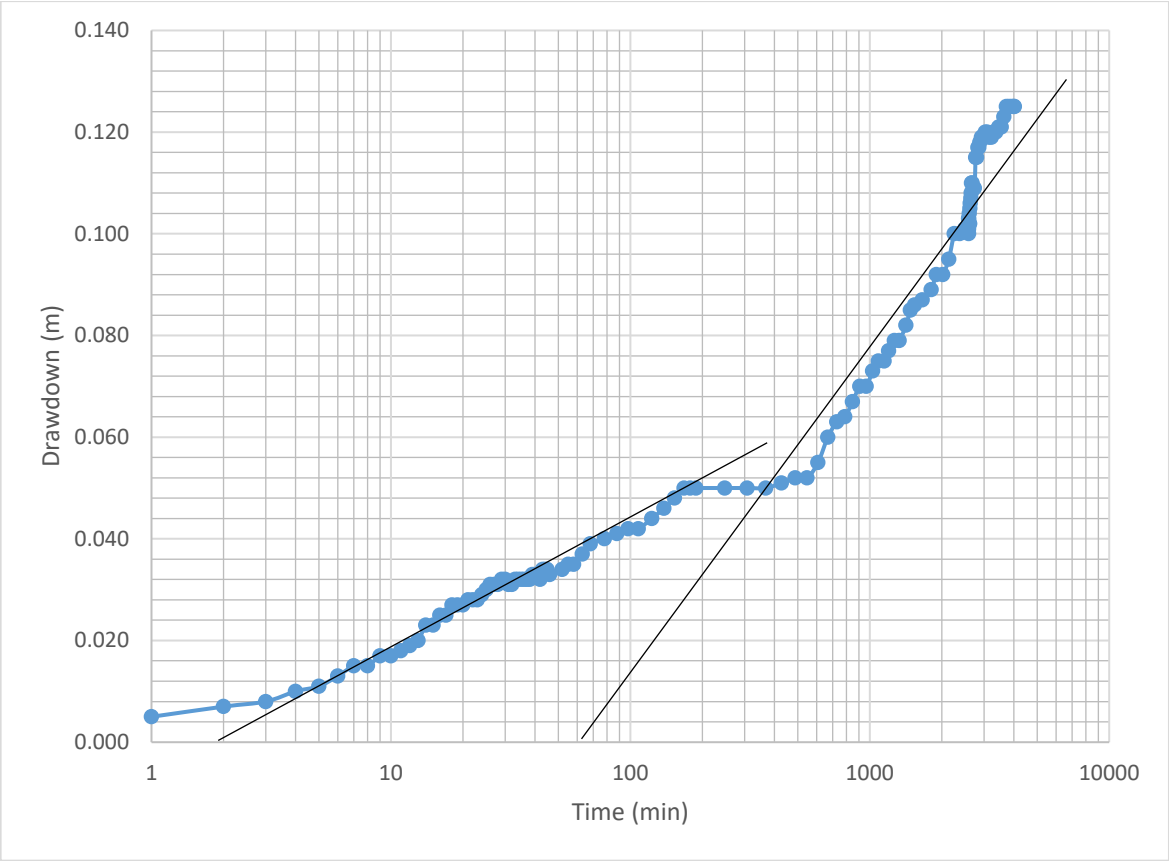

Figure 7.4: Variation of Drawdown vs Time for Observation Well 2

Straight-line fitted through the data as shown in the plot for the calculation of hydraulic parameters.

⇒ Transmissivity of the aquifer can be determined using Eqn 4.15

$$T = \frac{2.3Q}{4\pi\Delta s}$$

where, $Q = 60\ m^3/hr$

$\Delta s = (0.080 - 0.010) = 0.07$ m (from Figure 7.4)

$$\therefore T = \frac{2.3(60 \times 24)}{4 \times \pi \times 0.07} = 3765.15\ m^2/day \approx 3765\ m^2/day$$

⇒ Specific yield of the aquifer can be determined using Eqn 4.16

$$S_y = \frac{2.25Tt_{0y}}{r^2}$$

where, $t_{0y} = 50$ mins (from Figure 7.4)

$r = 30$ m (from Table 7.4)

$$\therefore S_y = \frac{2.25 \times 3765 \times \left(50 \times \frac{1}{1440}\right)}{30^2} = 0.3268$$

⇒ The Confined storativity can be determined using Eqn 4.17

$$S = \frac{2.25Tt_{0s}}{r^2}$$

where, $t_{0s} = 2$ mins (from Figure 7.4)

$$\therefore S = \frac{2.25 \times 3765 \times \left(2 \times \frac{1}{1440}\right)}{30^2} = 0.013$$

⇒ The Radius of Influence can be determined using Eqn 4.12

$$Q = \frac{2\pi Ts_w}{\ln \frac{R}{r_w}}$$

where, s_w = Drawdown at the end of pumping test = 0.125 m

$r_w = r = 30$ m (from Table 7.4)

$$\therefore 60 \times 24 = \frac{2 \times \pi \times 3765 \times 0.125}{\ln\left(\frac{R}{30}\right)}$$

$$\rightarrow R \approx 234 \text{ m}$$

7.2.1.3 Analysis of Observation Well 3

The drawdown variation obtained at observation well 3 following the pumping test with a constant discharge of $60 m^3/hr$ at the Main Well as per Table 6.4.

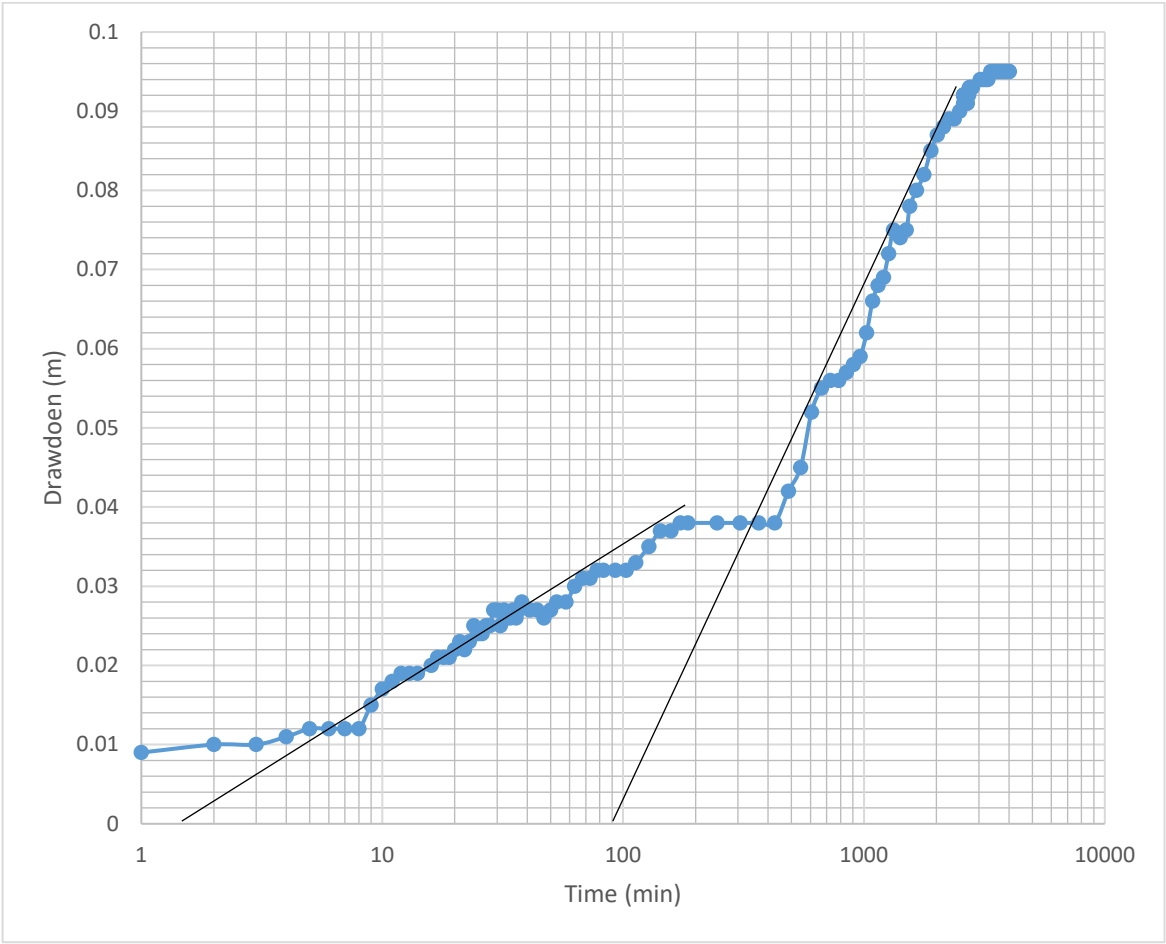

Figure 7.5: Variation of Drawdown vs Time for Observation Well 3

Straight-line fitted through the data as shown in the plot for the calculation of hydraulic parameters.

⇒ Transmissivity of the aquifer can be determined using Eqn 4.15

$$T = \frac{2.3Q}{4\pi\Delta s}$$

where, $Q = 60\ m^3/hr$

$\Delta s = (0.072 - 0.001) = 0.071$ m (from Figure 7.5)

$$\therefore T = \frac{2.3(60 \times 24)}{4 \times \pi \times 0.071} = 3712.12\ m^2/day \approx 3712\ m^2/day$$

⇒ Specific yield of the aquifer can be determined using Eqn 4.16

$$S_y = \frac{2.25Tt_{0y}}{r^2}$$

where, $t_{0y} = 90$ mins (from Figure 7.5)

$r = 40$ m (from Table 7.4)

$$\therefore S_y = \frac{2.25 \times 3712 \times \left(90 \times \frac{1}{1440}\right)}{40^2} = 0.3263$$

⇒ The Confined storativity can be determined using Eqn 4.17

$$S = \frac{2.25Tt_{0s}}{r^2}$$

where, $t_{0s} = 2$ mins (from Figure 7.5)

$$\therefore S = \frac{2.25 \times 3712 \times \left(2 \times \frac{1}{1440}\right)}{40^2} = 0.007$$

⇒ The Radius of Influence can be determined using Eqn 4.12

$$Q = \frac{2\pi Ts_w}{\ln \frac{R}{r_w}}$$

where, s_w = Drawdown at the end of pumping test $= 0.095$ m

$r_w = r = 40$ m (from Table 7.4)

$$\therefore 60 \times 24 = \frac{2 \times \pi \times 3712 \times 0.095}{\ln\left(\frac{R}{40}\right)}$$

$$\rightarrow R \approx 186 \text{ m}$$

After the analysis of the pumping test of the three observation wells, the aquifer properties with respect to the main well (380 m from the left bank) have been calculated as follows:

Table 7.5: Aquifer Properties of Observation wells w.r.t. Main Well

Well Id	Distance (m)	Storativity	Discharge (m^3/hr)	Transmissivity (m^2/day)	Maximum Drawdown (m)
Main Well	-	-	60	-	1.120
Obs 1	20	0.3633	60	3875	0.152
Obs 2	30	0.3268	60	3765	0.125
Obs 3	40	0.3263	60	3712	0.095
Average Transmissivity				3784 m^2/day	

All the distances of the observation wells are measured with respect to the respective main wells. The diameter of the main well is 200 mm and the depth is 9.75 m. The diameters of the observation wells are 50 mm each and the depth is 9.75 m.

7.2.2 Projected Drawdown

Projected Drawdown can be calculated using Eqn 5.1

$$\frac{Q_1}{Q_2} = \frac{s_1}{s_2}$$

where, $Q_1 = 60\ m^3/hr = 1440\ m^3/day$

$Q_2 = 16.5\ MLD = 16500\ m^3/day$

For Observation Well 1, $s_1 = 0.152$ m (from Table 7.5)

$$\therefore \frac{Q_1}{Q_2} = \frac{s_1}{s_2}$$

$$\Rightarrow \frac{1440}{16500} = \frac{0.152}{s_2}$$

$$\Rightarrow s_2 = 1.742\ m$$

Similarly the projected drawdowns of the other wells are shown in Table 7.6

Table 7.6: Projected Drawdown of Observation Wells

Well Id	Actual Discharge (m^3/day)	Projected Discharge (m^3/day)	Radius of Influence (m)	Projected Drawdown (m)
Obs 1	1440	16500	260	1.742
Obs 2	1440	16500	234	1.432
Obs 3	1440	16500	186	1.089

7.2.3 Recuperation Test

At the end of the pumping test when the pumping has been stopped, the water level in pumping well and observation wells will begin to rise. This is referred to as recovery of the groundwater level, while measurements of drawdown below the original static water level (prior to pumping) during this recovery period are known as residual drawdowns.

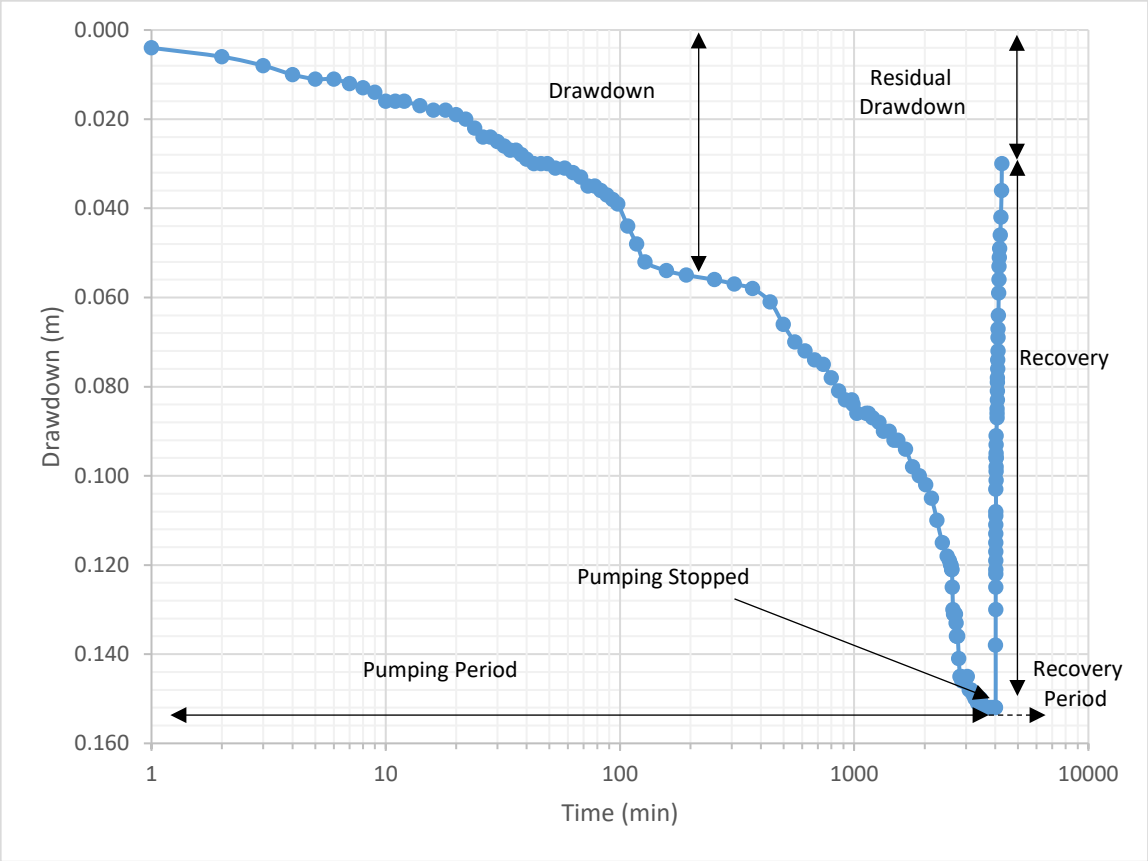

Figure 7.6: Variation of Drawdown with Time representing recuperation data for Observation Well 1

In the present study maximum drawdown in the observation well 1 is 0.152 m and the residual drawdown is 0.03 m which suggests 80.3 % recovery.

Table 7.7: Residual Drawdown and Percentage Recovery of observation wells

Well Id	Maximum Drawdown (m)	Residual Drawdown (m)	Percentage Recovery (%)
Obs 1	0.152	0.030	80.3
Obs 2	0.125	0.024	80.8
Obs 3	0.095	0.019	80.0

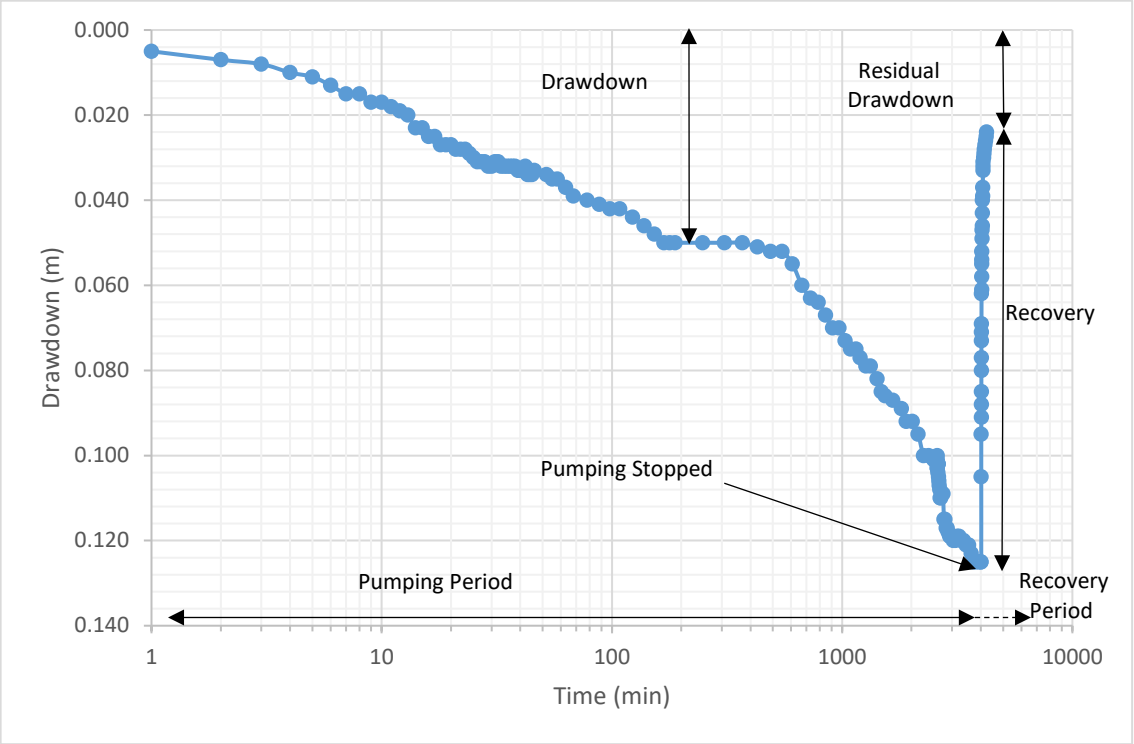

Figure 7.7: Variation of Drawdown with Time representing recuperation data for Observation Well 2

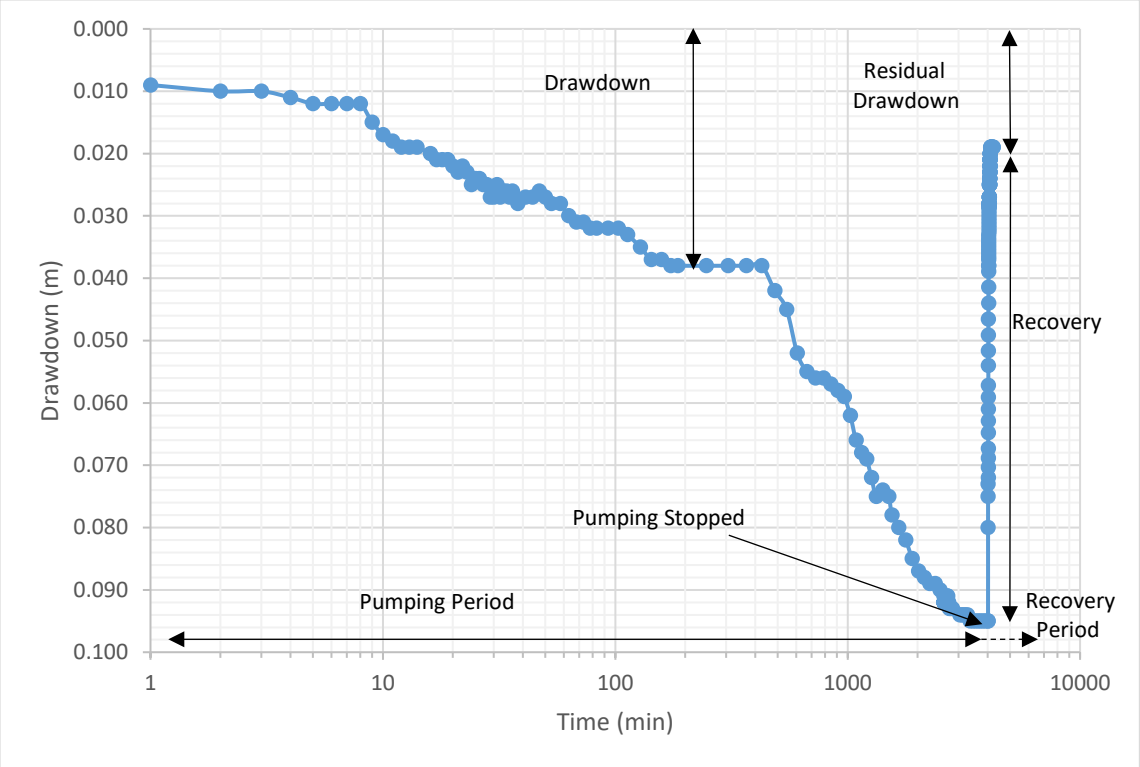

Figure 7.8: Variation of Drawdown with Time representing recuperation data for Observation Well 3

7.3 Design of Infiltration Gallery

7.3.1 Design as per CPHEEO

As discussed in the previous chapters the length of the infiltration gallery by considering equilibrium conditions as per CPHEEO Manual on Water Supply Treatment (1999) (page 66), GOI as given in Eqn 4.20.

$$L = \frac{1}{K}\left(\frac{2RQ}{H^2 - h^2}\right)$$

where, Q = Rate of flow in $m^3/day = 16500\ m^3/day$

K = Permeability constant in $m/d = \frac{T}{b}$ (where b = depth of aquifer)

L = Length of the infiltration gallery in m

H = Initial depth of water level in m =(b − static water level of main well),

h = Final depth of water level in m = Maximum allowable drawdown

R = Radius of influence in m

To calculate the Maximum allowable drawdown, the values of the projected drawdown can be considered as per Table 7.6. For Observation Well 1, the projected drawdown has come out to be 1.742 m. On the other hand, the pumping test was done in the winter season of the year, when the drawdown is relatively low due to the reasons other than pumping. Therefore, to consider the drawdown at the worst summer season, a safety factor of 2.5 can be used.

$$\Rightarrow h = 1.742 \times 2.5 = 4.3\ m$$

$$\Rightarrow H = 9.5 - 0.43 = 9.07\ m$$

$$\Rightarrow K = \frac{T}{b} = \frac{3784}{9.5} = 398.32\ m/day$$

$$\Rightarrow R = 260\ m$$

$$\therefore L = \frac{1}{K}\left(\frac{2RQ}{H^2 - h^2}\right) = \frac{1}{398.32}\left(\frac{2 \times 260 \times 16500}{9.07^2 - 4.3^2}\right) = 337.76\ m \approx 340\ m$$

Therefore as per CPHEEO design, the length of the infiltration gallery can be provided for a length of 340 m, with a collector well at a position of Slim-bore B1, and the two strainers of each 170 m can be placed towards slim-bore upstream and slim-bore downstream at an angle of 120° to 135° .

7.3.2 Design as per Ferris Drain Function

According to Ferris drain function D(u), the allowable drawdown can be calculated using Eqn 4.21 and Eqn 4.22.

$$s = \frac{Qx}{2T} D(u)$$

$$u^2 = \frac{x^2 S}{4Tt}$$

where,x = Distance from collector well (B1) to the point of observation = 45 m

s = Allowable drawdown= 4.3 m

S = Storativity= 0.3388

T = Transmissivity= 3784 m^2/day

t = Time to attain allowable drawdown= 250 days (non monsoon period of year)

$$\Rightarrow u^2 = \frac{x^2 S}{4Tt} = \frac{45^2 \times 0.3388}{4 \times 3784 \times 250} = 1.813 \times 10^{-4}$$

For $u^2 = 1.813 \times 10^{-4}$, D(u) = 42 (from Table 4.3)

For an allowable drawdown of 4.3 m,

$$\Rightarrow s = \frac{Qx}{2T} D(u)$$

$$\Rightarrow 4.3 = \frac{Q \times 45}{2 \times 3784} \times 42$$

$$\Rightarrow Q = 17.22 \text{ } m^3/\text{day/m of gallery}$$

Length of the Gallery required= $\frac{16500}{17.22}$ = 958.19 m ≈ 960 m

Therefore, as per the Ferris Drain Function Design of Infiltration Gallery, length of the gallery has come out to be 940 m, which is heavily overestimating the length as compared to the CPHEEO design. However, if it is to be provided as the design length then the same can be done as 470 m from B1 towards B U/S and B D/S each at an angle of 120° to 135° .

7.4 Estimation of Scour Depth

The mean scour depth below the Highest Flood Level (HFL) in a natural channel can be calculated in from following Eqn 4.23 as given in IRC: 78-2014:

$$d_{sm} = 1.34\left(\frac{D_b^2}{K_{sf}}\right)^{\frac{1}{3}}$$

where, D_b = Design discharge for substructure/foundation per meter width of the effective waterway.

K_{sf} = Silt factor for a representative sample of bed material obtained up to the level anticipated deepest scour.

The value of D_b may be determined by dividing the design discharge for foundation by lower of theoretical and actual effective linear waterway as given in IRC: 5:2015.

K_{sf} is given by the expression, $K_{sf} = 1.76\sqrt{d_m}$

where, d_m being the weighted mean diameter in millimetre.

$d_m = 0.725$ (from Table 4.4)

$\Rightarrow K_{sf} = 1.5$ (from Table 4.4)

To calculate D_b we can use Dickens Formula (1865) as given in Eqn 4.24

$$Q_p = C_D A^{3/4}$$

$C_D = 6$

A = 9850 sq km, (Sengupta et. al (2011))

$$\Rightarrow Q_p = 6 \times 9850^{3/4}$$

$$\Rightarrow Q_p \approx 6000 \text{ cumecs}$$

Width of the River = 760 m

$\therefore$ Flow per unit width of river (D_b) = 6000/760 = 7.9 cumecs

$$\Rightarrow d_{sm} = 1.34\left(\frac{D_b^2}{K_{sf}}\right)^{\frac{1}{3}} = 1.34 \times \left(\frac{7.9^2}{1.5}\right)^{\frac{1}{3}} = 4.65 \text{ m}$$

The maximum depth of scour below the highest flood level for the protection required=$2d_{sm} = 2 \times 4.65 = 9.3$ m

During the high flow, average depth of water taken = 7 m

So, the scouring below the bed level = $9.3 - 7.0 = 2.3$ m

Boulder Sausage work can be at a depth of 1m below the bed level of $= 2.3 - 1 = 1.3$ m

We can provide a collector well of 5m diameter at the location of Slim-bore B1 to collect the infiltrated water from the gallery. Considering the pump will operate for 22 hours a day.

$$\text{Designated Water requirement} = \frac{16500\ \text{m}^3/\text{day}}{22\ \text{hours}} = 750\ \text{m}^3/\text{hour} = 12500\ \text{lpm}$$

Considering the Infiltration Gallery Strainer size = 600 mm in diameter.

Depth of the Aquifer = 9.75 m

$\therefore$ Depth of Strainer $= \frac{2}{3} \times 9.75 = 6.5$ m

Therefore, the Strainer of the Infiltration Gallery can be placed at a depth of 6.5 m from the river bed level.

Keeping 15% opening area, the velocity at the entry of Strainer to yield 12500 lpm is,

$$Q = p\pi DlV \qquad \text{Eqn 7.1}$$

where, Q = Discharge = 12500 lpm

p = Percentage area opening

D = Diameter of Strainer = 600 mm

l = Length of Strainer = 340 m

V = Entrance velocity

$$\Rightarrow V = Q/(p\pi Dl) = 0.217\ \text{cm/sec}$$

The maximum permissible entrance velocity is 0.3 cm/sec, therefore the dimensions of the strainer can be accepted.

7.5 Design of Gravel Pack

As per the Ground Water Manual (1995), it is acceptable but the less desirable criterion is to use gravel pack material with C_u (Uniformity Coefficient) of aquifer material between 2.5 and 5. However artificial gravel pack is required when the aquifer material is homogeneous with a uniformity coefficient (C_u) of less than 3 and an effective grain size (D_{10}) of less than 0.25 mm.

According to the mechanical sieve analysis shown in the above sections, artificial gravel packing is not desirable because the C_u of the aquifer material is greater than 3, and D_{10} is greater than 0.25 mm. However the uniformity coefficient for main well is 2.526 as calculated in Table 6.5, and keeping a long design period in mind an artificial gravel pack may be introduced as per the in-situ conditions.

As discussed in the Section 4.6.4.3, if an artificial gravel pack is desired since $C_u <$ 3.0 for the coarse sand aquifer of Main Well, then, from the above mechanical sieve analysis data,

D_{30} (Gravel pack material) = 4 to 6 times D_{30} of aquifer material.

= 4 to 6 times 0.351 mm (from Table 6.5)

= 1.4 mm to 2.1 mm

With these points for D_{30} of gravel pack material, smooth curves are drawn such that C_u for the gravel pack material is 2.5.

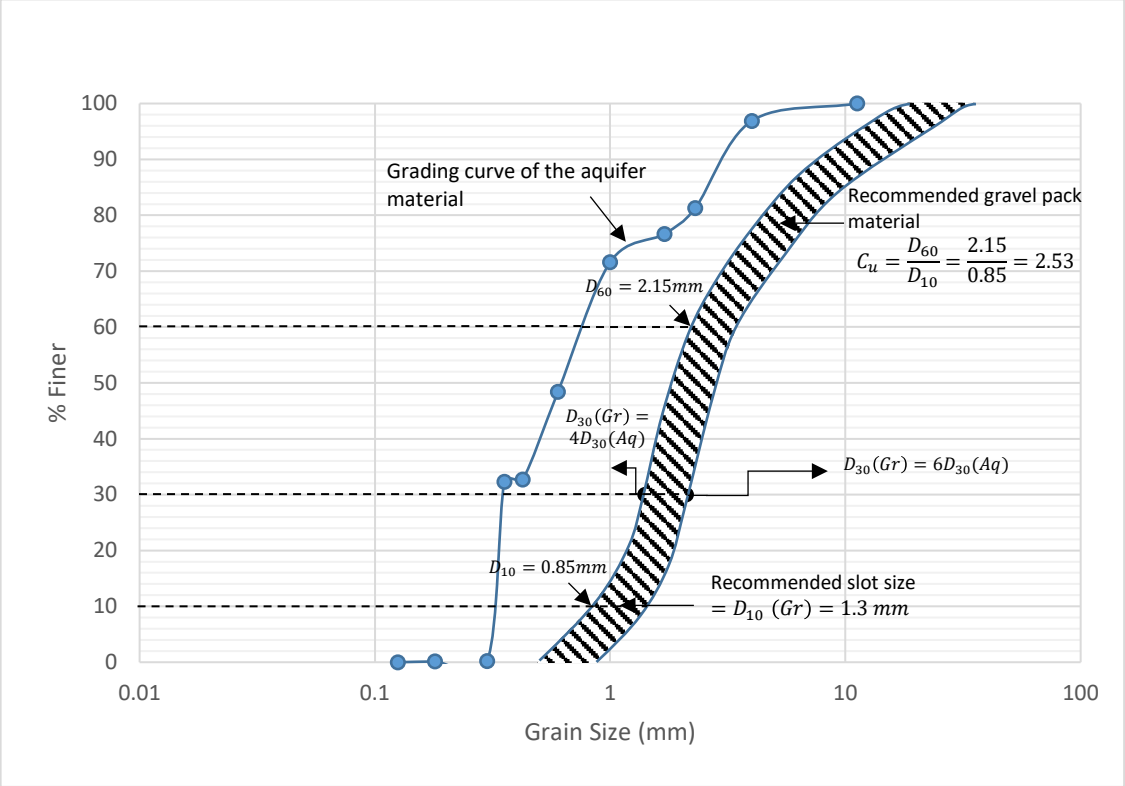

Figure 7.9: Grain Size Distribution for Artificial Gravel Pack

The shaded area in Figure 7.9, shows the recommended gravel pack material; clean pea gravels of size 1 to 10 mm may be used. Slot size may keep D_{10} of the gravel pack material which is 1.2 mm. The thickness of the artificial gravel pack may be 15 to 20 cm.

Check for Drawdown

$$K = CD_{10}{}^2 \quad (D_{10} \text{ in cm from Figure 7.9})$$

$$\Rightarrow K = 120 \times 0.13^2$$

$$\Rightarrow K = 2.028 \text{ cm/ sec}$$

Since Allen Hazen's formula overestimates K, taking 2/3 of the value

$$K = \frac{2}{3} \times 2.028 = 1.352 \text{ cm/sec}$$

$$\text{Transmissivity} = \text{Kb} = \frac{1.352}{100} \times 9.75 = 0.13182 \text{ m}^3/\text{sec/m}$$

$$\text{Specific Capacity} = \frac{\text{T}}{1.4} \times \text{Efficiency of Well (60\%)} = 0.0565 \text{ m}^3/\text{sec/m}$$

$$\text{Probable Drawdown} = \frac{12.5}{60 \times 0.0565} = 3.69 \text{ m} < 4.3 \text{ m, which is permissible.}$$

As per the CPHEO Manual (1999), galvanised pipes having bigger slots about 3 mm in width 750 mm in length are provided, on the basis of that slot size may be recommended ranging between 1.5 mm to 4 mm.

From the mechanical sieve analysis, it is very clear that only few positions are required to be provided with a gravel pack system. But the aquifer characteristic is not only the sole reason for a gravel pack. Clogging of the media is a very big problem in order to operate this type of substructures. Kalwa et. al. (2021) described about the necessity of a gravel pack in order to minimize the clogging problems to ensure less maintenance cost. Therefore we shall provide a 15 cm to 20 cm thick layer of gravel pack with clean pea gravels.

Chapter 8 Conclusion

It is very crucial and essential to investigate the vulnerability of groundwater aquifer system in the target area of Jhargram Municipality, West Bengal. The entire region is almost filled up with irregular groundwater extraction practices without having the knowledge of its influence to the nearest extraction point. This practice which can turn into a drastic situation of very less availability of groundwater resulting to a huge scarcity of both drinking water and domestic water supply in upcoming decades. Though several restrictions have been imposed since the last decade, but it becomes a huge problem for the increasing population of the area. The proposed infiltration gallery can extract the groundwater from the nearest Kangsabati river bed, to supply the demand of the entire Jhargram Municipal region without really hampering the groundwater storage. The hydraulic design has been done with keeping in mind of its safe yielding capacity and its recovery over time.

The design has been done with two different methods: the first one as per the CPHEEO guidelines with is a standard method to follow in India as instructed by the concerned department of Govt. of India. The second design criteria follows the Ferris Drain Function method, which heavily overestimates the length of the gallery.

As per CPHEEO, the length of infiltration gallery is provided with 340 meters along with a gravel pack surroundings with15-20cm of thickness. The gallery is to be laid in 2 halves of 170m each at an angle of ~120° with a collector well of 5m diameter at the centre.

8.1 Limitation & Future Scope of the Study

Infiltration galleries encourage natural groundwater recharge. Therefore, the rate of localised groundwater recharge can significantly increase. It must be noted that there is a risk of pollutants entering the groundwater system, from either upstream or construction related sources. Detail risk assessment study of emerging contaminant and other pollutant can also enrich the design sustainability. Application of numerical model more precise data collection and pumping test data analysis can also improve the design accuracy. In future application of software model (MIKE-Hydro River, HEC RAS) for uncertainty analysis can increase the reliability of the design.

References

- Amartya, K Bhattacharya, & Basack, Sudip. (2009). A Practical Design for Groundwater Extraction in Arid Regions Using Qanats Coupled with Vertical Risers. *Electronic Journal of Geotechnical Engineering*. 14.
- Amin, M. I., Kazi, R., & Downing, T. E. (1983). Efficiency of Infiltration Galleries as a Source of Water in Arid Lands. *Water International, Vol. 8, No. 4*, 158-165.
- Asare, Eb & Bosque-Hamilton, Ek. (2004). The performance of an infiltration gallery used as a simple water treatment option for a small rural community - Goviefe-Agodome in the Volta Region, Ghana. *Water SA. 30.* https://doi.org/10.4314/wsa.v30i2.5075
- Banerjee, G. (2012). Groundwater abstraction through river-bed collector well: a case study based on geophysical and hydrological investigation. *Clean Techn Environ Policy* 14, 573–587. https://doi.org/10.1007/s10098-011-0417-6
- Bekele, Elise & Toze, Simon & Patterson, Bradley & Fegg, Wolfgang & Shackleton, Mark & Higginson, Simon. (2013). Evaluating two infiltration gallery designs for managed aquifer recharge using secondary treated wastewater. *Journal of environmental management. 117C*. 115-120. https://doi.org/10.1016/j.jenvman.2012.12.018
- CPHEEO Manual (1999). Manual on Water Supply and Treatment. Third Edition – Revised and Updated. Central Public Health and Environmental Engineering Organisation, Ministry of Urban Development, New Delhi, India.
- Foucher, Pierre, Raghavan, Anand, Sheiretov, Todor, Engel, David, Babin, Christopher, Wurtz, Josh, Melvin, Hayden, and Francisco Garzon. (2022). Sand Control Screen Clogging Remediation with Innovative High-Density Slot Machining Solution. *SPE/ICoTA Well Intervention Conference and Exhibition*. https://doi.org/10.2118/209031-MS
- Gregory, M., & Arseneau, D.M. (2012). Design, Construction and Hydraulic Performance Assessment of an Infiltration Gallery. *The Journal of Water Management Modelling*. https://doi.org/10.14796/JWMM.R245-10
- Ground Water Manual (1995). Ground Water Manual. A Water Resources Technical Publication. A guide for the investigation, development, and management of ground-water resources", Second edition, U.S. Department of Interior, Bureau of Reclamation. Washington, USA.
- IRC: 78-2014. Standard Specifications and Code of Practice for Road Bridges, Section VII, Foundations and Substructure, Revised Edition. Indian Roads Congress, New Delhi, India.

- Jennings, Aaron & Baker, Kimberly. (2015). Hydraulic Performance of a Residential Stormwater Infiltration Gallery. *Journal of Environmental Engineering. 142.* 05015002. https://doi.org/10.1061/(ASCE)EE.1943-7870.0001063
- Jeong, H.Y., Jun, S., Cheon, J.Y., & Park, M.J. (2018). A review on clogging mechanisms and managements in aquifer storage and recovery (ASR) applications. *Geosciences Journal, 22*, 667-679. https://doi.org/10.1007/s12303-017-0073-x
- Jurel, Er. (2013). Infiltration Galleries:-A Solution To Drinking Water Supply For Urban Areas Near Rivers.". *IOSR Journal of Mechanical and Civil Engineering. 5*. 29-33. https://doi.org/10.9790/1684-0532933
- Jones, Anthony. (2008). Can we reposition the preferred geological conditions necessary for an infiltration gallery? The development of a synthetic infiltration gallery. *Desalination. 221.* 598-601. https://doi.org/10.1016/j.desal.2007.05.028
- Kalwa, F., Binder, M., Händel, F., Grüneberg, L., & Liedl, R. (2021). Biological and Physical Clogging in Infiltration Wells: Effects of Well Diameter and Gravel Pack. *Ground water*, *59*(6), 819–828. https://doi.org/10.1111/gwat.13104
- Kusuma, Maritha & Hadi, Wahyono & Wirjodirdjo, Budisantoso. (2018). Preliminary study of infiltration gallery for water treatment towards Universal Access 2019 in Indonesia. *Soil & Environment. 37*. 83-88. https://doi.org/10.25252/SE/18/51284
- Kusuma, M. N., Wirjodirjo, B., Hadi, W., & Fitriani, N. (2021). Scenarios modification of hydraulic conductivity to time period of clogging in infiltration gallery. *Pollution Research*, 40(1), 178-181.
- Macuha RN. (2019). Estimating the Yield of a Collector Well with Parallel Infiltration Galleries as Laterals. *Philippine Engineering Journal Vol. 40. No. 2*. 1-14.
- Maity, Prabir & Das, Subhasish & Das, Rajib. (2017). Methodology for Groundwater Extraction in the Coastal Aquifers of Purba Midnapur District of West Bengal in India under the Constraint of Saline Water Intrusion. *Asian Journal of Water*. 14. 1-12. https://doi.org/10.3233/AJW-170011
- Mansilha, Catarina & Melo, Armindo & Ferreira, I & Pinho, Carina & Domingues, Valentina & Castro Pinho, Olívia & Gameiro, Paula. (2011). Groundwater from Infiltration Galleries Used for Small Public Water Supply Systems: Contamination with Pesticides and Endocrine Disruptors. *Bulletin of environmental contamination and toxicology. 87*. 312-318. https://doi.org/10.1007/s00128-011-0337-5

- Marazuela, M. Á., García-Gil, A., Santamarta, J. C., Gasco-Cavero, S., Cruz-Pérez, N., & Hofmann, T. (2022). Stormwater management in urban areas using dry gallery infiltration systems. *The Science of the total environment, 823,* 153705. https://doi.org/10.1016/j.scitotenv.2022.153705
- Muhammad Fahim Aslam, Habib-ur-Rehman, Noor Muhammad Khan. (2021). Assessing the Role of Infiltration Galleries to Enhance Groundwater Recharge in Model Town Lahore. *American Journal of Water Science and Engineering. Volume 7, Issue 1.* 14-23. https://doi.org/10.11648/j.ajwse.20210701.12
- Raghunath, H.M. (2011). Ground Water. New Age International Publishers, India.
- Schwartz, F.W. and Zang, H. (2003). Fundamentals of groundwater. John Willy & Sons, 258-272.
- SENGUPTA, S., MANDAL, B., & PRADHAN, D. (2012). Exceptional heavy rainfall over Ajoy, Mayurakshi and Kansabati catchments and QPF verification during flood season of September 2009. *MAUSAM, 63(3)*, 479–488.https://doi.org/10.54302/mausam.v63i3.1233
- Shende, S., & Chau, K. W. (2019). Attenuation of Pathogen Shock Load: Analytical Analysis of Infiltration Gallery in Riverbank Filtration during Stream Stage Rise. *Journal of Hazardous, Toxic, and Radioactive Waste, 23(4)*, [04019009]. https://doi.org/10.1061/(ASCE)HZ.2153-5515.0000445
- Sikdar, P. K., Dey, S., Ghosal, U., & Chakraborty, S. (2020). Base flow and drinking water supply in semi-arid and fluoride affected areas: the example of River Brahmani, Birbhum district, West Bengal, India. *International Association of Hydrogeologists, Vol 1*, 42-55.
- Subramanya, K. (2017). Engineering Hydrology, 4th Edition. McGraw-Hill Education, India.
- Todd, D.K. (2009). Groundwater Hydrology. John Willy & Sons, USA.

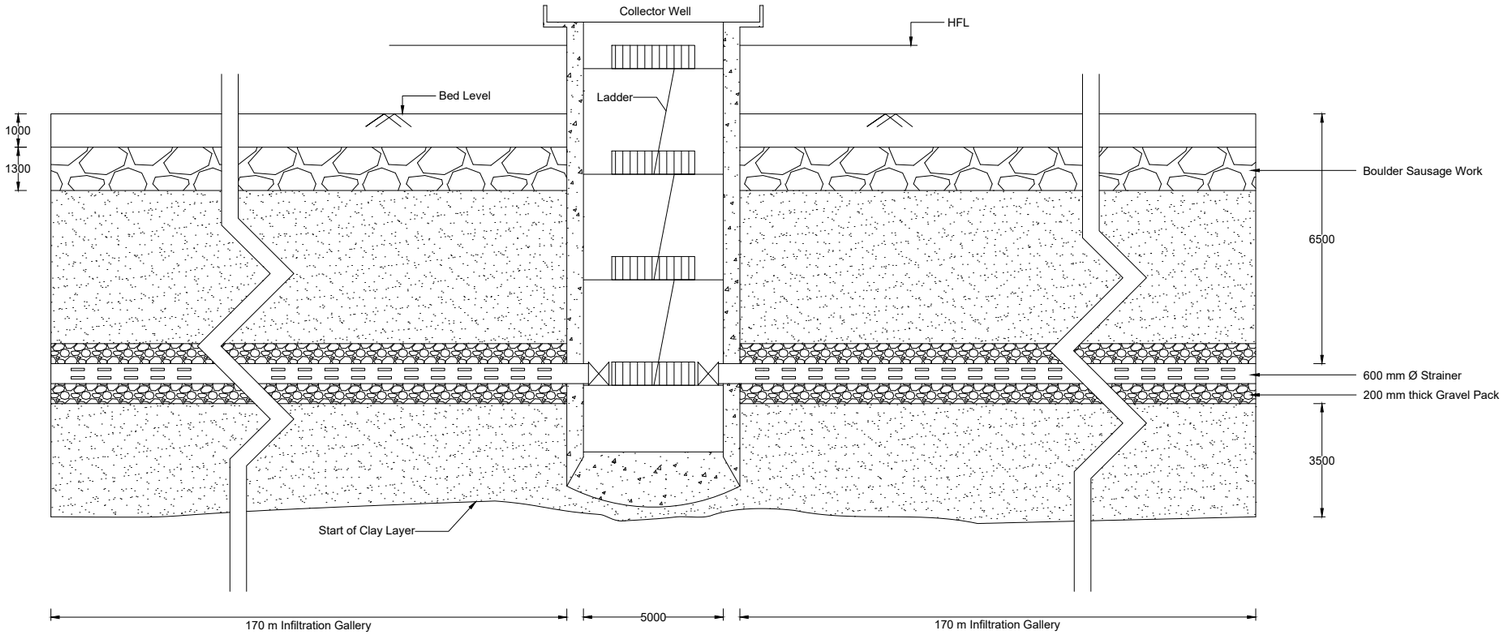

LONGITUDINAL SECTIONAL VIEW OF INFILTRATION GALLERY SYSTEM

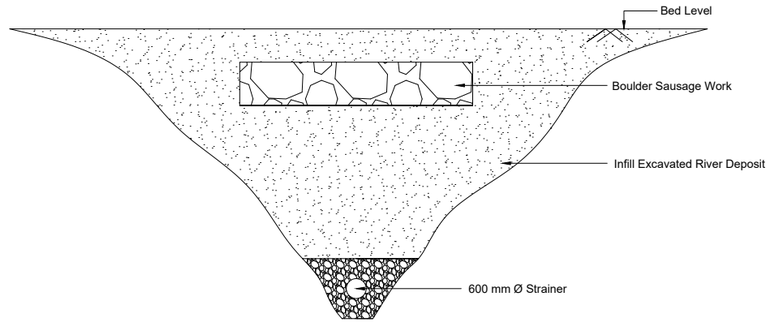

TRANSVERSE SECTIONAL VIEW OF INFILTRATION GALLERY

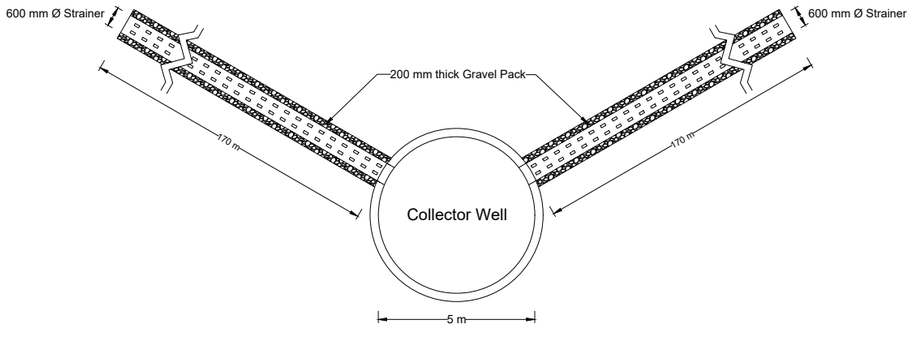

PLAN VIEW OF INFILTRATION GALLERY SYSTEM

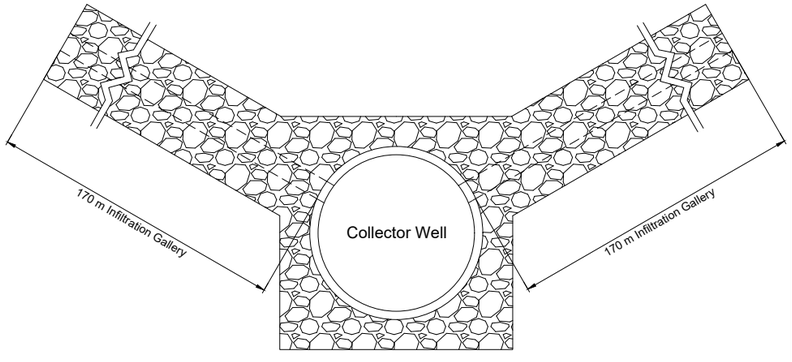

PLAN VIEW OF BOULDER SAUSAGE WORK

NOTE: ALL DIMENSIONS ARE IN "MM" OTHERWISE MENTIONED

TITLE: **GENERAL ARRANGEMENT DRAWING OF THE RIVER BED INFILTRATION GALLERY SYSTEM**

Prepared by:

KABEER AHMED TAIYABJI
Exam roll: M4WRE22012
ME Water Resources and Hydraulic Engineering

SCHOOL OF WATER RESOURCES ENGINEERING
JADAVPUR UNIVERSITY
2022